

North East Scotland Salmon and Sea Trout Tracking Array

River Dee Trust (RDT) and Marine Scotland Science (MSS)

Robert Main⁽¹⁾, Al Reeve⁽³⁾, Jonathan Archer⁽⁴⁾, Rory O'Hara Murray⁽¹⁾, Matt Newton⁽¹⁾ Ross Gardiner⁽²⁾, Bas Buddendorf⁽³⁾, John Armstrong⁽²⁾, Ian Davies⁽¹⁾ and Lorraine Hawkins⁽³⁾



Scottish Government
Marine Scotland Science⁽¹⁾
Marine Laboratory
375 Victoria Road
Aberdeen
AB11 9DB

Marine Scotland Science ⁽²⁾
Freshwater Fisheries
Laboratory
Faskally
Pitlochry
Perthshire
PH16 5LB

River Dee Trust⁽³⁾
River Office
Mill of Dinnet
Aboyne
Aberdeenshire
AB34 5LA



Scottish Government
Riaghaltas na h-Alba
gov.scot



1

⁽⁴⁾Scottish Centre for Ecology and the Natural Environment, Institute of Biodiversity, Animal Health and Comparative Medicine, College of Medical, Veterinary and Life Sciences, University of Glasgow

1 Executive Summary

This research project, funded by Vattenfall European Offshore Wind Deployment Centre, investigated the spatial distribution of seaward-migrating juvenile Atlantic salmon (*Salmo salar*) and brown trout (sea trout, *Salmo trutta*) leaving the Rivers Dee and Don in North East Scotland.

In recent decades Atlantic salmon populations in the North East of Scotland and throughout the North Atlantic have been in serious decline across their range. Juvenile salmon exit rivers to migrate to northern feeding grounds in areas such as in the Norwegian Sea each springtime., As such the Scottish Government have identified marine developments as a potential pressure on salmon stocks where there is potential for overlap. The aim of this work was therefore to establish nearshore migration routes of salmon and habitat use of sea trout, to identify potential for overlap between migrating fish and future marine development sites. Modelling to determine the swimming vectors leading to the observed migration paths was also carried out so that this information could be applied to salmon populations from other rivers.

Fish movements from the river, through the estuary and into the marine environment – extending to 20km from shore – were tracked over 3 years by tagging juvenile salmon and sea trout each year in the Rivers Dee and Don and tracking their location with up to 158 fixed-position receivers. After a trial study in 2017 (60 salmon smolts), 187 Dee salmon, 125 Don salmon, and 98 Dee sea trout were tagged over 3 years (2018, 2019, 2021). After accounting for losses in the river, 144 Dee salmon smolts, 49 Don salmon smolts and 53 Dee sea trout smolts formed part of the study.

Salmon travelled at an average speed of 0.45ms^{-1} from the exit of Aberdeen Harbour to 4km from the coast. Their speed then significantly dropped between 4 and 20km from shore to 0.24ms^{-1} . Fish tagged with depth sensors mostly swam within the top 3m of the water surface.

Salmon from the River Dee tended to travel in an easterly direction for the first 4km from shore; this was similar in all 3 years (mean annual bearings $96\text{-}106^\circ$ from North). After reaching 4km from shore, the direction of travel became slightly more southerly, with a mean bearing from 4-10km from shore of 128° (2018) and from 4-20km from shore of 117° (2019).

Direct measurement of marine currents was used to account for tidal effects on tagged fish. Once tidal corrections were made, the direction of travel of Dee salmon from the harbour to 4km from shore ranged from northeast to southeast with mean annual bearings of 75-107°. The corrections also meant that at 4-10km from shore, the direction of travel became significantly more south-easterly (bearing 158°) in 2018. The direction of travel from 4–20km from shore remained between east and southeast after correction (114°) in 2019. Similar trajectories were seen in 2021, although the change in the receiver locations prevented statistical comparison.

For the River Don, salmon smolts showed a similar south-easterly direction to 20km offshore. However, there was a portion of salmon smolts that headed in a north easterly direction. This was only observed in 2021 due to a paucity of tagged fish in 2019 due to high loss rates.

Particle tracking simulations were run to model the trajectories of juvenile salmon exiting the River Dee, assuming current flows as calculated in the Scottish Shelf Model (Marine Scotland Science). A range of behaviours of these juvenile salmon were tested to determine which behaviour produced simulations most representative of the observed tracked migration paths.

The modelled behaviour that was most similar to the observed tracks of tagged fish was the 'variable rheotaxis' behaviour, whereby 'particles' (modelled fish) followed the tide but only swam when the current was broadly heading away (easterly) from the coast. When the simulations were run over a 9-month period, only about 50% of the particles made it to high latitudes and not until late in the year. However, field studies reported juvenile salmon reaching these northerly locations much earlier in the year. The simulated scenario using the 'constant bearing' behaviour was most successful at producing particles that reached high latitudes by May-Jun, fitting with other tracking studies. These results from particle simulation suggest a possible behaviour change at some point during the migration, where fish transition from a current-following behaviour to a constant bearing, or to a 'variable rheotaxis' behaviour that follows a northerly current.

The overall east to south-easterly migration of juvenile salmon from the Dee was consistent over all three years of the study, providing strong evidence that this is the regular migratory route when emigrating from the Dee. These fish must, at some point in their migration, make a course adjustment to allow for a more northerly trajectory to the feeding grounds in the Norwegian Sea.

Sea trout observed in this study did not tend to migrate to oceanic feeding areas but instead remained in the nearshore environment. Tracked individuals exhibited highly variable migration strategies, categorised as freshwater migration only (potamodromous; 18% of tagged individuals), migration from freshwater to estuary (semi-anadromous; 37%) and migration from freshwater to marine (anadromous; 45%). Anadromous fish showed behavioural variation in terms of time they spent in the estuary before entering the marine habitat and in the number of times they moved between estuarine and marine habitats. Anadromous sea trout tended to either spend a short time in the Dee estuary (mean of 21 hours) or a much longer time (mean of 19 days).

The marine distribution of anadromous sea trout was mainly around the harbour mouth and out to 4km from shore. Their distribution was analysed to determine any preference between littoral, shallow and pelagic habitat. No difference between habitat types was found. Sea trout tended to stay within the top 3 metres in the estuary area. These data suggest that sea trout may be present in areas where harbour developments and both near and offshore developments occur due to their wide ranging and highly plastic behaviour.

This study has demonstrated that salmon and sea trout tend to exhibit different behaviours with salmon smolts rapidly leaving their rivers and heading in an easterly or south easterly direction and sea trout smolts showing a range of different behaviours including remaining in harbour/estuarine areas and close inshore. This means that sea trout are more likely than salmon to be present in areas where harbour and inshore marine industry activities occur. Simulation modelling predicted salmon smolts to head eastwards across the North Sea before heading north, towards high latitude feeding grounds. This means salmon are more likely to be present in areas of offshore development, such as future offshore wind development. Given the conservation status of both these species, further work is needed to investigate the extent to which salmon and sea trout interact with marine industry activities and to identify any potential negative effects on protected populations.

2 Acknowledgements

This project would never have been possible without the hard work and dedication of the River Dee Trust staff who aided in the capture of migrating fish, deployment and recovery of receivers and discussions with stakeholder groups.

The crew of the Scottish Government research vessel MRV Alba na Mara have deployed and recovered hundreds of moorings over the 4 years this project and pilot have run. Also the crew of the vessel Waterfall have been indispensable in using their remotely operated vehicle (ROV) in some very challenging circumstances to recover over a hundred moorings from within the study.

This project has provided data for two MSc projects from the Scottish Centre for Ecology and the Natural Environment (SCENE), University of Glasgow. The theses from these two MSc projects are available online and contain wider information on both salmon and sea trout which may be of interest ([Migration of Atlantic salmon \(*Salmo salar*\) smolts and post-smolts from a Scottish east coast river - Enlighten: Theses \(gla.ac.uk\)](#) [River and coastal marine habitat use and the continuum of migration strategies by brown trout \(*Salmo trutta*\) smolts from the River Dee \(Aberdeenshire\) - Enlighten Theses \(gla.ac.uk\)](#)).

Contents

1	Executive Summary.....	2
2	Acknowledgements	5
3	Project background.....	21
4	General Introduction.....	23
5	Aims of this Study.....	24
5.1	Salmon Smolts.....	24
5.2	Brown Trout Smolts (Sea Trout).....	24
6	General Methods.....	25
6.1	Study Location	25
6.2	Fish Tagging	27
6.3	Range testing.....	28
6.3.1	Pre study.....	28
6.3.2	Within the Study.....	29
6.4	Receiver Locations	30
7	Salmon.....	33
7.1	Introduction	33
7.2	Methods	35
7.2.1	Tag Specification	35
7.2.2	Fish migration behaviour	36
7.2.3	Marine Directionality	37
7.3	Particle Tracking.....	38
7.3.1	Hydrodynamic model description and validation.....	38
7.3.2	Near-field simulations	42
7.3.3	Far-field simulations.....	43
7.3.4	Data analyses	44
7.4	Results	44
7.4.1	Depth and temperature data.....	46
7.4.2	Harbour Transit Time (HTT)	48
7.4.3	Rate of Marine Migration	48

7.4.4	Direction of Marine Travel (Transmitter Detections)	50
7.4.5	Grid Array 2021	52
7.5	Detection Efficiency	53
7.5.1	Predation Events	56
7.6	Particle tracking	59
7.6.1	2018 near-field simulation spatial analysis	59
7.6.2	2019 near-field simulations spatial analysis	63
7.6.3	Near-field simulation temporal analysis	66
7.6.4	Far-field simulations	69
7.7	Discussion	73
7.8	Conclusion (Salmon)	77
8	Sea Trout	80
8.1	Introduction	80
8.2	Methods	81
8.2.1	Tag Specifications	81
8.2.2	Study Array for 2018 and 2019	82
8.2.3	Defining habitat at ALS locations	82
8.2.4	Data Handling	83
8.2.5	Categorising of migration strategies	84
8.2.6	Statistical analysis	86
8.2.7	A framework to describe the continuum of behaviours available to anadromous trout with the marine environment	90
8.3	Results	93
8.3.1	Detected Predation Events	93
8.3.2	Hypotheses test results	95
8.3.3	Anadromous smolts use on marine curtains A, B, C and D	101
8.3.4	Temperature and Depth	102
8.3.5	Continuum of anadromous smolts behaviour results	104
8.4	Discussion	106

8.5	Conclusion Sea Trout	109
9	Overall Conclusions.....	111
10	References	113
11	Appendix A – Far-field particle density plots for faster swim speeds	119
12	Appendix B – Near-field particle density plots for 2018 simulations with faster swim speeds – first detections	121
13	Appendix C – Near-field particle density plots for 2018 simulations with faster swim speeds – all detections	123
14	Appendix D – Near-field particle density plots for 2019 simulations with faster swim speeds – first detections	125
15	Appendix E – Near-field particle density plots for 2019 simulations with faster swim speeds – all detections	127
16	Appendix F – Near-field temporal analysis with faster swim speeds	129

List of Figures

FIGURE 6.1: ABERDEEN BAY SMOLT TRACKING ARRAY SHOWING THE LOCATION OF AUTOMATIC LISTENING STATIONS (ALS) IN CURTAINS A (BLACK CIRCLES, 2017, 2018 AND 2019), B (BLACK CROSSES, 2018) C (BLACK SQUARES, 2018) AND D (BLACK TRIANGLES, 2019 AND 2021). IN EACH CURTAIN RANGE TEST TAGS ARE MARKED WITH A HOLLOW SYMBOL MATCHING THE CURTAIN SYMBOL. THE 2016 RANGE TEST LAYOUT IS ALSO SHOWN AS HOLLOW SYMBOLS. RIVER ALSs (BLACK HOLLOW DIAMONDS) AND HARBOUR ALS (BLACK STARS) ARE ALSO SHOWN. INSET B HIGHLIGHTS THE STUDY AREA WITHIN THE CONTEXT OF SCOTLAND INCLUDING BUILT (OUTLINED IN GREY) AND PLANNED (OUTLINED IN BLACK) WINDFARM LOCATIONS.26

FIGURE 6.2 RESULTS FROM A 5 DAY RANGE TEST IN IN ABERDEEN BAY DURING 2016 SHOWING THE PERCENTAGE OF TAG SIGNALS DETECTED BY THE AUTOMATIC LISTENING STATION (ALS) ACROSS A RANGE OF DISTANCES. THE SOLID BLUE SQUARES ARE THE AVERAGE DETECTION PERCENTAGE AT EACH ALS LOCATION; BLUE VERTICAL BARS INDICATE 95% CONFIDENCE INTERVALS AND WHITE SQUARES ARE OUTLIERS.29

FIGURE 6.3: ALS GRID (BLACK CIRCLES) AND CURTAIN D (BLACK TRIANGLES) PLACEMENTS IN 2021, RANGE TEST TAGS IN CURTAIN D ARE MARKED (HOLLOW TRIANGLE. RIVER ALSs (BLACK HOLLOW DIAMONDS) AND HARBOUR ALS (BLACK STARS) ARE ALSO SHOWN. ACOUSTIC DOPPLER CURRENT PROFILER (ADCP) IS ALSO SHOWN (BLACK HOLLOW START). INSET B SHOWS THE STUDY SITE IN THE CONTEXT OF SCOTLAND INCLUDING BUILT (OUTLINED IN GREY) AND PLANNED (OUTLINED IN BLACK) WINDFARM LOCATIONS.31

FIGURE 7.1: COMPARISON OF ADCP AND MODELLED TIME SERIES OF SEA SURFACE HEIGHT, AND SURFACE VELOCITIES FOR A 15 DAY PERIOD IN MAY 2018. THE PARTICLE RELEASE TIMES ARE INDICATED BY THE DARK VERTICAL GREY LINES IN THE SEA SURFACE HEIGHT SUB-FIGURE. 40

FIGURE 7.2: COMPARISON OF TIDAL ELLIPSE FROM ADCP AND SSW-RS FOR MAY-AUG 2018. .41

FIGURE 7.3 PERCENTAGE OF DETECTED TRANSMITTERS AT DISTANCES RELATIVE TO R12 (0KM), HARBOUR (H1 AND H2) COMBINED DETECTIONS. DATA LINES CEASE AT MOST SEAWARD MARINE CURTAIN; CURTAINS A (4KM, 2017), C (10KM, 2018) AND D (20KM, 2019).44

FIGURE 7.4: BOXPLOT OF SALMON SMOLT SWIMMING DEPTHS(M) FROM SEA SURFACE IN THE LOWER RIVER (R12), HARBOUR (H1 AND H2) AND MARINE CURTAINS (CURTAIN A, CURTAIN C) FOR 2017 AND 201847

FIGURE 7.5: SMOLT SWIMMING TEMPERATURES (°C) THE LOWER RIVER (R12), HARBOUR (H1 AND H2) AND MARINE CURTAINS (CURTAIN A, CURTAIN C) FOR 2017 AND 2018. PREDATION EVENTS HAVE BEEN REMOVED.....47

FIGURE 7.6: PLOTS SHOWING RECORDED FISH BEARINGS (BLACK DOTS) WITH MEAN EBB TIDE (RED ARROW) AND MEAN FLOOD TIDE (BLUE ARROW) DIRECTIONS, WITH ARROWS SHOWING THE OVERALL MEAN MOVEMENT DIRECTIONS (BLACK).....51

FIGURE 7.7 TRAJECTORIES OF TRANSMITTERS FROM THE DEE TRANSITING THROUGH A GRID ARRAY OF ALS IN 2021. COLOURS IDENTIFY UNIQUE INDIVIDUALS52

FIGURE 7.8 TRAJECTORIES OF TRANSMITTERS FROM THE DON TRANSITING THROUGH A GRID ARRAY OF ALS IN 2021. COLOURS IDENTIFY UNIQUE INDIVIDUALS53

FIGURE 7.9: EXAMPLE OF SIMULATED FISH PATHS (GREY LINE) WITH TAG TRANSMISSIONS (BLACK DOTS) BASED ON THE TAGS USED AND FISH SWIMMING SPEEDS RECORDED AS FISH PASS AN ALS LINE (RED DOTS REPRESENT RECEIVERS).....55

FIGURE 7.10: SIMULATIONS OF THE PROBABILITY OF DETECTING A TAGGED FISH BASED ON THE RANGE TEST RESULTS SHOWING FISH DETECTIONS PROBABILITIES AT VARYING FISH SWIMMING SPEEDS (A, B) AND AT DIFFERING RECEIVER SPACING (C AND D).56

FIGURE 7.11 TEMPERATURE PLOT FROM TRANSMITTER (TAG) SERIAL NUMBER 20 IN 2018 SHOWING A DROP IN TEMPERATURE FOLLOWED BY A RAPID INCREASE TO 36.4°C. COLOURED DOTS REPRESENT THE ALS THE TAG WAS DETECTED AT.57

FIGURE 7.12: DEPTH PLOT FROM TRANSMITTER (TAG) SERIAL NUMBERS 23 AND 35 IN 2018 SHOWING AN INCREASE IN SWIMMING DEPTH. COLOURED SHAPES REPRESENT TAG SERIAL NUMBER 23 (ROUND) AND TAG 35 (TRIANGULAR) WITH THE COLOUR REPRESENTING THE ALS STATION NUMBER.....58

FIGURE 7.13: (A) – (E) SHOW PARTICLE DENSITY PLOTS FOR FIRST DETECTIONS OF 2018 SIMULATIONS AROUND ABERDEEN BAY FOR (A) PASSIVE (B) NEGATIVE RHEOTAXIS (C) VARIABLE RHEOTAXIS (D) NORTHERLY BEARING AND (E) NORTH-EASTERLY BEARING BEHAVIOURS, WITH SMOLT SWIM SPEED SET TO 1.5 BL S-1 FOR (B)-(E). SMOLT BODY LENGTH WAS INITIALLY SET TO 0.14 M. THE 2018 INNER AND OUTER ARRAYS OF ACOUSTIC RECEIVERS ARE INDICATED WITH RED LINES. THE FIRST DETECTIONS OF THE PARTICLES ON THE ARRAYS ARE SHOWN BY THE BLUE DOTS, THE SIZE OF WHICH INDICATE THE NUMBER OF FIRST PARTICLE DETECTIONS AT EACH RECEIVER LOCATION. (F) SHOWS THE FIRST DETECTIONS OF TAGGED SALMON SMOLTS AT THE TWO CURTAINS (A AND C), WITH THE SIZE INDICATING THE NUMBER OF UNIQUE DETECTIONS AT ANY ONE RECEIVER.61

FIGURE 7.14: (A) – (E) SHOW PARTICLE DENSITY PLOTS FOR ALL DETECTIONS 2018 SIMULATIONS AROUND ABERDEEN BAY FOR (A) PASSIVE (B) NEGATIVE RHEOTAXIS (C) VARIABLE RHEOTAXIS (D) NORTHERLY BEARING AND (E) NORTH-EASTERLY BEARING BEHAVIOURS, WITH SMOLT SWIM SPEED SET TO 1.5 BL S-1 FOR (B)-(E). SMOLT BODY LENGTH WAS INITIALLY SET TO 0.14 M. THE 4KM AND 10KM CURTAINS (A AND C) ARE INDICATED WITH RED LINES. THE DETECTIONS OF THE PARTICLES ON THE ARRAYS ARE SHOWN BY THE BLUE DOTS, THE SIZE OF WHICH INDICATE THE NUMBER OF PARTICLE DETECTIONS AT EACH RECEIVER LOCATION. (F) SHOWS THE DETECTIONS OF TAGGED SALMON SMOLTS AT THE TWO ARRAYS, WITH THE SIZE INDICATING THE NUMBER OF DETECTIONS AT ANY ONE RECEIVER.62

FIGURE 7.15: (A) – (E) SHOW PARTICLE DENSITY PLOTS FIRST DETECTION OF PARTICLES IN 2019 SIMULATIONS AROUND ABERDEEN BAY FOR (A) PASSIVE (B) NEGATIVE RHEOTAXIS (C) VARIABLE RHEOTAXIS (D) NORTHERLY BEARING AND (E) NORTH-EASTERLY BEARING

BEHAVIOURS, WITH SMOLT SWIM SPEED SET TO 1.5 BL S-1 FOR (B)-(E). SMOLT BODY LENGTH WAS INITIALLY SET TO 0.14 M. THE 2019 4KM (A) AND 20KM (D) CURTAINS OF ACOUSTIC RECEIVERS ARE INDICATED WITH RED LINES. THE FIRST DETECTIONS OF THE PARTICLES ON THE ARRAYS ARE SHOWN BY THE BLUE DOTS, THE SIZE OF WHICH INDICATE THE NUMBER OF FIRST PARTICLE DETECTIONS AT EACH RECEIVER LOCATION. (F) SHOWS THE FIRST DETECTIONS OF TAGGED SALMON SMOLTS AT THE TWO CURTAINS, WITH THE SIZE INDICATING THE NUMBER OF UNIQUE DETECTIONS AT ANY ONE RECEIVER.....64

FIGURE 7.16: (A) – (E) SHOW PARTICLE DENSITY PLOTS FOR ALL DETECTIONS IN 2019 SIMULATIONS AROUND ABERDEEN BAY FOR (A) PASSIVE (B) NEGATIVE RHEOTAXIS (C) VARIABLE RHEOTAXIS (D) NORTHERLY BEARING AND (E) NORTH-EASTERLY BEARING BEHAVIOURS, WITH SMOLT SWIM SPEED SET TO 1.5 BL S⁻¹ FOR (B)-(E). SMOLT BODY LENGTH WAS INITIALLY SET TO 0.14 M. THE 2019 4KM (A) AND 20KM (D) CURTAINS OF ACOUSTIC RECEIVERS ARE INDICATED WITH RED LINES. THE DETECTIONS OF THE PARTICLES ON THE ARRAYS ARE SHOWN BY THE BLUE DOTS, THE SIZE OF WHICH INDICATE THE NUMBER OF PARTICLE DETECTIONS AT EACH RECEIVER LOCATION. (F) SHOWS THE DETECTIONS OF TAGGED SALMON SMOLTS AT THE TWO CURTAINS, WITH THE SIZE INDICATING THE NUMBER OF DETECTIONS AT ANY ONE RECEIVER.65

FIGURE 7.17: BOXPLOTS SHOWING THE TIME FOR PARTICLES TO BE FIRST DETECTED AT THE INNER (TOP) AND OUTER (BOTTOM) ARRAYS FOR THE 2018 (LEFT) AND 2019 (RIGHT) SIMULATIONS, UNDER THE DIFFERENT BEHAVIOURS WITH SMOLT SWIM SPEEDS SET TO 1.5 BL S-1. RED LINES SHOW MEDIAN VALUES FOR THE PARTICLES TRACKED, OR DETECTIONS MADE, BOXES SHOW THE 25TH AND 75TH PERCENTILES, THE WHISKERS SHOW THE LOWER AND UPPER ADJACENT VALUES AND THE RED CROSSES SHOW ANY OUTLIERS.....69

FIGURE 7.18: PARTICLE DENSITY PLOTS FOR (A) PASSIVE (B) NEGATIVE RHEOTAXIS (C) VARIABLE RHEOTAXIS (D) NORTHERLY BEARING AND (E) NORTH-EASTERLY BEARING BEHAVIOURS FOR 2018, WITH SMOLT SWIM SPEED SET TO 1.5 BL S-1 FOR (B)-(E). SMOLT BODY LENGTH WAS INITIALLY SET TO 0.125M.....71

FIGURE 7.19: PERCENTAGE OF PARTICLES FURTHER NORTH THAN 61°N AS A FUNCTION OF TIME FOR THE FIVE BEHAVIOURS – PASSIVE, NEGATIVE AND VARIABLE RHEOTAXIS AND CONSTANT BEARING TO THE NORTH (BEARING 000) AND NORTH-EAST (BEARING 045), AND THREE SWIM

SPEEDS 1.5, 2.5, AND 3.55 BL S-1, (A), (B) AND (C), RESPECTIVELY. THE VERTICAL GREY AREA SHOWS THE SECOND HALF OF MAY WHEN SMOLTS HAVE BEEN OBSERVED AROUND 61° N (HAUGLAND *ET AL.* 2006).....72

FIGURE 8.1: THE STUDY SITE WITH THE LOCATION OF ALS AND RELEASE LOCATIONS, CURTAIN A, B AND C IN 2018, CURTAINS A AND D 2019. VATTENFALL’S EUROPEAN OFFSHORE WIND DEPLOYMENT CENTRE (EOWDC) AND KINCARDINE OFFSHORE WIND FARM (KOWL) ARE DENOTED BY A DASHED BORDER. INSERT B: STUDY SITE WITHIN LARGER GEOGRAPHIC AREA INCLUDING BUILT (OUTLINED IN GREY) AND PLANNED (OUTLINED IN BLACK) WINDFARM LOCATIONS. INSERT C: HARBOUR ALS LOCATIONS.82

FIGURE 8.2: MARINE HABITAT CLASSIFICATION WHERE ALS WERE DEPLOYED WERE; LITTORAL (≤ 10 M, BLACK X), SHALLOW WATER ($>10 - 25$ M, CIRCLE BISECTED WITH BLACK PLUS AND), PELAGIC (>25 M, BOLD BLACK PLUS).....83

FIGURE 8.3: MAP OF THE ALS ON CURTAIN A. NOTES: THE ALS WERE POSITIONED IN THE SAME PLACE IN 2018 AND 2019 FOR YEARLY COMPARISON. HABITAT WHERE ALSS WERE DEPLOYED WAS SPLIT INTO LITTORAL (BLACK CROSS), PELAGIC (BOLD PLUS SIGN) AND SHALLOW WATER (CIRCLE BISECTED WITH PLUS SIGN). GAPS IN THE MARINE CURTAIN ARE WHERE ALS WERE LOST IN ONE YEAR AND THEREFORE CANNOT BE COMPARED TO THE OTHER YEAR.90

FIGURE 8.4: DETECTION PLOTS OF THE FOUR SMOLTS THAT WERE CLASSED AS PREDATED. RED CIRCLES INDICATE WHEN PREDATION COULD HAVE TAKEN PLACE. TAGS A69-1105-143 AND A69-1105-161 ARE OF SMOLTS FROM 2018 WITH THELMA BIOTEL TEMPERATURE AND DEPTHS TAGS. TAGS A69-9006-5297 AND A69-9006-5218 WERE SMOLTS OF 2019 WITH VEMCO PREDATION TAGS. USING $D = \text{DEPTH (M)}$, $T = (\text{°C})$, $ADC = \text{DIGESTION SENSOR}$. RMOUTH IS THE ALS R1294

FIGURE 8.5: THE SMOLT THAT MIGRATED DOWNSTREAM THEN SWAM BACK 23KM UPSTREAM TO THE AREA THAT THE SMOLT WAS RELEASED. THE BLACK-HASHED LINE IS THE DATE TIME OF SMOLTS RELEASE. THE FIRST VERTICAL (GREY) LINE IS DATE TIME OF FIRST DETECTION. THE LAST VERTICAL (HASHED) LINE IS THE LAST KNOWN DETECTION. ORANGE DOTS ARE DETECTIONS

ON AN ALS WITHIN THE RIVER.....95

FIGURE 8.6: SEMI-ANADROMOUS AND ANADROMOUS SMOLTS' MEAN GROUND SPEEDS DOWN THE RIVER, IN RELATION TO THEIR FORK LENGTH. THE BLUE LINE INDICATES THE SMOLTS' MEAN GROUND SPEED THROUGH RIVER. THE GREY AREA DENOTES 95% CONFIDENCE INTERVALS. BLACK DOTS ARE INDIVIDUAL SMOLTS.98

FIGURE 8.7: SMOLTS' OCCUPANCY TIME IN THE ESTUARY IN RELATION TO THEIR MIGRATION STRATEGY (SEMI-ANADROMOUS IN BLUE AND ANADROMOUS IN RED) AND TIME OF ARRIVAL AT THE ESTUARY. GREY AREAS ARE 95% CONFIDENCE INTERVALS OF THE MEAN. DOTS ARE INDIVIDUAL SMOLTS.....99

FIGURE 8.8: TIME DIFFERENCE BETWEEN BOTH SEMI-ANADROMOUS AND ANADROMOUS SMOLTS IN THE TWO ESTUARINE HABITATS (RIVER MOUTH WAS ALS R12, HARBOUR WAS H1 AND H2B). NOTES: THE BLACK HORIZONTAL LINE IS THE MEDIAN; THE BOX IS THE INTERQUARTILE RANGE, AND THE VERTICAL LINES ARE MINIMUM AND MAXIMUM VALUES. THE GREY LINES BETWEEN BLACK DOTS DENOTE THE DIFFERENCE IN TIME BETWEEN INDIVIDUALS IN THE HABITATS... 100

FIGURE 8.9: MAP OF THE STUDY AREA WITH WHITE DOTS INDICATING A RESIDENCY EVENT FOR 2018 AND THE BLACK DOTS INDICATING A RESIDENCY EVENT FOR 2019. THE DOT SIZE INDICATES THE TOTAL TIME THE ANADROMOUS SMOLTS SPENT ON THE ALS. RESIDENCY TIMES IN ESTUARY AND RIVER ARE NOT SHOWN.....101

FIGURE 8.10: DISTANCE FROM SHORE THE ANADROMOUS SMOLTS WERE DETECTED FROM THE NEAREST LANDMASS. NOTE: BLACK HORIZONTAL LINE IS THE MEDIAN, THE BOX IS THE INTERQUARTILE RANGE, AND THE VERTICAL LINES ARE MINIMUM AND MAXIMUM VALUES. BLACK DOTS BEYOND VERTICAL LINES ARE OUTLIERS..... 102

FIGURE 8.11: ANADROMOUS SMOLTS SWIMMING DEPTH COMPARED TO THE DEPTH OF WATER THAT THE ALS WERE DEPLOYED AT. RED POINTS INDICATE DEPLOYMENT DEPTH OF ALS (ON THE SEABED). BLUE POINTS INDICATE THE SWIMMING DEPTH OF ANADROMOUS SMOLTS AT THOSE

FIGURE 11.1 PARTICLE DENSITY PLOTS FOR (A) PASSIVE (B) NEGATIVE RHEOTAXIS (C) VARIABLE RHEOTAXIS (D) NORTHERLY BEARING AND (E) NORTH-EASTERLY BEARING BEHAVIOURS FOR 2018, WITH SMOLT SWIM SPEED SET TO 2.5 BL S-1 FOR (B)-(E). SMOLT BODY LENGTH WAS INITIALLY SET TO 0.125M.....119

FIGURE 11.2 PARTICLE DENSITY PLOTS FOR (A) PASSIVE (B) NEGATIVE RHEOTAXIS (C) VARIABLE RHEOTAXIS (D) NORTHERLY BEARING AND (E) NORTH-EASTERLY BEARING BEHAVIOURS FOR 2018, WITH SMOLT SWIM SPEED SET TO 3.5 BL S-1 FOR (B)-(E). SMOLT BODY LENGTH WAS INITIALLY SET TO 0.125M.....120

FIGURE 12.1 (A) – (E) SHOW PARTICLE DENSITY PLOTS FOR 2018 SIMULATIONS AROUND ABERDEEN BAY FOR (A) PASSIVE (B) NEGATIVE RHEOTAXIS (C) VARIABLE RHEOTAXIS (D) NORTHERLY BEARING AND (E) NORTH-EASTERLY BEARING BEHAVIOURS, WITH SMOLT SWIM SPEED SET TO 2.5 BL S-1 FOR (B)-(E). SMOLT BODY LENGTH WAS INITIALLY SET TO 0.14 M. THE 2018 INNER AND OUTER ARRAYS OF ACOUSTIC RECEIVERS ARE INDICATED WITH RED LINES. THE FIRST DETECTIONS OF THE PARTICLES ON THE ARRAYS ARE SHOWN BY THE BLUE DOTS, THE SIZE OF WHICH INDICATE THE NUMBER OF FIRST PARTICLE DETECTIONS AT EACH RECEIVER LOCATION. (F) SHOWS THE FIRST DETECTIONS OF TAGGED SALMON SMOLTS AT THE TWO ARRAYS, WITH THE SIZE INDICATING THE NUMBER OF UNIQUE DETECTIONS AT ANY ONE RECEIVER.121

FIGURE 12.2 (A) – (E) SHOW PARTICLE DENSITY PLOTS FOR 2018 SIMULATIONS AROUND ABERDEEN BAY FOR (A) PASSIVE (B) NEGATIVE RHEOTAXIS (C) VARIABLE RHEOTAXIS (D) NORTHERLY BEARING AND (E) NORTH-EASTERLY BEARING BEHAVIOURS, WITH SMOLT SWIM SPEED SET TO 3.5 BL S-1 FOR (B) -(E). SMOLT BODY LENGTH WAS INITIALLY SET TO 0.14 M. THE 2018 INNER AND OUTER ARRAYS OF ACOUSTIC RECEIVERS ARE INDICATED WITH RED LINES. THE FIRST DETECTIONS OF THE PARTICLES ON THE ARRAYS ARE SHOWN BY THE BLUE DOTS, THE SIZE OF WHICH INDICATE THE NUMBER OF FIRST PARTICLE DETECTIONS AT EACH RECEIVER LOCATION. (F) SHOWS THE FIRST DETECTIONS OF TAGGED SALMON SMOLTS AT THE TWO ARRAYS, WITH THE SIZE INDICATING THE NUMBER OF UNIQUE DETECTIONS AT ANY ONE RECEIVER.122

FIGURE 13.1 (A) – (E) SHOW PARTICLE DENSITY PLOTS FOR 2018 SIMULATIONS AROUND ABERDEEN BAY FOR (A) PASSIVE (B) NEGATIVE RHEOTAXIS (C) VARIABLE RHEOTAXIS (D) NORTHERLY BEARING AND (E) NORTH-EASTERLY BEARING BEHAVIOURS, WITH SMOLT SWIM SPEED SET TO 2.5 BL S-1 FOR (B)-(E). SMOLT BODY LENGTH WAS INITIALLY SET TO 0.14 M. THE 2018 INNER AND OUTER ARRAYS OF ACOUSTIC RECEIVERS ARE INDICATED WITH RED LINES. THE DETECTIONS OF THE PARTICLES ON THE ARRAYS ARE SHOWN BY THE BLUE DOTS, THE SIZE OF WHICH INDICATE THE NUMBER OF PARTICLE DETECTIONS AT EACH RECEIVER LOCATION. (F) SHOWS THE DETECTIONS OF TAGGED SALMON SMOLTS AT THE TWO ARRAYS, WITH THE SIZE INDICATING THE NUMBER OF DETECTIONS AT ANY ONE RECEIVER. 123

FIGURE 13.2 (A) – (E) SHOW PARTICLE DENSITY PLOTS FOR 2018 SIMULATIONS AROUND ABERDEEN BAY FOR (A) PASSIVE (B) NEGATIVE RHEOTAXIS (C) VARIABLE RHEOTAXIS (D) NORTHERLY BEARING AND (E) NORTH-EASTERLY BEARING BEHAVIOURS, WITH SMOLT SWIM SPEED SET TO 3.5 BL S-1 FOR (B) – (E). SMOLT BODY LENGTH WAS INITIALLY SET TO 0.14 M. THE 2018 INNER AND OUTER ARRAYS OF ACOUSTIC RECEIVERS ARE INDICATED WITH RED LINES. THE DETECTIONS OF THE PARTICLES ON THE ARRAYS ARE SHOWN BY THE BLUE DOTS, THE SIZE OF WHICH INDICATE THE NUMBER OF PARTICLE DETECTIONS AT EACH RECEIVER LOCATION. (F) SHOWS THE DETECTIONS OF TAGGED SALMON SMOLTS AT THE TWO ARRAYS, WITH THE SIZE INDICATING THE NUMBER OF DETECTIONS AT ANY ONE RECEIVER. 124

FIGURE 14.1 (A) – (E) SHOW PARTICLE DENSITY PLOTS FOR 2019 SIMULATIONS AROUND ABERDEEN BAY FOR (A) PASSIVE (B) NEGATIVE RHEOTAXIS (C) VARIABLE RHEOTAXIS (D) NORTHERLY BEARING AND (E) NORTH-EASTERLY BEARING BEHAVIOURS, WITH SMOLT SWIM SPEED SET TO 2.5 BL S-1 FOR (B) -(E). SMOLT BODY LENGTH WAS INITIALLY SET TO 0.14 M. THE 2019 INNER AND OUTER ARRAYS OF ACOUSTIC RECEIVERS ARE INDICATED WITH RED LINES. THE FIRST DETECTIONS OF THE PARTICLES ON THE ARRAYS ARE SHOWN BY THE BLUE DOTS, THE SIZE OF WHICH INDICATE THE NUMBER OF FIRST PARTICLE DETECTIONS AT EACH RECEIVER LOCATION. (F) SHOWS THE FIRST DETECTIONS OF TAGGED SALMON SMOLTS AT THE TWO ARRAYS, WITH THE SIZE INDICATING THE NUMBER OF UNIQUE DETECTIONS AT ANY ONE RECEIVER. 125

FIGURE 14.2 (A) – (E) SHOW PARTICLE DENSITY PLOTS FOR 2019 SIMULATIONS AROUND ABERDEEN BAY FOR (A) PASSIVE (B) NEGATIVE RHEOTAXIS (C) VARIABLE RHEOTAXIS (D) NORTHERLY BEARING AND (E) NORTH-EASTERLY BEARING BEHAVIOURS, WITH SMOLT SWIM SPEED SET TO 3.5 BL S-1 FOR (B)-(E). SMOLT BODY LENGTH WAS INITIALLY SET TO 0.14 M. THE 2019 INNER

AND OUTER ARRAYS OF ACOUSTIC RECEIVERS ARE INDICATED WITH RED LINES. THE FIRST DETECTIONS OF THE PARTICLES ON THE ARRAYS ARE SHOWN BY THE BLUE DOTS, THE SIZE OF WHICH INDICATE THE NUMBER OF FIRST PARTICLE DETECTIONS AT EACH RECEIVER LOCATION. (F) SHOWS THE FIRST DETECTIONS OF TAGGED SALMON SMOLTS AT THE TWO ARRAYS, WITH THE SIZE INDICATING THE NUMBER OF UNIQUE DETECTIONS AT ANY ONE RECEIVER. 126

FIGURE 15.1 (A) – (E) SHOW PARTICLE DENSITY PLOTS FOR 2019 SIMULATIONS AROUND ABERDEEN BAY FOR (A) PASSIVE (B) NEGATIVE RHEOTAXIS (C) VARIABLE RHEOTAXIS (D) NORTHERLY BEARING AND (E) NORTH-EASTERLY BEARING BEHAVIOURS, WITH SMOLT SWIM SPEED SET TO 2.5 BL S-1 FOR (B)-(E). SMOLT BODY LENGTH WAS INITIALLY SET TO 0.14 M. THE 2019 INNER AND OUTER ARRAYS OF ACOUSTIC RECEIVERS ARE INDICATED WITH RED LINES. THE DETECTIONS OF THE PARTICLES ON THE ARRAYS ARE SHOWN BY THE BLUE DOTS, THE SIZE OF WHICH INDICATE THE NUMBER OF PARTICLE DETECTIONS AT EACH RECEIVER LOCATION. (F) SHOWS THE DETECTIONS OF TAGGED SALMON SMOLTS AT THE TWO ARRAYS, WITH THE SIZE INDICATING THE NUMBER OF DETECTIONS AT ANY ONE RECEIVER. 127

FIGURE 15.2 (A) – (E) SHOW PARTICLE DENSITY PLOTS FOR 2019 SIMULATIONS AROUND ABERDEEN BAY FOR (A) PASSIVE (B) NEGATIVE RHEOTAXIS (C) VARIABLE RHEOTAXIS (D) NORTHERLY BEARING AND (E) NORTH-EASTERLY BEARING BEHAVIOURS, WITH SMOLT SWIM SPEED SET TO 3.5 BL S-1 FOR (B)-(E). SMOLT BODY LENGTH WAS INITIALLY SET TO 0.14 M. THE 2019 INNER AND OUTER ARRAYS OF ACOUSTIC RECEIVERS ARE INDICATED WITH RED LINES. THE DETECTIONS OF THE PARTICLES ON THE ARRAYS ARE SHOWN BY THE BLUE DOTS, THE SIZE OF WHICH INDICATE THE NUMBER OF PARTICLE DETECTIONS AT EACH RECEIVER LOCATION. (F) SHOWS THE DETECTIONS OF TAGGED SALMON SMOLTS AT THE TWO ARRAYS, WITH THE SIZE INDICATING THE NUMBER OF DETECTIONS AT ANY ONE RECEIVER. 128

FIGURE 16.1 BOXPLOTS SHOWING THE TIME FOR PARTICLES TO BE FIRST DETECTED AT THE INNER (TOP) AND OUTER (BOTTOM) ARRAYS FOR THE 2018 (LEFT) AND 2019 (RIGHT) SIMULATIONS, UNDER THE DIFFERENT BEHAVIOURS WITH SMOLT SWIM SPEEDS SET TO 2.5 BL S-1. RED LINES SHOW MEDIAN VALUES FOR THE PARTICLES TRACKED, OR DETECTIONS MADE, BOXES SHOW THE 25TH AND 75TH PERCENTILES, THE WHISKERS SHOW THE LOWER AND UPPER ADJACENT VALUES AND THE RED CROSSES SHOW ANY OUTLIERS. 129

FIGURE 16.2 BOXPLOTS SHOWING THE TIME FOR PARTICLES TO BE FIRST DETECTED AT THE INNER (TOP) AND OUTER (BOTTOM) ARRAYS FOR THE 2018 (LEFT) AND 2019 (RIGHT) SIMULATIONS, UNDER THE DIFFERENT BEHAVIOURS WITH SMOLT SWIM SPEEDS SET TO 3.5 BL S-1. RED LINES SHOW MEDIAN VALUES FOR THE PARTICLES TRACKED, OR DETECTIONS MADE, BOXES SHOW THE 25TH AND 75TH PERCENTILES, THE WHISKERS SHOW THE LOWER AND UPPER ADJACENT VALUES AND THE RED CROSSES SHOW ANY OUTLIERS. 130

LIST OF TABLES

TABLE 7.1: DESCRIPTIVE DATA FOR HARBOUR TRANSIT TIMES (HOURS)	48
TABLE 7.2: RATES OF ATLANTIC SALMON SMOLT MOVEMENTS BETWEEN H2 AND MARINE CURTAINS	49
TABLE 7.3: BEARING OF TRANSMITTER TRAJECTORIES OF ACTUAL DETECTIONS AND CORRECTED BEARINGS WHERE TIDE COMPONENTS HAVE BEEN REMOVED.	50
TABLE 7.4: DETECTION EFFICIENCY (%) OF EACH GATE AND CURTAIN ACROSS YEARS, WITH RAW NUMBERS OF FISH MISSED REPRESENTED IN BRACKETS.	53
TABLE 7.5: TIME FOR PARTICLES TO BE DETECTED FOR THE FIRST TIME AT CURTAIN A AND C DURING THE 2018 AND CURTAIN D 2019 SIMULATIONS, UNDER THE DIFFERENT BEHAVIOURS AND SMOLT SWIM SPEEDS IN BODY LENGTHS PER SECOND (BL S ⁻¹). THE ARRAY DATA SHOWS THE TIMES DERIVED FROM THE DETECTED TAGS. THE INITIAL SMOLT SIZE WAS 0.14 M FOR ALL SIMULATIONS. THE MEAN, MEDIAN AND STANDARD DEVIATION (SD) FOR ALL PARTICLE, OR DETECTED TAGS FOR THE ARRAY DATA, ARE SHOWN.	67
TABLE 8.1: THE ALLOCATION OF MIGRATION OUTCOMES AND THEIR DEFINITIONS.....	85
TABLE 8.2: SHOWING MODELS 1 AND 2, VARIABLES, THEIR DESCRIPTION, AND THE MODEL THEY WERE USED IN.....	88
TABLE 8.3: ALLOCATION OF TAGGED SEA TROUT SMOLTS INTO EACH OF THE FIVE CATEGORIES BY TAGGING SITE AND YEAR, USING DEFINITIONS AS DESCRIBED IN TABLE 9.1. NOTE: N/A FOR POTAMODROMOUS 2019 AS THERE WERE NO ALS WITHIN THE FRESHWATER PART OF THE RIVER DEE IN 2019.....	96

TABLE 8.4: BIOLOGICAL DIFFERENCES BETWEEN SMOLTS IN THE FOUR DIFFERENT MIGRATION GROUPS, 2018 AND 2019 DATA COMBINED.....	97
TABLE 8.5: TABLE SHOWING THE MEAN NUMBER OF DETECTIONS PER SMOLT WITHIN A YEAR AND WITHIN EACH HABITAT	100
TABLE 8.6: TEMPERATURE THE SMOLTS EXPERIENCED DURING THEIR MIGRATION TO MARINE CURTAIN C IN 2018.....	103
TABLE 8.7: SWIMMING DEPTHS (M) RECORDED OF SMOLTS WITHIN EACH HABITAT, USING THELMA BIOTEL TEMPERATURE AND DEPTH TAGS.....	103
TABLE 8.8: THE VARIOUS MIGRATION STRATEGIES EXHIBITED BY THE RIVER DEE ANADROMOUS SEA TROUT SMOLTS	105

3 Project background

This report details the research project funded by Vattenfall's European Offshore Wind Deployment Centre to investigate the spatial distribution of seaward migrating juvenile Atlantic salmon (*Salmo salar*) and Brown trout (*Salmo trutta*) (both salmonids) leaving the Dee and Don Rivers (North East Scotland).

The Scottish Energy Strategy has a vision for a greener future with 50% of Scotland's overall energy consumption coming from renewable sources by 2030 and almost complete decarbonisation by 2050. With the passing of the Climate Change (Emissions Reduction Targets)(Scotland) Act, in September 2019 this target has been brought forward to 2045. Several Offshore wind farms are, as of 2022, commercially producing power and with the latest ScotWind leasing round in January 2022 providing seabed leases for a potential 27.6GW of further offshore wind generation. Additional development is likely to arise through the Innovation and Targeted Oil & Gas (INTOG) leasing round for offshore wind (2023)

Numbers of Atlantic salmon returning to the Rivers Dee and Don have shown strong declines over the past several decades (data collected by Marine Scotland Science since 1952), which have similarly occurred in other North East rivers and throughout Scotland. Numbers of salmon in the North Atlantic have declined by two-thirds in the last 40 years, Scotland's salmon catches were the lowest on record in 2021. The River Don salmon population is assessed under the Conservation Regulations (2016) as having a low probability of meeting its Conservation Limit ([Conservation of wild salmon - Salmon and recreational fisheries - gov.scot \(www.gov.scot\)](https://www.gov.scot/publications/conservation-of-wild-salmon-salmon-and-recreational-fisheries-2016/pages/1-10.aspx)).

Scottish Government launched the [Wild Salmon Strategy](#) (Scottish Government, 2022) and subsequently its [implementation plan](#) (Scottish Government, 2023) where understanding and mitigating pressures in the marine and coastal environment has been highlighted as a priority theme. The Strategy identifies pressures facing Scottish salmon stocks, including from developments in the marine environment. Noise, water quality, turbine strike and electromagnetic field effects, are some of the potential impact mechanisms identified in the Strategy, which may arise from marine renewable developments.

This project has sought to address evidence gaps relating to the migration routes that Atlantic salmon smolts take to get to their feeding grounds, which are thought to be in the Norwegian Sea. It also seeks to add light to the inshore movements of brown trout smolts (more commonly

known as sea trout). Identifying overlap between migration routes and marine development sites is an important step in assessing any impact on these vulnerable populations.

The report is structured so that common methods applicable to both species of work are presented together to avoid repetition, whilst unique information and analysis methods are presented within each specific chapter. Information on salmon and sea trout analysis are presented within separate chapters for ease of dissemination. Analysis of 2018 and 2019 data have been presented previously (Salmon Tracking Interim Reports, February 2019, July 2020).

Within the salmon chapter a 'smolt' should be assumed to be a salmon whilst in the sea trout chapter a 'smolt' should be deemed to be a sea trout

4 General Introduction.

The knowledge of the spatial and temporal distribution of salmonids within the marine environment is a basic requirement to help inform policy, planning and consenting decisions in relation to licenced marine activities and conservation. In January 2022 Crown Estate Scotland announced seabed leases for up to 27.6GW of generating capacity of offshore wind around Scotland. The potential impact mechanisms from marine renewables on salmonids include; underwater noise, predator aggregations, collision with tidal underwater turbines and navigational effects from electromagnetic fields produced by subsea cabling, with the risk of disruption to migration routes, delays to migration, disorientation and vulnerability to predation, which could all impact on salmon survival rates.

As such, there is a need to determine the offshore movements of fish as they enter the open ocean. The potential for interactions between migratory salmonids and offshore renewables was highlighted by Malcolm *et al.* (2010) and Ounsley *et al.* (2019), yet both studies identify a severe lack of information on actual swimming vectors and behaviours of salmonids in the marine environment to enable reliable predictions of the nature and extent of interactions with marine renewables to be estimated.

The use of electronic acoustic transmitters is now regarded an effective technology for identifying movements and migrations of aquatic species in coastal, estuarine and freshwater ecosystems (Cooke *et al.* 2013). The developments and benefits of telemetry have previously been covered extensively (Lucas and Baras, 2000; Hodder *et al.* 2007; Halttunen *et al.* 2009; Cooke and Thorstad, 2011). Acoustic telemetry requires a transmitter, attached to an individual study animal, which transmits information wirelessly to a receiver comprising a hydrophone and usually a data logger where information is recorded and stored. Acoustic tags are uniquely coded allowing individuals to be identified, and are able to determine and send information to the receiver on environmental parameters (e.g. depth and temperature and predation) being experienced by the transmitter implanted in the fish at that exact moment in time. The deployment of hydrophones within a study enables the movement of tags to be derived and thus give an insight to the migration of study fish. This allows the knowledge gaps in behaviour to be investigated.

The broad aim of this project was to use acoustic telemetry to determine the near shore (<20km) spatial distribution and movement of salmon and sea trout emigrating from the Rivers Dee and Don. More specifically, the project aimed to use simultaneous measurements of

salmon smolt dispersal vectors and local currents to estimate actual swimming vectors. These data have then been combined with outputs from the Scottish Shelf Model (SSM), a hydrodynamic model developed by Marine Scotland Science, to provide a general picture of salmon smolt dispersion in the North Sea. Sea trout behaviour was investigated in the same manner. However, dispersal vectors were not compared with the hydrodynamic model. Sea trout are more likely to utilise near shore habitats for feeding rather than migrating further afield.

Due to the Covid-19 pandemic some of these aims have been refined due to Government restrictions on ways of working. All fieldwork was suspended in 2020, and this had knock on effects into 2021 with the reduction in tag battery life and ongoing Government restrictions playing a role in the cessation of all tagging work on the river Ythan and the change in capture location on the river Dee. These changes impacted some of the overall aims of the project, and significantly impacted the sea trout work, with fish only being tagged on the Dee. This should however be seen in the context of four successful years of tagging and tracking work over a large geographic area.

5 Aims of this Study

5.1 Salmon Smolts

- a) What is the predicted spatial distribution of salmon smolts from the Rivers Dee, Don and Ythan upon leaving their rivers?
- b) How does the distribution of smolts vary depending on variation in smolt size (and hence swimming speed), weather and date of sea entry?
- c) Is there evidence of narrow or wide dispersal of smolts from each river? This question is important for establishing whether a marine or coastal development might be encountered by a large or small proportion of the fish from a given river.

5.2 Brown Trout Smolts (Sea Trout)

- a) What is the predicted spatial distribution of sea trout smolts from the Rivers Dee, Don and Ythan

6 General Methods

6.1 Study Location

The River Dee in Aberdeenshire, Scotland, rises in the Cairngorms and flows eastwards through Aberdeenshire before discharging into the North Sea via Aberdeen Harbour (NGR: NJ 95690 05589) some 140 km from its source. The North Sea east of Aberdeen Harbour steadily increases in depth to about 60m, four kilometres from shore and is predominantly a sandy substrate. Immediately east of the harbour breakwaters, it offers migrating smolts 180 degrees of open sea from North to South with an easterly aspect (Figure 6.1). The River Dee supports a high quality Atlantic salmon population, which is an interest feature of the River Dee Special Area of Conservation (SAC). SAC are a network of European sites protected under the Conservation (Natural Habitats &c.) Regulations 1994 (as amended) in Scotland commonly referred to as the Habitats Directive. The Dee also supports an internationally renowned rod fishery (catch and release only).

The River Don also, rises in the Cairngorms and flows eastwards through Aberdeenshire discharging into the North Sea at the Bridge of Don, approximately 4km north of Aberdeen Harbour. The Don has a natural estuary which is relatively un-impacted by anthropogenic development compared to the estuary of the Dee. The River Don itself is highly modified with several weirs along its course. The Don has a salmon population but is renowned for its trout population, which supports rod fisheries (now catch and release only).

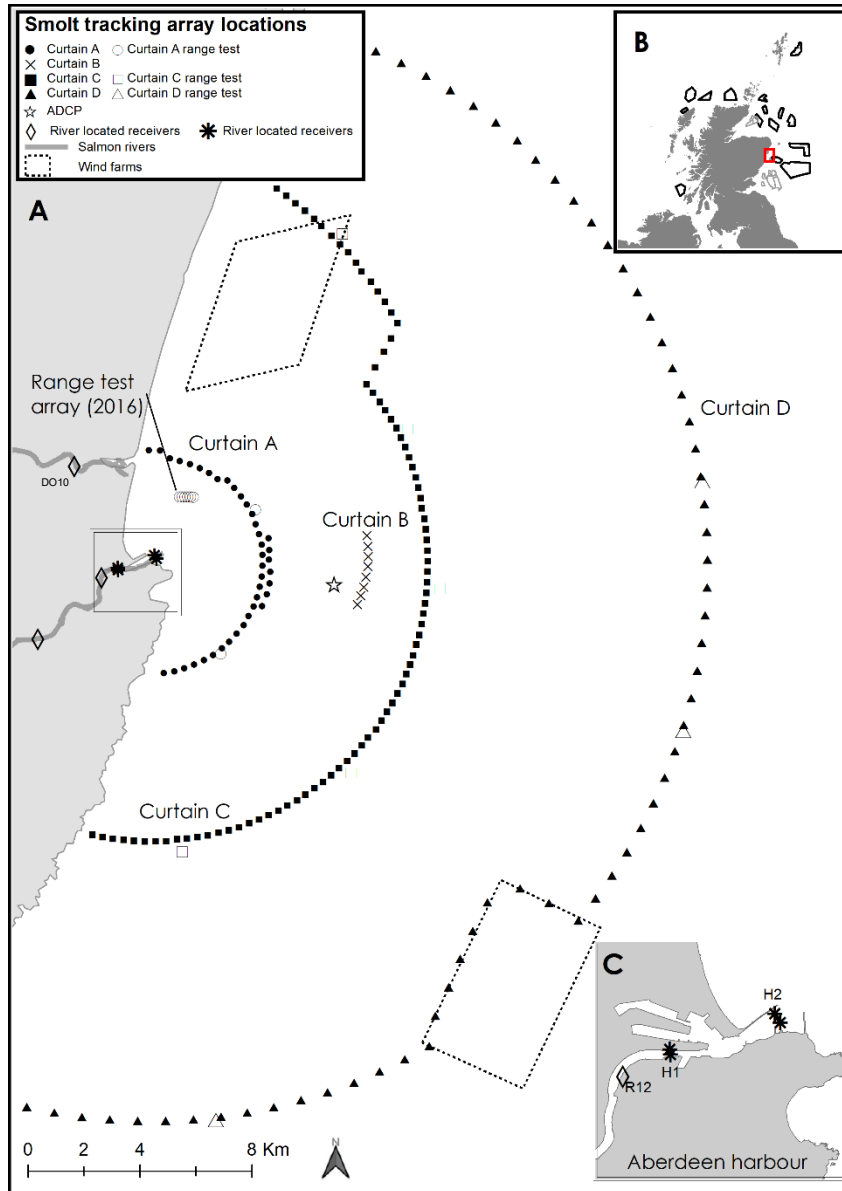


Figure 6.1: Aberdeen Bay Smolt Tracking Array showing the location of Automatic Listening Stations (ALS) in Curtains A (black circles, 2017, 2018 and 2019), B (black crosses, 2018) C (black squares, 2018) and D (black triangles, 2019 and 2021). In each Curtain range test tags are marked with a hollow symbol matching the curtain symbol. The 2016 range test layout is also shown as hollow symbols. River ALSs (black hollow diamonds) and harbour ALS (black stars) are also shown. Inset B highlights the study area within the context of Scotland including built (outlined in grey) and planned (outlined in Black) windfarm locations. .

6.2 Fish Tagging

Fish were tagged in April and May of each year with numbers tagged generally reflecting the numbers of fish migrating through the system as a whole. The number of fish trapped on any day are a subset of the total number of fish migrating at any time, Fish greater than 135mm were selected for tagging.

Smolts were captured by both Rotary Screw Traps (RSTs) and fyke nets (FNs) which were checked daily (between 9am - 2pm); captured smolts were processed and released on the same day. Smolts greater than 135 mm fork length (Thelma Biotel and Vemco V7 tags) and greater than 140mm fork length (Vemco V7P tags) were anaesthetised by immersion in five litres of solution containing tricaine methanesulfonate (MS-222, 0.08 mg l⁻¹). Anaesthetised smolts were measured for length (fork length - L_f , mm) and mass (M, g) prior to tagging.

Once measured and weighed, fish were placed on a surgical platform consisting of a foam board with a v-shaped groove which had been pre-soaked in river water. All equipment was sterilised, using 70% ethanol, between each fish and care was taken, as far as possible in a field location, to ensure aseptic conditions. An incision between 10-12 mm was made using a single use scalpel in the ventral surface of the smolt, anterior to the pelvic girdle. Tags were activated following the manufacturer's instructions, and tested prior to sterilisation in a bath of 70% ethanol or Videne Antiseptic Solution (for predation tags). The activated tag was then rinsed in sterile saline solution, inserted into the peritoneal cavity, and the incision closed with two interrupted sutures (Vicryl 4-0 violet, Ethicon, Johnson & Johnson Medical N.V., Belgium) secured with surgeon knots. Fish were aspirated with a 0.04 mg l⁻¹ MS-222 solution throughout the procedure. Fish tagging was carried out under Home Office Licence (numbers 60/4411 (2017) and 70/8928 (2018), PD2D1240E (2019 and 2021)).

After the tag was implanted, smolts were placed into a bucket with fresh river water, which was aerated using a battery-operated air pump and observed until they regained their swimming equilibrium and exhibited a fluid and consistent operculum (breathing) movement. The smolts were then transferred to a holding pen within the river providing a flow of water in a protected environment. The smolts remained within the pen for a minimum of two hours before being released 100 metres downstream of the capture location, with other smolts (untagged) which were trapped at the same time.

6.3 Range testing

The detection of a tagged fish will only occur if the hydrophone is able to hear the tag within the surrounding background noise. Thus, depending on spatial and temporal variability in the acoustic scape, the ability of an individual automatic listening station (ALS) to detect an individual tag varies considerably. The rate at which an ALS detects a tag is known as its detection efficiency. Should detection efficiency be low, confidence in the output of results is reduced as there is potential that the study fails to detect a large proportion of tagged fish present. If detection efficiency is high the results should be considered robust and strong evidence of the true presence of the tagged population. Within the study a variety of methods were employed to determine detection efficiency.

6.3.1 *Pre study*

Prior to the study, a five-day tag detection range test was carried out in Aberdeen Bay in November 2016 to estimate the optimal spacing of ALSs for the study. Six ALSs were deployed (comprising an underwater hydrophone (Innovasea model: VR2AR), rope canister and weights) in a transect approximately 300 metres long with receivers spaced roughly 60 metres apart. Attached to two ALS at either end of the transect were range test Thelma Biotel ART-LP-7,3 tags which were representative of the size and power output of tags to be used in the study. These tags were moored approximately 12m below the water surface. A shallower mooring may have been more representative of a swimming smolt. However, navigation concerns of high shipping levels prevented shallower deployment. The weather during this period ranged from flat calm, Beaufort Force 1 to rough seas at Beaufort Force 7-8. This gave a wide range of conditions over which detection probability was assessed. Data were pooled into hourly windows to determine the detection efficiency by dividing the number of detected pings from an individual tag by the number of expected pings (determined by the pre-defined ping rate of the tag).

Data from range tests indicated that tags were detected by receivers 300m away at approximately 40% efficiency (i.e. for every 100 tag transmissions 40 were detected) but with considerable variation (Figure 6.2). Efficiency increased as distance between tag and receiver decreased and at 190m between tag and receiver detection efficiency was on average 77%. Subsequently, it was determined that receivers should be placed 380m apart (i.e. a maximum distance of 190m between a passing tagged fish and the nearest receiver) to maximise the distance covered by the ALS curtain but also retain high detection efficiencies.

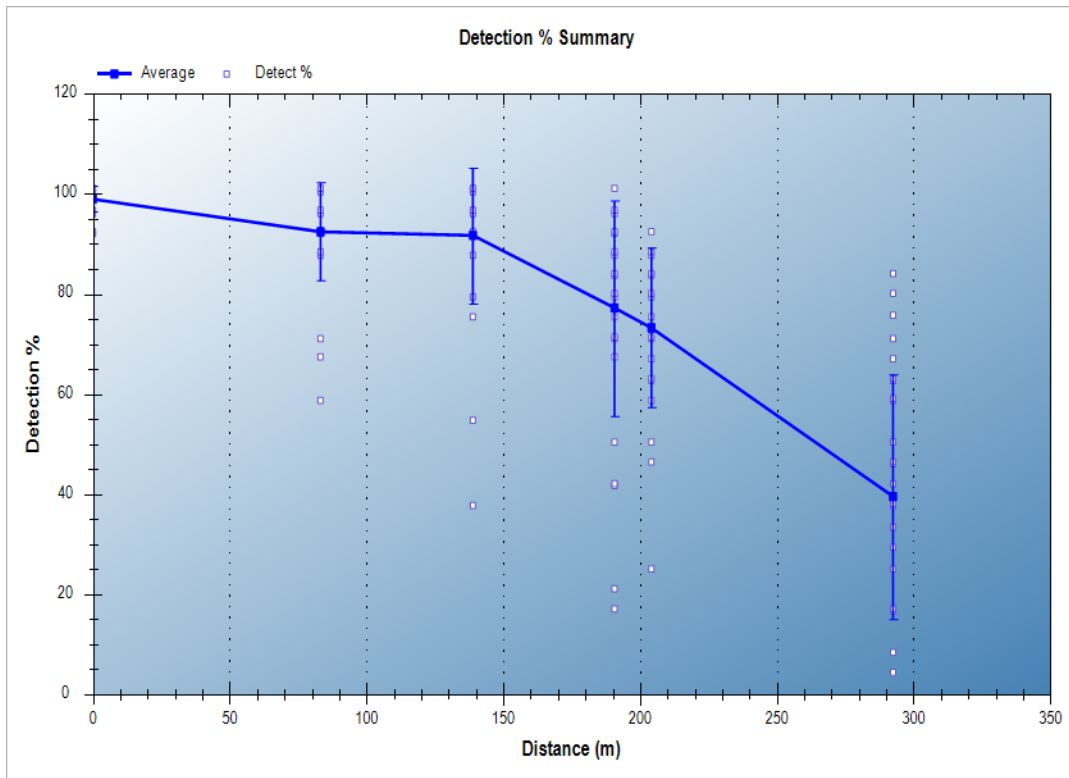


Figure 6.2 Results from a 5 day range test in in Aberdeen Bay during 2016 showing the percentage of tag signals detected by the Automatic Listening Station (ALS) across a range of distances. The solid blue squares are the average detection percentage at each ALS location; blue vertical bars indicate 95% confidence intervals and white squares are outliers.

6.3.2 Within the Study

Several methods of range testing were used during the study. Corrections from missed detections were made where transmitters were detected on subsequent downstream receivers in the river, gates in the harbour or curtains in the marine environment, that had not been previously detected at an upstream ALS. This is not possible at the outermost curtains where subsequent seaward ALS do not exist.

During each study year range test tags were attached to ALS deployed slightly offset (<300m) from each marine curtain (Curtain A, C and D). These tags reflected the same manufacturer of tags and power output to be used in fish within that year. All range test tags were moored approximately 12m from the water surface to best represent the expected smolt swimming depth whilst also avoiding shipping collisions.

These data were analysed to estimate detection efficiencies across the curtain of interest. In addition, data from these range test tags were used to model the likelihood of a smolt migrating

through a receiver curtain undetected. Simulations were based on the model proposed by Hayden *et al.* (2016).

In this simulation, virtual fish are “swum” at a curtain of ALS, a simulated signal from a tag is transmitted, either at a fixed delay of 30 s during simulations for 2017 or a random delay between 50-100 s for simulations in 2018. The virtual fish were given a random speed within the inter quartile range of recorded fish speeds (within the study) and passed at varying distances from receivers and the distance between transmission location and each receiver is calculated. A detection range curve is then used to calculate the probability (p) that the signal was detected on each receiver. Detection or non-detection at each receiver is determined by drawing from a Bernoulli distribution with a probability of p . Detection range curves were generated from range test tags positioned within the curtain of interest and probabilities of detection were calculated for 3 hour periods during the time fish were actively migrating over the ALS curtain. The simulation was repeated 10,000 times to estimate the mean probability of detecting a fish crossing the array.

Probabilities of detecting single transmissions from tags are not the same as an actual fish detection. Despite high probabilities of detection, or good detection efficiency estimates, it is still possible for fish to pass an ALS undetected. Indeed the soundscape at a specific location at any time can be significantly affected by localised conditions, for example ships passing overhead, which would reduce detection efficiency considerably for a short period of time.

6.4 Receiver Locations

Fish passage down river and out to sea was monitored remotely using moored Acoustic Listening Stations (ALSs). Three types of Vemco receivers were used in this project (VR2W, VR2AR and VR2Tx). The overall array arrangement of ALSs in this project consisted of single ALSs in strategic positions in the river, pairs of ALSs in the harbour forming gates, arcs of ALSs in the marine forming larger curtains, and in 2021 a grid of ALS (Figure 6.1 and Figure 6.3) as described below.

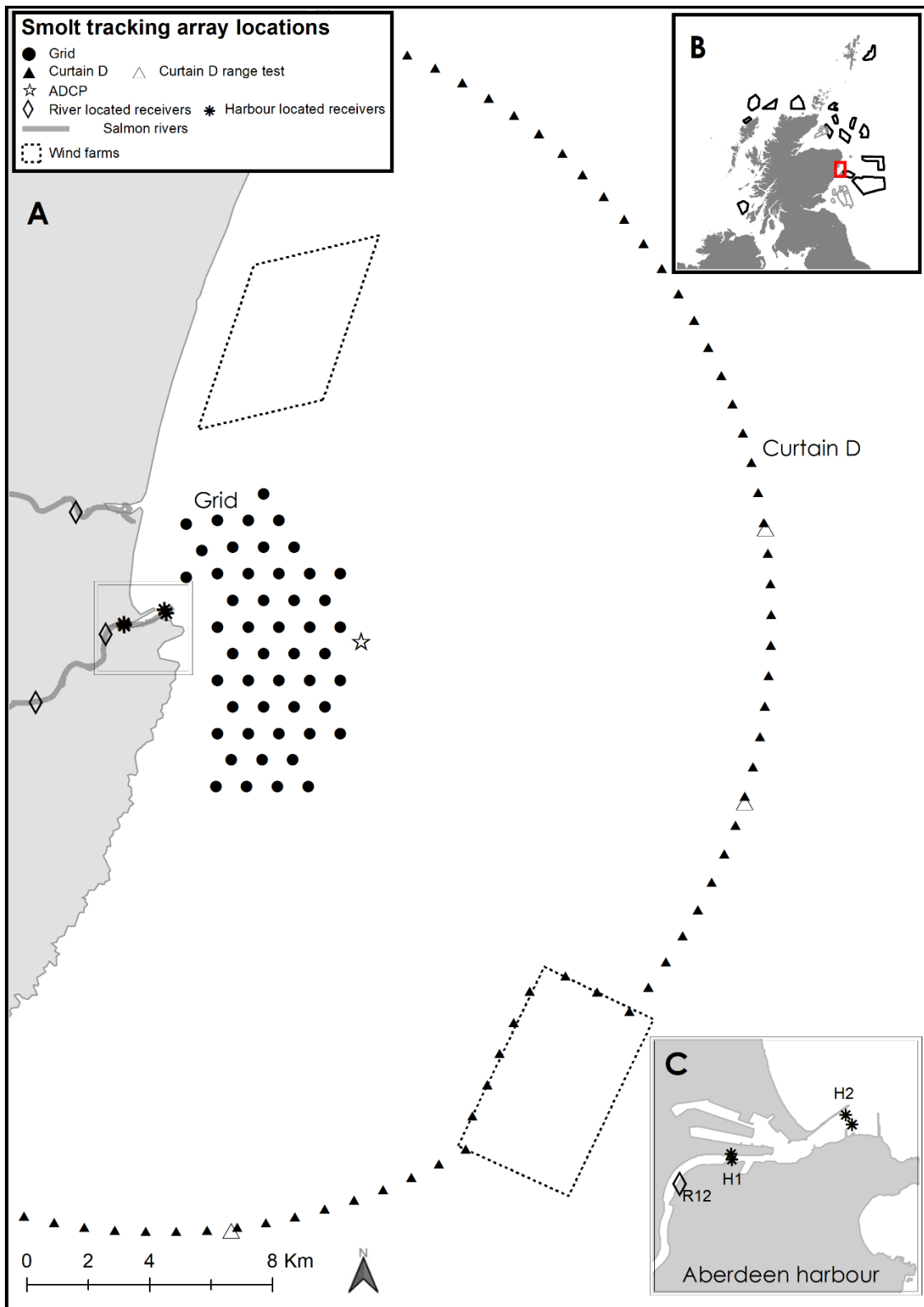


Figure 6.3: ALS Grid (black circles) and curtain D (black triangles) placements in 2021, range test tags in Curtain D are marked (hollow triangle). River ALSs (black hollow diamonds) and harbour ALS (black stars) are also shown. Acoustic Doppler Current Profiler (ADCP) is also shown (Black hollow star). Inset B shows the study site in the context of Scotland including built (outlined in grey) and planned (outlined in Black) windfarm locations..

Within the River Dee an acoustic receiver (ALS R12) (Figure 6.1: inset C) was placed in the lower river at the same location each year. Within Aberdeen Harbour, two gates (H1 and H2) were created by positioning two ALSs opposite each other to create complete overlap in detection zones.

Within the marine environment, arcs of ALSs were placed to the east of the Harbour mouth. In 2017, 2018 and 2019 an arc of ALS was deployed approximately 4km from the Harbour mouth and is referred to as curtain A (Figure 6.1). ALS were spaced at 380m and two range test tags also deployed just beyond the curtain (Figure 6.1). In 2018 an additional 96 ALSs were deployed in an arc forming the marine curtain C, 10 km from the mouth of Aberdeen Harbour, again with a 380 m spacing, along with a further 5 range test ALS stations just beyond the curtain (Figure 6.1). The second curtain dog-legged to avoid construction activities at the EOWDC in Aberdeen Bay. In 2019 and 2021, curtain C was moved further offshore, 20km from the harbour mouth and consisted of 64 ALS spaced at approximately 1 km intervals and formed curtain D which doglegged to avoid the Kincardine Offshore Windfarm. In addition, in 2021, 47 ALS were deployed in a grid formation approximately 5km from the harbour mouth (discussed in further detail in section 7.4.5)

7 Salmon

7.1 Introduction

The numbers of adult Atlantic salmon (*Salmo salar* .L) returning to spawn in fresh water are declining, primarily as a result of poor survival at sea (Chaput *et al.* 2012; ICES 2019). After 1-3 years in the river, salmon migrate from nursery grounds in fresh water to feed at sea for a year or more in Norwegian or Greenlandic waters. The migrants face a broad range of challenges on this journey which, to be successful, juvenile salmon need to adapt to cross osmotic boundaries, identify new prey items, and evade novel predators (Hoar, 1988; Rikardsen and Dempson, 2011). They also have to face multiple anthropogenically-induced stressors including those from Atlantic salmon farming, pollution, fisheries, offshore renewable and other coastal developments and activities (Thorstad *et al.* 2012, ICES 2020, Scottish Government, 2022). The early stages of marine migration, where juvenile salmon are faced with physical and physiological challenges, are therefore a critical phase of the life cycle of Atlantic salmon (Thorstad *et al.* 2012), yet there is limited information on the movement and behaviour of juvenile salmon at this crucial stage (McIlvenny *et al.* 2021, Ounsley *et al.* 2019, Strøm *et al.* 2018).

Scotland's wind energy sector is increasing in size and distribution as demand for clean local wind energy increases. In 2022, lease options were awarded for 17 new offshore renewable projects covering an area of over 7000km² of Scottish waters. The impacts of offshore renewable energy developments on migratory fish are uncertain and could include physical, acoustic, and electromagnetic effects (Gill *et al.* 2012, Harding *et al.* 2016). The likelihood of impact will depend on the interaction between the distribution and behaviour of fish within and around the offshore development and the effect of each technology on individual fish (Malcolm *et al.* 2010), and the resilience of the populations.

Particle tracking simulations have been used as a predictive tool to understand potential migration strategies of animals at sea (Byron and Burke, 2014; Ounsley *et al.* 2019). Behavioural components may be introduced within individual based models (IBM) in combination with hydrodynamic models to simulate migratory behaviour. A number of authors have used such methods to investigate the potential migration routes of Atlantic salmon populations (Booker *et al.* 2008; Mork *et al.* 2012; Byron *et al.* 2014; Moriarty *et al.* 2016). Recently, Ounsley *et al.* (2019) simulated migration routes from multiple locations around the Scottish coast with the results suggesting that salmon cannot rely on current-following behaviours to reach their feeding grounds in the North Atlantic. Indeed, the authors suggest

that particles from the East coast of Scotland generally had a better success rate when swimming in a north or northeast trajectory.

Simulations require ground truthing with actual migratory data collected from real individuals, which until relatively recently has not been achievable. However, with the advancement of acoustic technology it is now possible to track wild emigrating smolts in excess of 250km from their natal river (Barry *et al.* 2020; Green *et al.* 2022). Newton *et al.* (2021) combined IBM particle tracking models with real time telemetry to determine that fish emigrating from the Cromarty firth (north east Scotland) were swimming at approximately 70° from North in an easterly bearing, but not following the marine currents.

The strategic deployment of acoustic receivers and tracking studies has been identified as one of the next steps required to make advances in the knowledge of the marine migration of Atlantic salmon (Ounsley *et al.*, 2019). The combination of real-time telemetry data with IBM particle tracking models is essential in determining the marine migrations of emigrating Atlantic salmon. The tracking of fish further into the marine environment, and from multiple locations, is a necessary requirement to improve the ability of these models to determine fish migrations in the marine environment.

Here we present a study using simultaneous measurements of salmon smolt dispersal vectors and local currents to estimate actual swimming vectors. These data are then combined with outputs from the Scottish Shelf Model (SSM), a hydrodynamic model developed by Marine Scotland Science to provide a general picture of smolt dispersal at both the near field and far field level. With the incorporation of the observed movements of acoustically-tagged smolts into this hydrodynamic model, this work aims to address; 1) The predicted spatial and temporal distribution of salmon smolts emigrating from the Rivers Dee and Don;. 2) Whether the distribution of smolts varies depending on variation in smolt size (and hence swimming speed), weather and date of sea entry, 3) If there is evidence of narrow or wide dispersal of smolts from each river.

7.2 Methods

7.2.1 *Tag Specification*

Numbers of tags available varied between years and across rivers. To minimise risk of failing to capture fish of suitable size the initial focus of tagging was within the Dee at locations where good numbers of smolts had been captured previously. In later years, fish from the Don were also included. However, more fish, in general, were tagged on the Dee. Logistical constraints determined where and the number of fish to be tagged in any year. In total 247 Dee and 150 Don salmon smolts were tagged between 2017 and 2021.

In 2017, 60 Thelma Biotel (www.Thelmabiotel.com) tags were used within the River Dee. Fifteen of these tags (tag type: ADTT-LP-7) transmitted temperature and depth along with associated unique IDs. A further 45 tags transmitted only ID (tag type: ATID-LP-7,3). All tags had a fixed delay of 30 seconds between code transmissions.

In 2018, 100 Vemco (www.Innovasea.com) tags were used to tag salmon in the River Dee. Thirty of these tags were capable of transmitting depth and temperature (V7TP-2L-069k-1). The remaining 70 were ID only tags (V7-2L-069k-1). These tags were set to transmit with a random delay between 50 and 100 seconds to reduce the risk of multiple tags persistently transmitting at the same time.

In 2019, 124 Vemco tags were used to tag salmon. Fifty smolts in the Dee were tagged with ID tags (V7-2L-069k-1). A further 24 smolts were tagged with predator tags (V7D-2x-069k-1) which transmit both ID and a unique signal when a predation event occurs, this is activated by the dissolving of a biopolymer switch in a predators stomach. In the Don, 50 salmon smolts were tagged with ID tags (V7-2L-069k-1).

In 2021, 88 Vemco tags were used to tag salmon. Eight salmon smolts were tagged with ID tags (V7-2L-069k-1) in the Dee and a further five fish with predator tags (V7D-2x-069k-1). In the Don, 50 salmon smolts were tagged with predator tags (V7D-2x-069k-1), and a further 25 salmon smolts with ID tags (V7-2L-069k-1). The low numbers seen in the Dee resulted from a new and more challenging single tagging location which failed to produce smolts in the size range and quantity required for tagging.

7.2.2 Fish migration behaviour

Fish migration behaviour was inferred from the pattern of detections of tags at, and between, the fixed position ALSs. Migration in salmon smolts is primarily a downstream movement and therefore can be measured by the progression of detections on ALSs towards the sea.

Fish were classed as starting a migration upon first tag detection on a river ALS (this was calculated regardless of what river receiver a tag was detected on, i.e. if a tag was detected at the bottom of the river it was assumed to have been missed on the previous upstream receivers). Across all years, successful marine migrations were defined as tags passing out of the river and over curtain A,. Fish missed on curtain A but detected on the curtain C were also classed as successful marine migrants..

Tags that were detected on an ALS and subsequently failed to appear at any other ALS, gate or curtain were assumed lost to the study and therefore unsuccessful in their migration in either the river or marine environment depending on where loss occurred. There are many factors which could contribute to this loss including tag failure, tag ejection, noise, predation or other causes of mortality. However in most cases, the fate of lost tags cannot be determined. Some detection of tags may not present the 'typical behaviour' of a smolt (continuous downstream movement) and these were individually investigated to assess whether the tag remained within the original study animal. This involved looking at the specific behaviour of a tag to see if it progressed back up the river or increases in temperature or unusual tag depths (continued depths below 10m for example) out with the usual patterns seen in the study.

The movement of tags between ALSs can be broken down into two parts: residency events and movement events. *Residency events*, in this study, are defined as two consecutive detections on the same ALS or gate, within one hour of each other. *Movement events* are defined as periods between residency events when fish are detected on different ALSs or gates. These two event types were calculated using the Vtrack package in R. In addition specific migration behaviours were used to describe the migration of smolts, these are detailed below:

Ground Speed ($m.s^{-1}$) was calculated as the time difference between last detection at gate H2 to the first detection on an individual ALS within curtain A, divided by the straight-line distance from the midpoint of H2 gate to that individual ALS. This gives the minimum Ground Speed,

as fish may not have taken a direct route from one point of detection to the next point of detection.

Harbour Transit Time (HTT, Hours) was calculated as time difference in hours between the last detection on the lower river receiver (ASL R12) to the last detection on the most outward harbour gate (H2). This area comprises of 500m of lower river which is tidal and experiences fluctuations in salinity depending on tidal cycle and freshwater inputs from upstream, and 1.8km of Aberdeen harbour (Figure 6.1).

Direction of Tag Travel (Degree) was calculated as the straight line bearing from the midpoint of gate H2 to the location of first detection on an ALS within Curtain A. If fish were subsequently detected on the curtain C a *direction of tag travel* was also calculated between the location of the last detection on curtain A and the first detection on curtain C or curtain D.

7.2.3 Marine Directionality

To determine accurate estimates of actual fish swimming behaviour, data derived from Acoustic Doppler Current Profiler (ADCP) measurements were used to estimate the effect of marine currents on fish.

The ADCP was deployed in the same location in 2018 and 2021 (Figure 6.1). It was programmed to record current speed and direction in various depth bins over the smolt migration period. The water column was divided into five separate bins 0-6 m, 6.01-12 m, 12.01-20 m, 20.01-40 m and 40.01-60 m deep. The upper bin (0-6 m) also provides a rough metric of sea surface state as the data become noisier and incomplete as the sea surface become disturbed by worsening weather and increasing wave heights.

To predict tidal currents and elevations during 2017 and 2019, the data collected using the ADCP in 2018 were analysed using the T_Tide toolbox in Matlab (Pawlowicz *et al.* 2002). The same toolbox was used to predict eastward and northward velocities (u and v components of velocity) and water elevation, using only constituents with a signal-to-noise ratio greater than one, to ensure good quality of predictions. The analysis and modelling of hydrographic data were carried out by the Oceanography section in Marine Scotland Science in Aberdeen. This prediction is also based on the bottom bins (40-60 m) of ADCP data, which removes the elements of interference from surface wind and other non-tidal factors. This allowed a comparison of current influence on individual fish in 2017, 2018, 2019 and 2021. Although

they are the most accurate information available, these data lack the individual weather and other factors that may play a part in the surface water movements.

Data from the ADCP were used to extract the u (velocity) and v (velocity) components of the current which could be subtracted from the Ground Speed and *direction of tag travel* to determine *Actual Fish Swimming Speeds* and *Actual fish Headings* with the effect of the current being removed.

7.3 Particle Tracking

Particle tracking simulations were performed modelling the trajectories of smolts originating from the River Dee in April-May 2018 and 2019. Different smolt behaviours were simulated and the resulting trajectories compared, enabling different hypothesis to be tested. Two sets of simulations were performed. The first set were 2 month simulations with particles (simulating individual smolts) released from Aberdeen harbour at the exact times that individual smolts were last detected by the harbour entrance receivers. This first set of results were designed to investigate the near field behaviour of smolts and the results were compared with the 2018 and 2019 smolt tag data from Aberdeen Bay. The second set of simulations were nine month simulations starting in April 2018 with particles (simulating smolts) released from a near shore location in Aberdeen bay every 12 hours during April and May, designed to investigate the far field migration of smolts.

7.3.1 *Hydrodynamic model description and validation*

The underlying flow fields used for the particle tracking were data from the Scottish Shelf Waters Reanalysis Service (SSW-RS, <https://tinyurl.com/SSW-Reanalysis>), a 27 year reanalysis of the Scottish Shelf Model (SSM) for 1993-2019. The SSM is an implementation of the Finite Volume Community Ocean Model (FVCOM, Chen *et al.* 2003), a hydrodynamic model with an unstructured grid resolving the Scottish coastline at around 500-1000 m resolution. The SSW-RS uses a hybrid vertical sigma layer scheme. In water depths > 37 m, the model has 2 fixed surface (and 2 fixed bottom) layers each 1.5 m in thickness, and 16 intermediate terrain following layers of equal thickness. In shallower regions (< 37 m) the model has 20 terrain following sigma layers.

Data from the ADCP was compared to modelled sea surface height, and near surface velocity from the SSW-RS reanalysis for 15 days in May 2018 (Figure 7.1). The sea surface height compare well with the tide in-phase and elevations closely matching. The tidal range is around

1.5 m at neap tides and 3.5 m at spring tides. Similarly, the velocity compares well, particularly the dominant north-south component, with the semi-diurnal tidal phase and spring neap cycle well reproduced. The peak current speeds are around 0.4 and 1 m/s during neap and spring tides, respectively. Figure 7.2 is a comparison of the near surface flow between the ADCP and SSW-RS, showing the tidal ellipses. The SSW-RS has a little more scatter, but the amplitude and tidal direction are well reproduced, with the tide running dominantly in a north north east – south south west direction. The flood tide is in the south south west direction.

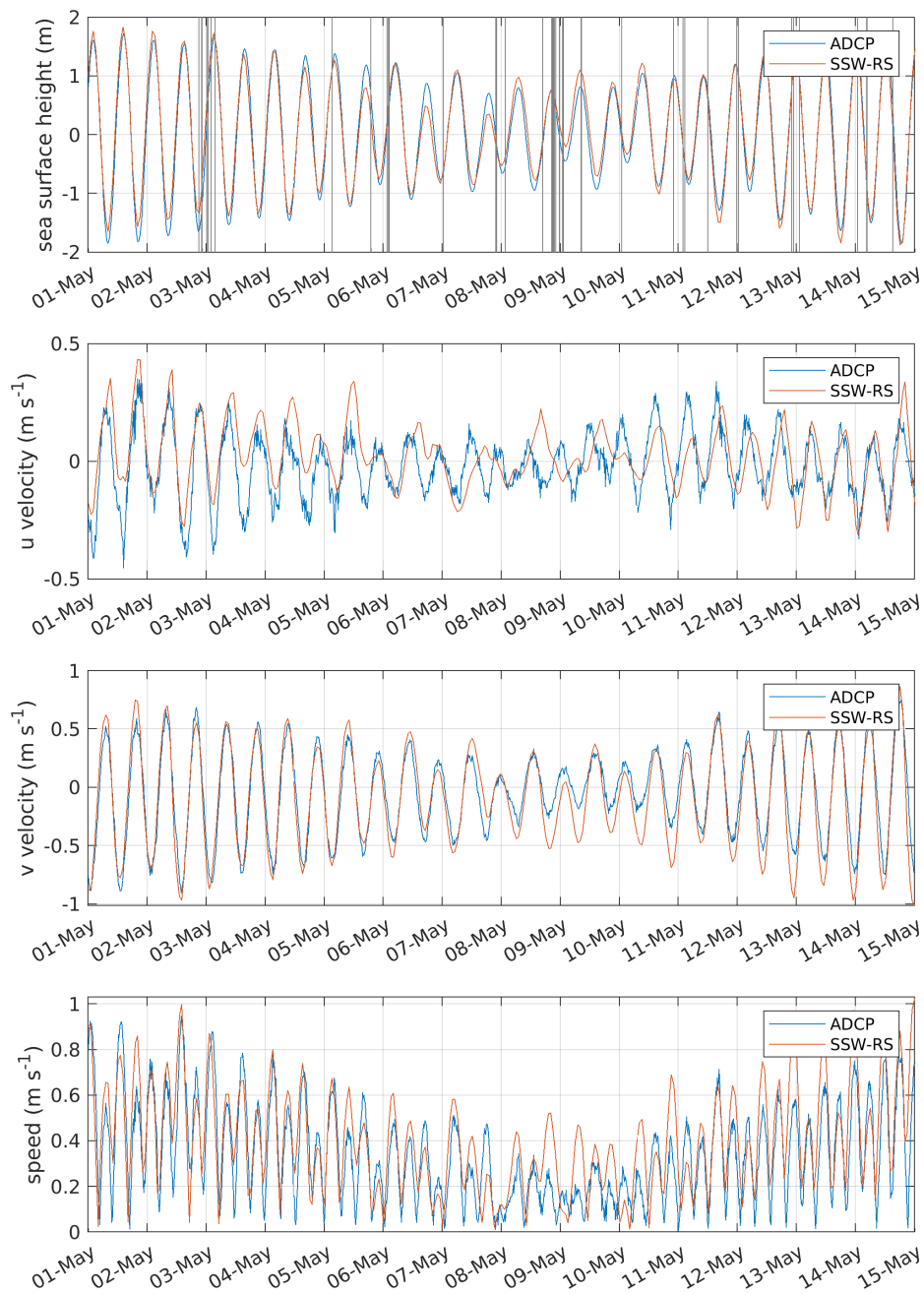


Figure 7.1: Comparison of ADCP and modelled time series of sea surface height, and surface velocities for a 15 day period in May 2018. The particle release times are indicated by the dark vertical grey lines in the sea surface height sub-figure.

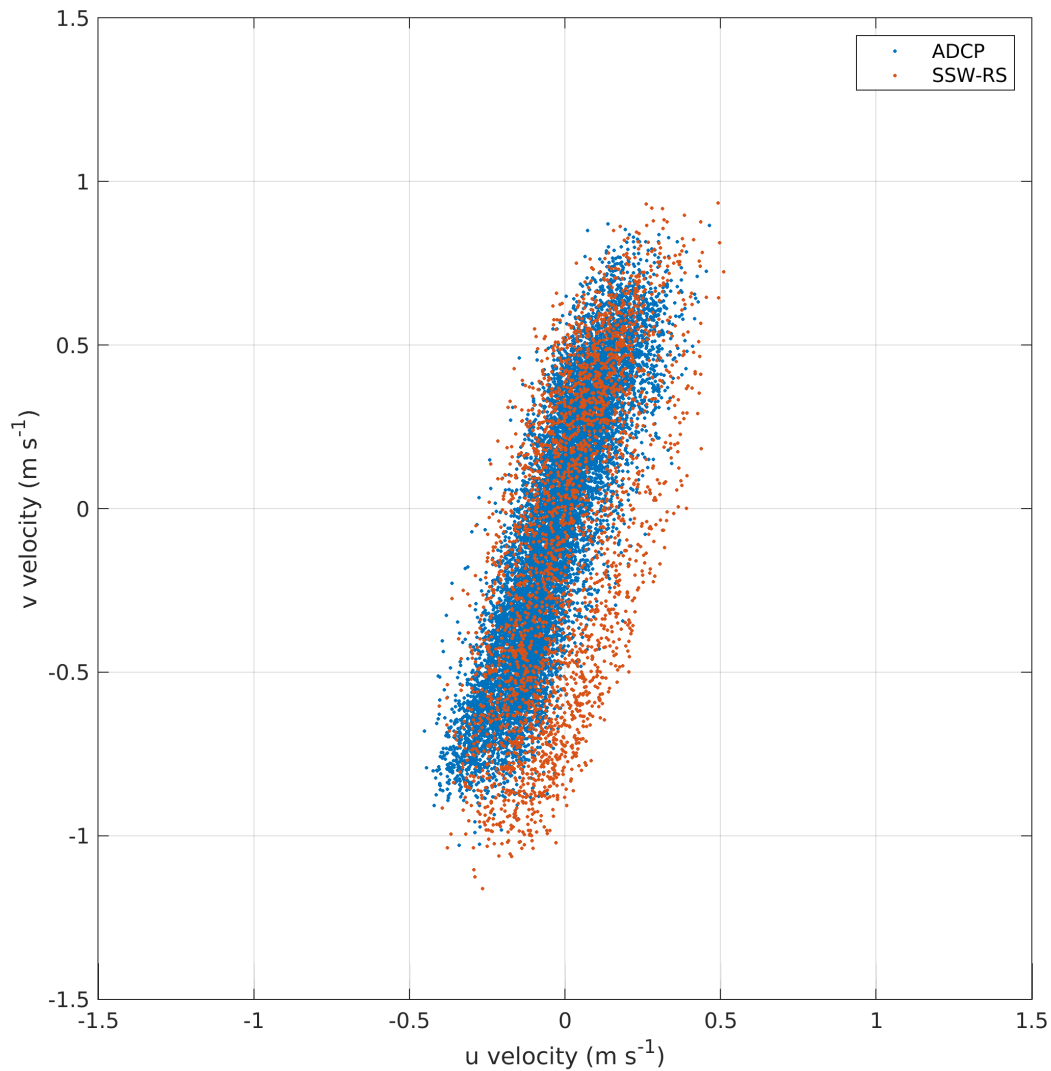


Figure 7.2: Comparison of tidal ellipse from ADCP and SSW-RS for May-Aug 2018.

All the particle tracking simulations forced particles to remain at 2 m depth, which used flow data from the second sigma layer in depths > 37 m, and flow data from deeper sigma layers in shallower regions. The FVCOM i-state configuration model (FISCM, <https://github.com/GeoffCowles/fiscm>) particle tracking software (Liu *et al.* 2015), and smolt behaviours implemented by Ounsley *et al.* (2019), were used. No stochastic horizontal variability (e.g. diffusion) was included in the simulations and variability was introduced by spreading the release of particles in time and space. The first simulations used passive particles, where the particles had no behaviour other than being forced to stay at 2 m depth. Negative rheotaxis behaviour was then implemented, where the particles are forced to swim with the current at all times, and a constant bearing behaviour where the particles were forced

to swim with a certain trajectory at all times. Two constant bearing simulations were run, with a north and northeast bearing each with a 20° variance about the central bearing. We also tested a *variable rheotaxis* behaviour, where the particles were forced to swim with the current only when the current has an easterly component to it (i.e. only when the east-west velocity component was positive). Following the approach of Ounsley *et al.* (2019) a smolt exponential growth model (Mork *et al.* 2012) was used for all the model runs, and the effect of smolt swim speed (as a function of smolt body length) was explored with swim speeds varying between 1.5 to 4.5 body lengths per second. The particle tracking simulations received hourly flow data from the SSW-RS and had a particle tracking time step of 10 minutes.

7.3.2 Near-field simulations

These 2 month long simulations were designed to investigate the near-field movement of particles in the vicinity of the acoustic arrays deployed in Aberdeen bay. For this reason the results were saved every 10 minutes. The acoustic tag data were examined to determine when tags were detected by the receivers close to the harbour mouth. In total 51 and 33 unique tags were detected by these harbour mouth receivers in 2018 and 2019, respectively. The last detection of the tags on the H2 gate at the exit of Aberdeen Harbour was taken as a release time of a single particle, and the 2018 release times are indicated in Figure 7.1 by the vertical grey lines. Thus, each particle represented an individual tag departing the harbour. The initial smolt length was larger than that used for the far-field simulations, 0.14 m, as this better represented the smolts that were tagged in the Dee.

The arrival time and location of each particle/smolt on each array of receivers were determined as follows. A circular buffer was created around each receiver location and the times that particles entered each buffer determined. A number of buffer radii were tested, ensuring there were no gaps between adjacent buffers and between the buffers closest to the coast and the model coastline. It was found that with the higher swim speeds (typically > 2.5 bl s⁻¹) and smaller buffer sizes (250 m) a small number (<10) particles were not detected by the inner array. This was because the particles moved through the buffers in less than the model time step (10 minutes). A minimum buffer radius of 350 m was therefore chosen. This was more than adequate for both the inner and outer 2018 arrays, but the outer 2019 array was more widely spaced and, to ensure no gaps were available for a particle to pass undetected, a 800 m buffer radius was used for all but 4 of the outer array receiver locations. The remaining four (two of which were the receivers closest to the coast) had buffer radii of 1000 m.

The times that the particles resided in each buffer region on each array (inner and outer) was recorded, along with the receivers they coincided with. The first detection location for each particle was recorded, as was the total number of detections at each receiver location. These were then used to create maps showing where on the arrays the first detections were, the number of first detections, and total number of detections at each receiver location. The acoustic tag data were then examined and the first time and location each tagged smolt was detected on each array was recorded, to give equivalent first detection data. The total number of tagged smolt detections at each receiver on the two arrays was recorded to give an equivalent to the total number of particle detections at each receiver location. These two methods, examining the particle tracking and tag data, were designed to be as similar as possible in order to compare the results.

7.3.3 Far-field simulations

These simulations were designed to investigate the far-field migration of smolts, similar to the work of Ounsley *et al.* (2019). The simulations ran for 9 months from start April – end December 2018 and 2019. Only the 2018 results are discussed here, as the 2019 results did not differ significantly and were only run to examine annual variation in the flow fields. The initial smolt length was set to 0.125 m, as was used by Ounsley *et al.* (2019) and is a better representation of the length of the whole population rather than the tagged population where larger individuals (>135mm) are selected. Particles were continuously released over a two month period, with 5 particles released from 5 locations 100 m apart on a north-south line close to the river Aberdeen harbour entrance, every 12 hours. 600 particles were released during each simulation. The dominant semi-diurnal tidal period (M2) is about 12.4 hours, so over the 2 month period particles were released at a range of tidal conditions through a semi-diurnal and spring-neap cycles. The 100 m separation between particles further ensured that the released particles encountered a range of flow velocities at release time, contributing to the ultimate variability of the simulations given that they do not include stochastic variability. Five sets of simulations were performed, each with different behaviours: passive, negative rheotaxis, variable rheotaxis, constant bearing to the north (000°) and constant bearing to the north east (045°). For each behaviour, other than passive, three simulations were performed with differing swim speeds – 1.5, 2.5 and 3.5 body lengths per second.

7.3.4 Data analyses

Movement data were tested for normality using a Shapiro-Wilk test. Depending on whether the data were normally distributed or not, the difference between years and between marine curtains in 2018 was tested with a t-test or a Wilcoxon Test. A Watson's two-sample Test of Homogeneity was used for bearings in circular data.

7.4 Results

In 2017, 60 salmon smolts were caught at three different sites on the River Dee (Dinnet Burn n= 46, Beltie Burn n= 10 and the Sheeoch Burn n= 4) and tags implanted. Of these 60 fish tagged, 22 tags, (representing 36% of tags), were subsequently not detected on any ALS. Thirty-three tags (55%) were detected at the lower river (R12; Figure 7.3) prior to entering the harbour and all 33 were detected leaving the last set of harbour ALSs (H2). Twenty-six tags (43%) were detected at curtain A (4 km from the harbour mouth) (Figure 7.3).

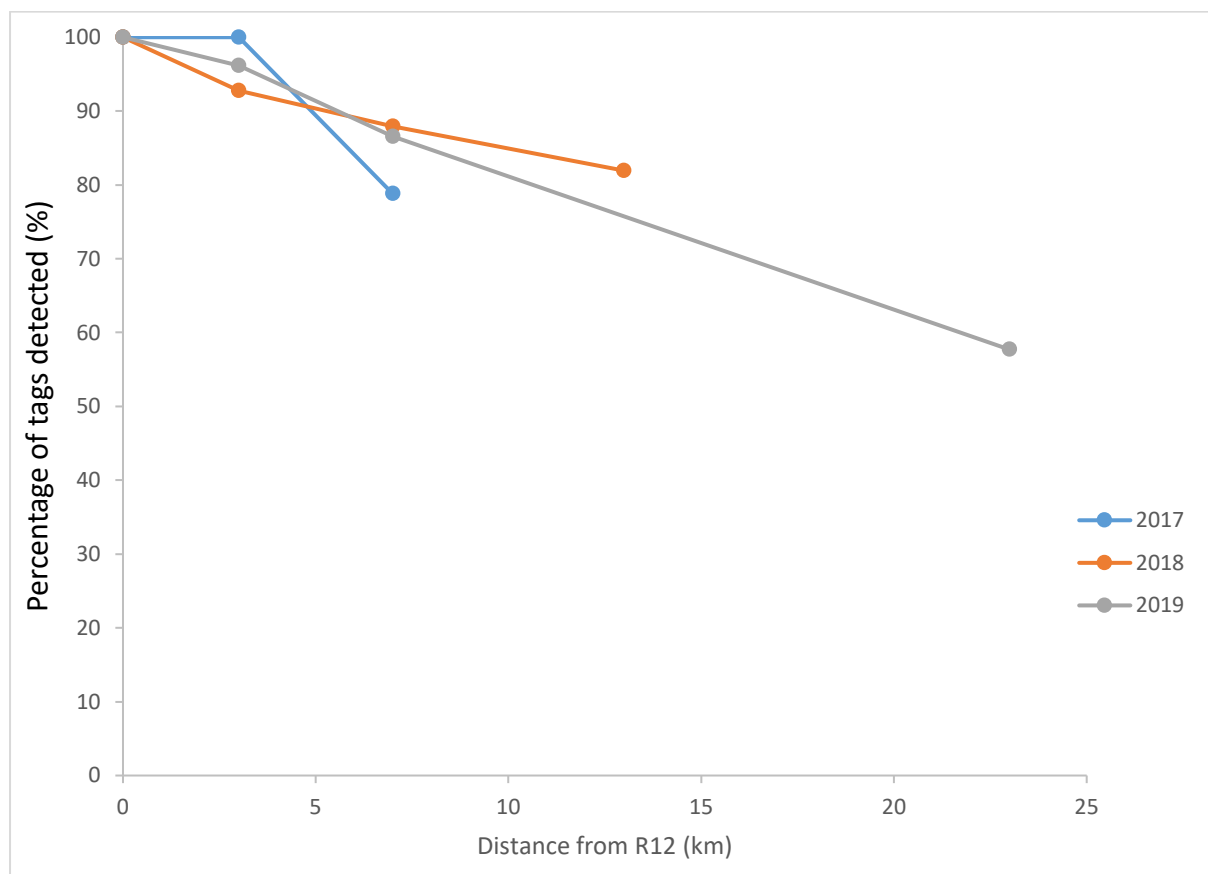


Figure 7.3 Percentage of detected transmitters at distances relative to R12 (0km), harbour (H1 and H2) combined detections. Data lines cease at most seaward marine curtain; curtains A (4km, 2017), C (10km, 2018) and D (20km, 2019).

In 2018, 100 salmon smolts were caught on the River Dee at the same 3 sites (Dinnet Burn n= 6, Beltie Burn n= 32 and the Sheeoch Burn n= 62). Of these, 11 tags (11%) were not detected on any ALS. Eighty three tags were detected in the lower river (R12) prior to entering the harbour and 77 were detected leaving the last set of harbour ALSs (H2). Seventy three tags (73%) were detected at curtain A (4 kilometres from the harbour mouth) and 68 tags (68%) were detected at curtain C (10 km from the harbour mouth) (Figure 7.3). These data have been corrected for tags missed at curtain A and subsequently detected at curtain C (n=6).

In 2019, 74 salmon smolts were tagged in the River Dee at sites used in previous years (Dinnet Burn n= 10, Beltie Burn n= 64). No salmon smolts of the correct size were caught at the Sheeoch Burn. Of these, 22 tags (30%) were not detected on any ALS. Fifty two tags (74%) were detected at the lower river (R12) gate prior to entering the harbour and 50 tags (68%) were detected at the last gate within the Harbour (H2). Forty five (61%) tags were detected at curtain A (4km from harbour mouth). Finally 30 tags (40%) were detected at curtain D (20km from the harbour mouth).

Also in 2019, 50 salmon smolts were tagged on the River Don. Of these fifty, only 4 were detected in the lower river at DO10 (8% of the tags, Figure 6.1 Figure 7.3). Two of these tags were detected at curtain A (4km from harbour) (4%), the same two tags were also detected at curtain D (20km).

In 2021, 13 salmon smolts were tagged on the main stem of the Dee and eleven of the tags were detected at the lower river ALS (R12, 85%). Eleven fish were subsequently detected leaving the harbour at H2, although one of these tags began to transmit a predation signal (see section 7.5.1). Nine tags (69%) passed through the grid array (Figure 6.3) providing detailed tracks. Six (46%) were subsequently detected at curtain D (20km) (46%).

Also in 2021, Seventy-five salmon smolts were tagged on the River Don. Twenty-one (28%) of these tags were not detected again, and 47 (63%) were detected on the lower river receiver (DO10), and 17 at curtain D (20km) (23%,Figure 7.3) at A total of 16 fish (21%) were detected on the grid array. However, ten fish were detected at curtain D, (20km) that were not detected swimming through the grid.

Transmitter loss between the lowest river ALS (R12) and the outermost marine curtain was relatively low. Over 80% of the fish detected at R12 were also detected at curtain A (4km) and curtain C (10km). The numbers of transmitters detected at curtain D (20km) was considerably lower but likely as a result of the wider spacing between ALS enabling transmitters to pass undetected. The high detectability of transmitters where ALSs are closely spaced indicates that performance of the receivers was in general high. This is supported by the range testing results and simulations using actual detections. It is not possible to determine if each transmitter accurately represents a swimming smolt as it may have been consumed by a predator.

7.4.1 Depth and temperature data

The transmissions from tags capable of sensing depth and temperature (2017 and 2018 only) were recorded through both years (2017 n=15 and 2018 n=30). The range of depths (Figure 7.4) and temperatures (Figure 7.5) recorded by these tags are shown below. Fish were detected within the top 3m of the water surface and within the top 2m when crossing marine curtains.

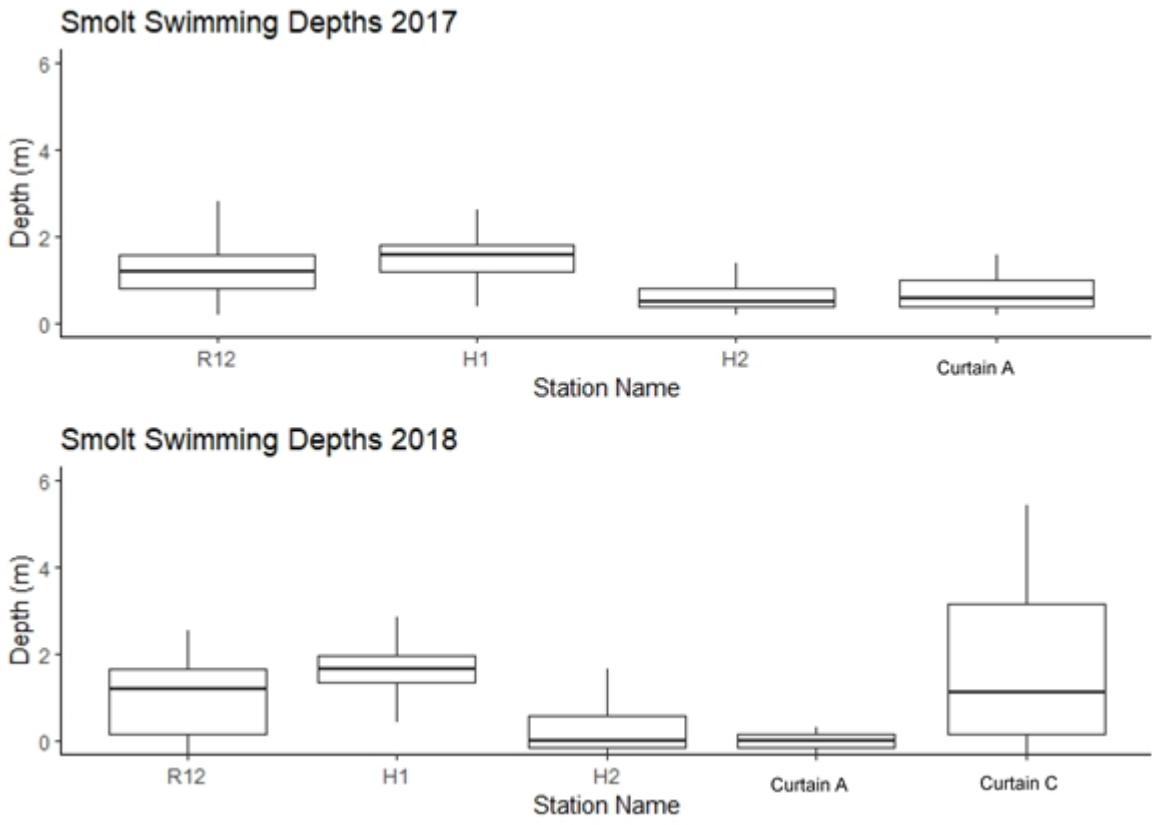


Figure 7.4: Boxplot of salmon smolt swimming depths(m) from sea surface in the lower river (R12), harbour (H1 and H2) and marine curtains (Curtain A, Curtain C) for 2017 and 2018

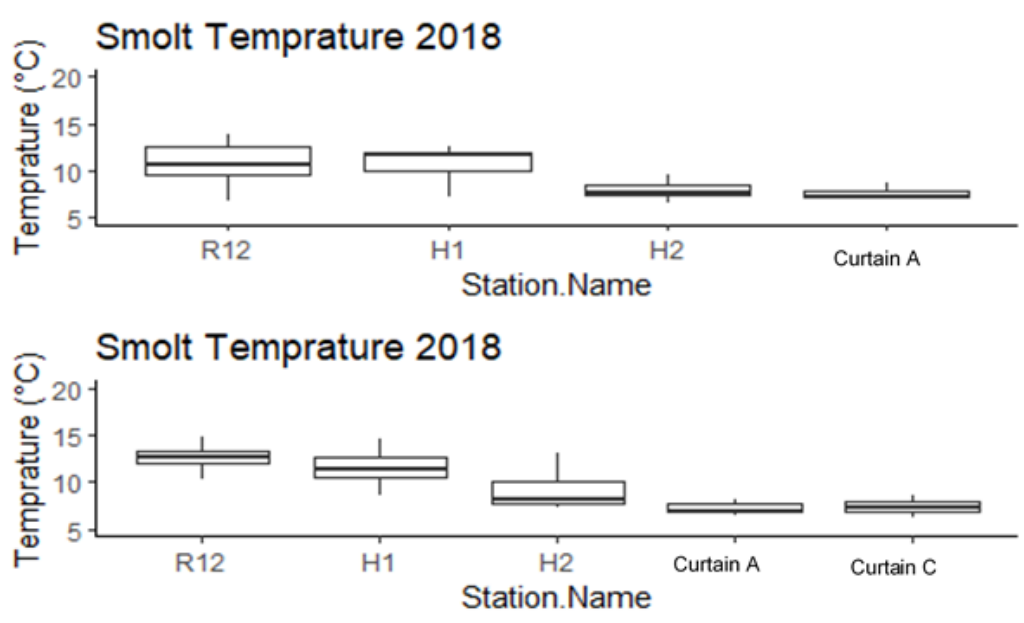


Figure 7.5: Smolt swimming temperatures (°C) the lower river (R12), harbour (H1 and H2) and marine curtains (Curtain A, Curtain C) for 2017 and 2018. Predation events have been removed.

7.4.2 Harbour Transit Time (HTT)

Time taken to migrate from the lower river (R12) through to the harbour exit (H2) was compared across years (see Table 7.1). The median migration time from last detection on R12 to last detection at H2 ranged between 1.17 hours (in 2021) and 2.52 hours (in 2017) with the majority of fish transiting through the harbour in under 27 hours (Table 7.1). Some fish took multiple days to leave the lower river with transit times of over 48 hours recorded in 2017 and 2018. A Kruskal Wallis test indicated there were significant differences in the transit time of fish across years (Kruskal-Wallis chi-squared = 10.42, df = 3, p-value = 0.02) with a Dunn test indicating the significant difference came between 2017 and 2019 ($z = 2.72$, p-value = 0.04) specifically.

Table 7.1: Descriptive data for Harbour Transit Times (hours)

Year	No. fish	Hours				
		Min	Median	Mean	Interquartile Range (IQR)	Max
2021	10	0.08	1.17	3.19	0.9-1.58	20.80
2019	49	0.12	1.37	3.15	0.97-3.45	23.12
2018	77	0.25	1.63	14.01	1.15-7.75	185.37
2017	33	0.75	2.52	27.66	1.23-27.02	133.00

7.4.3 Rate of Marine Migration

Ground Speed was calculated between Aberdeen Harbour and the marine curtains (Table 7.2). Median Ground Speed between the end of the Harbour (H2) and curtain A (4km) was similar across all years (2017 – 0.44 ms⁻¹, 2018 – 0.45 ms⁻¹, 2019 – 0.45 ms⁻¹) with no significant difference in Ground Speed from the end of the Harbour (H2) to curtain A (4km) between years (Anova, p =0.75). As fish migrated further out to sea, median Ground Speed generally decreased (curtain A to curtain C) [2018] – 0.37 ms⁻¹, curtain A to curtain D [2019] – 0.24 ms⁻¹) whilst variation (interquartile range) in Ground Speed also decreased (curtain A to curtain C [2018]: 0.21 – 0.58 ms⁻¹, curtain A to curtain D [2019] – 0.19 – 0.31 ms⁻¹). The reduction in speed was significantly (T.test, df = 29.9, p = <0.001) different in 2019 for movements between the end of the Harbour (H2) and curtain A (4km) compared to speeds between curtain A and curtain D. However, there was no significant difference in 2018 for

speeds between the end of the Harbour (H2) and curtain A, compared with speeds between curtain A and curtain C (10km), (T.test, P = 0.34))

The data gathered from the ADCP were used to adjust the detected ground speeds recorded on ALS to account for the effects of tide on the tagged fish (Table 7.2). This showed no significant difference in the AFSS between the end of the Harbour (H2) and curtain A (4km) in 2017, 2018, and 2019 (Anova, P = 0.79). There was, however, a significant difference in the AFSS when comparing the movements between the end of the Harbour (H2) to curtain A and H2 to curtain C (10km) in 2018 and H2 to curtain D (20km) in 2019 (T.test, P=0.005 and P=1.586e⁻⁰⁶ respectively).

Table 7.2: Rates of Atlantic salmon smolt movements between H2 and marine curtains

Year	Movement	Median Ground Speed ms ⁻¹ [Lfs ⁻¹]	IQR ms ⁻¹ [Lfs ⁻¹]	Median AFSS ms ⁻¹ [Lfs ⁻¹]	IQR ms ⁻¹ [Lfs ⁻¹]
2017	H2 – curtain A	0.44 [3.16]	0.38 – 0.54 [2.57 – 3.76]	0.40 [2.76]	0.34 – 0.55 [2.33 – 3.89]
2018	H2 – curtain A	0.45 [3.24]	0.37 – 0.53 [2.64 – 3.73]	0.46 [3.31]	0.37 – 0.51 [2.75 – 3.64]
2019	H2 – curtain A	0.45 [3.31]	0.41 – 0.58 [3.02 – 4.27]	0.47 [3.45]	0.42 – 0.53 [3.00 – 3.85]
2018	curtain A – curtain C	0.37 [3.45]	0.21 - 0.58 [1.80 – 4.99]	0.32 [2.53]	0.25 – 0.45 [1.72 – 3.17]
2019	curtain A – curtain D	0.24 [1.80]	0.19 – 0.31 [1.37 – 2.15]	0.23 [1.67]	0.16 – 0.36 [1.15 – 1.93]

7.4.4 Direction of Marine Travel (Transmitter Detections)

The directional vector of smolt migration direction was calculated between Aberdeen Harbour H2 and curtain A (4km) and from curtain A to either curtain C (2018) or curtain D (2019). The directional vector on the initial heading between the last harbour gate (H2) and curtain A was not significantly different between years (2017, 2018, 2019, Table 7.3) Watson-wheeler Test ($P = 0.144$). In 2018 fish headed on a more southerly bearing between curtain A (4km) and curtain C (10km) than between last harbour gate (H2) and curtain A, Watson two sample: Test Statistic: 0.30, Level 0.05, Critical Value: 0.187), however in 2019 between the last harbour gate (H2) and curtain D (20km) this difference was not detected (Watson two sample: Test Statistic: 0.03, Level 0.05, Critical Value: 0.187). Although measured across different distances there was also no difference in trajectory between the curtain A (4km) and the curtain (10km) bearings in 2018 and 4km Curtain (A) to 20km Curtain (D) in 2019 (Watson two sample: Test stat 0.007, level 0.05, Critical value, 0.187).

The data gathered from the ADCP were used to adjust the detected movements recorded on ALS to account for the effects of tidal currents on the tagged fish. Once corrected for tidal effects, fish in 2017 were heading at a significantly more southerly bearing between H2 and curtain A than in 2018 (Watson two sample: Test statistic: 0.27, Level: 0.05, Critical Value: 0.187). However there was no difference in bearing from H2 and curtain A between 2017 and 2019 (Watson two sample: Test statistic: 0.168, Level: 0.05, Critical Value: 0.187) or 2018 and 2019 (Watson two sample: Test statistic: 0.038, Level: 0.05, Critical Value: 0.187). Further offshore, fish took a significantly more southerly bearing between curtain A and curtain C (curtain D in 2019) than from H2 to curtain A in both 2018 (Watson two sample: Test statistic: 0.459, Level: 0.05, Critical Value: 0.187) and 2019 (Watson two sample: Test statistic: 0.21, Level: 0.05, Critical Value: 0.187).

Table 7.3: Bearing of transmitter trajectories of actual detections and corrected bearings where tide components have been removed.

Year	Movement	Mean Bearing \pm circular SD (Degree from North)	Corrected Bearing \pm circular SD (Degree from North)
2017	H2 – Curtain A (4km)	106° \pm 39°	94° \pm 23°
2018	H2 – Curtain A (4km)	96° \pm 34°	107° \pm 49°
2019	H2 – Curtain A (4km)	97° \pm 50°	75° \pm 30°
2018	Curtain A (4km) – Curtain C (10km)	128° \pm 46°	158° \pm 37°
2019	Curtain A (4km) – Curtain D (20km)	117° \pm 49°	114° \pm 43°

The situation in 2021 was more complex with a grid array deployed to try and capture fine scale movements of fish. Due to the small number of fish tagged on the Dee in 2021 this data should be treated with caution. However, even with few fish tagged we see the same pattern as fish leave the Dee in an easterly direction. This pattern was also seen with fish from the Don, however, the grid does not extend north of the Don to the same extent as the Dee and therefore only tags making a more southerly passage are detected; for this reason the last river ALS in the Don (Don DO10) – curtain D (20km) movement is also shown.

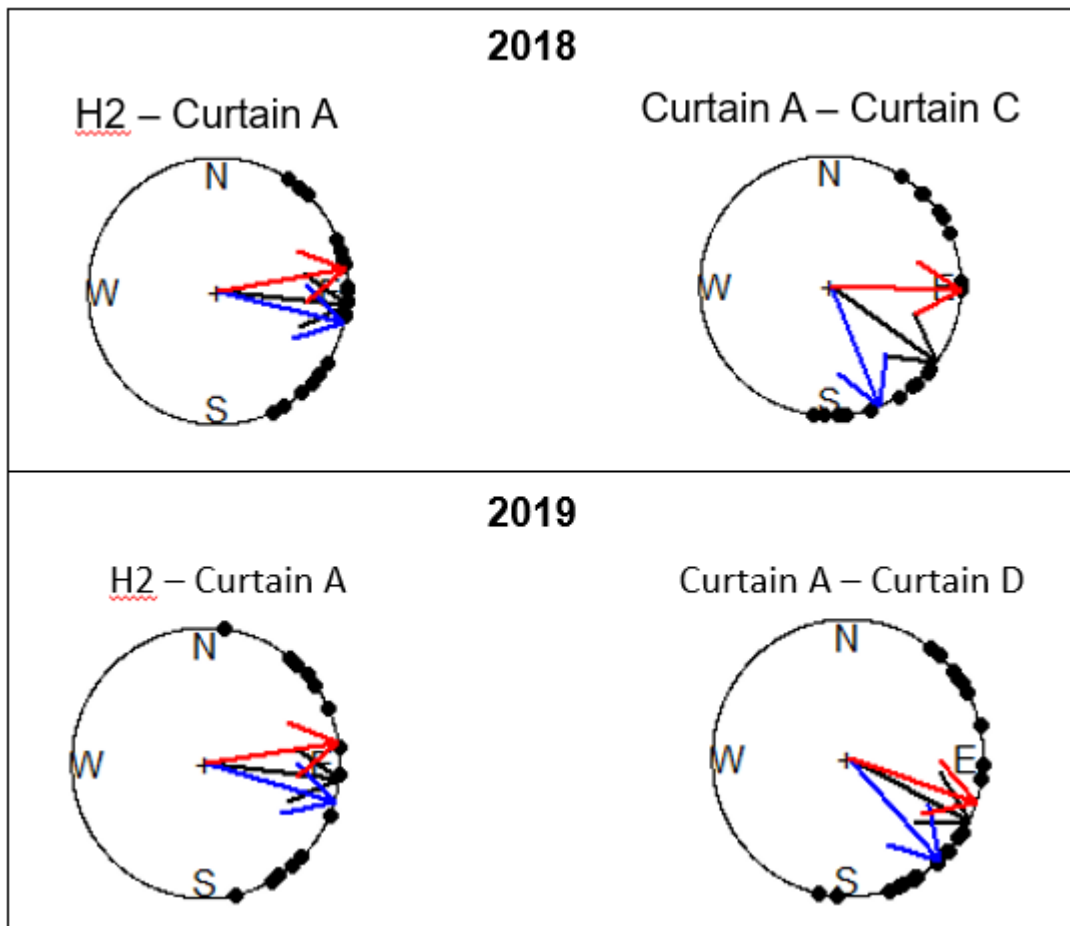


Figure 7.6: Plots showing recorded fish bearings (black dots) with mean ebb tide (red arrow) and mean flood tide (blue arrow) directions, with arrows showing the overall mean movement directions (black)

7.4.5 Grid Array 2021

Very few fish were tagged within the River Dee in 2021 and as such it is difficult to determine with any rigour robust results. However, of the 9 fish detected within the grid in 2021, the dispersal pattern is similar to previous years' work in the nearshore, with fish heading in an easterly to south easterly direction, though subsequent detections at curtain D (20km) further to the south for the majority of fish (Figure 7.7).

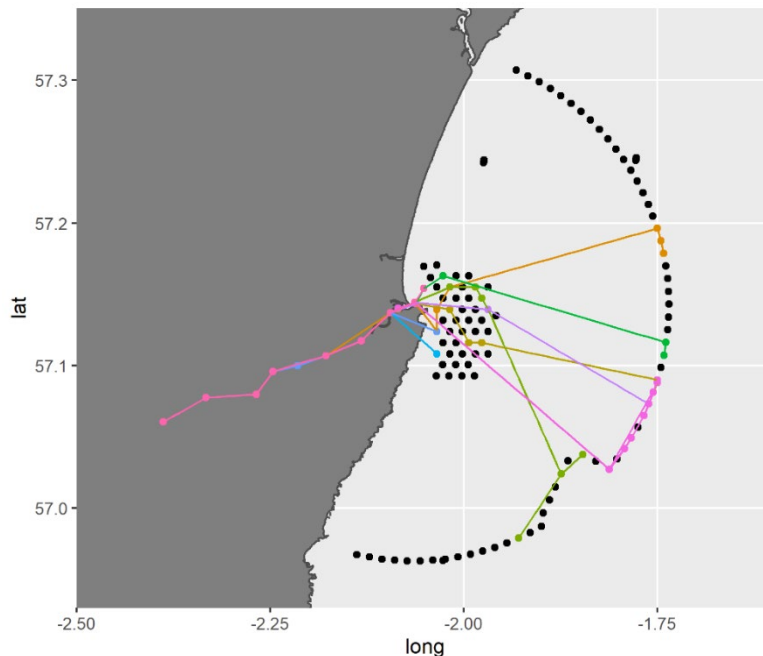


Figure 7.7: Trajectories of transmitters from the Dee transiting through a grid array of ALS in 2021. Colours identify unique individuals.

In 2021 sixteen fish from the River Don were detected on the grid array, again those which were detected were generally heading in a south easterly direction. Three fish were missed on the grid array but detected further south on the curtain D (20km) suggesting an initial northerly movement before heading south and thus missing detections on the grid (Figure 7.8). Interestingly, seven of the fish from the Don were detected heading in a north easterly heading, opposite to what has been seen in the Dee (Figure 7.7).

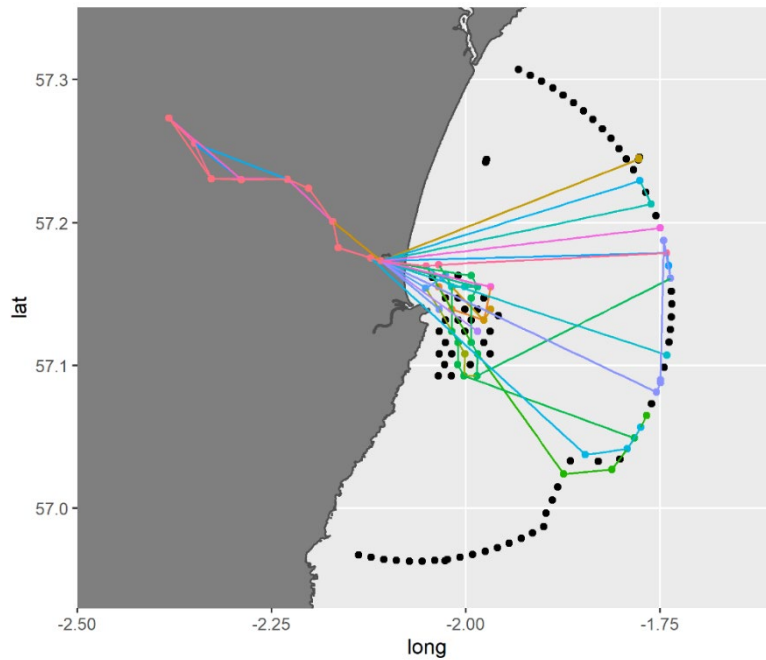


Figure 7.8: Trajectories of transmitters from the Don transiting through a grid array of ALS in 2021. Colours identify unique individuals.

7.5 Detection Efficiency

Throughout the study period, detection efficiency was, in general, high (Table 7.4). Most variable were the Harbour gates which is likely due to the high levels of shipping traffic creating highly variable detection efficiencies at ALSs located here.

Table 7.4: Detection efficiency (%) of each gate and curtain across years, with raw numbers of fish missed represented in brackets.

		2017	2018	2019	2021
River Dee	Lower River (R12)	90.9 (3)	100 (0)	100	100 (0)
	Harbour Entry (H1)	90.9 (3)	55 (36)	74.5 (13)	18 (9)
	Harbour Exit (H2)	97 (1)	93.5 (5)	70 (15)	82 (2)
	Curtain A (4km)		91.8 (6)	95.6 (2)	
River Don	Lower River Don (DO10)			100 (0)	98 (1)

Using data gathered from the range testing within the marine curtains, fish passage simulations were run to estimate the detection probability within curtain A in 2017 and 2018, and curtain C in 2018. ALS spacing within the simulations were set to the same as the ALS curtain being tested, the detection probability curve was drawn from the worst performing range test location within each curtain and virtual fish were assigned a random swimming speed within the IQR of fish swimming speed (ground speed) within the study (Figure 7.9). The mean probability of detecting a tag transiting the curtain A in 2017 and 2018 across 10,000 simulations in each year was 1. However, in 2018, six fish were detected curtain C (2018) that were not detected passing curtain A (4km). In 2018, using the worst performing range test location to generate a probability of detection curve for the simulations, across 10,000 simulations the probability of a fish being detected crossing the curtain C was 0.95 (\pm 0.05 SD). The results of these simulations will be better than can be expected in reality as environmental factors such as noise from vessels will affect the detection probability.

Simulations were also run to determine the effect of swim speed on the probability of detecting a fish. As speed increases the probability of detection decreases. However, this was not the same across each location. Detection probability within curtain A began to reduce after swim speeds reached 1.3 ms^{-1} whereas detection probability reduced continuously with increased swim speed in the curtain C (10km) and at a much greater rate than at curtain A (4km) (Figure 7.10). Similarly, at both locations as receiver spacing increases the probability of detection decreases, however the rate of reduction within curtain A is much slower than at curtain D (Figure 7.10).

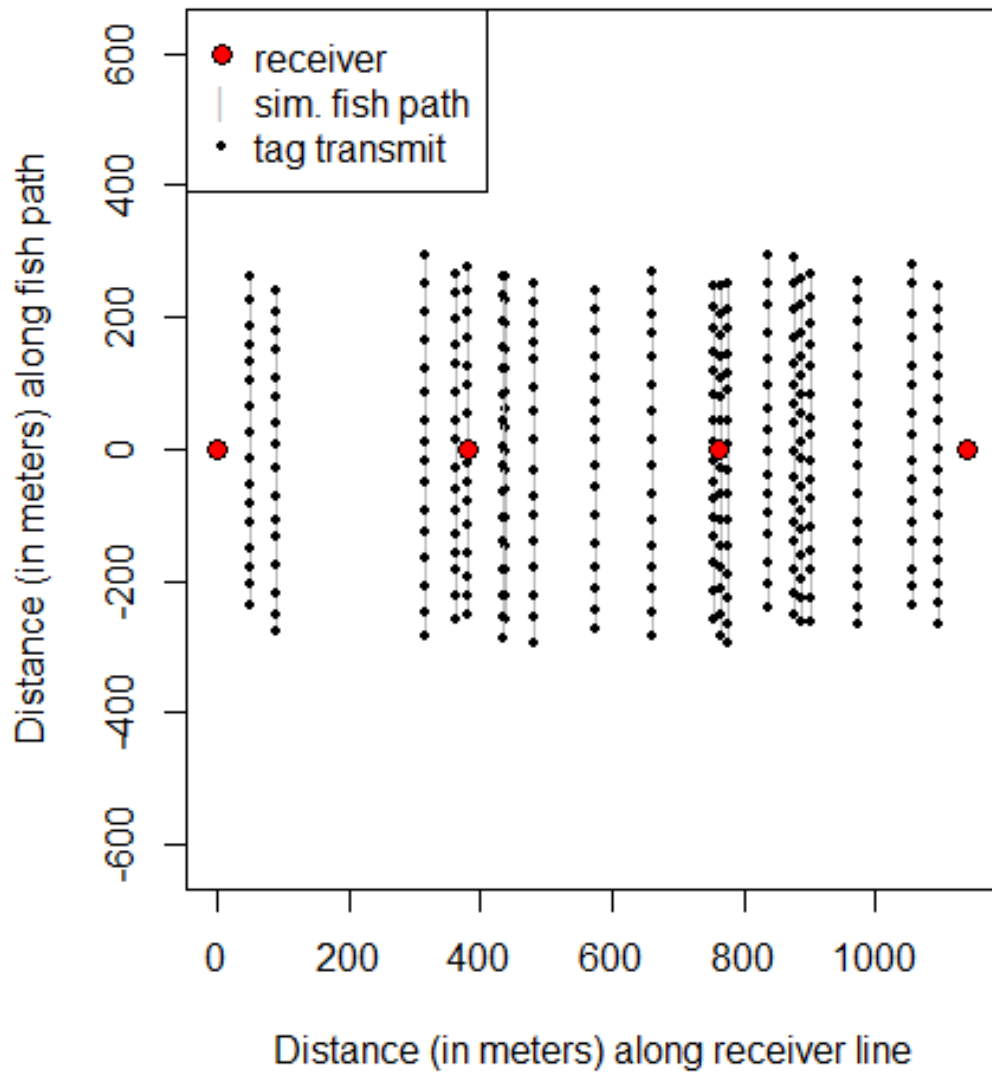


Figure 7.9: Example of simulated fish paths (grey line) with tag transmissions (black dots) based on the tags used and fish swimming speeds recorded as fish pass an ALS line (red dots represent receivers).

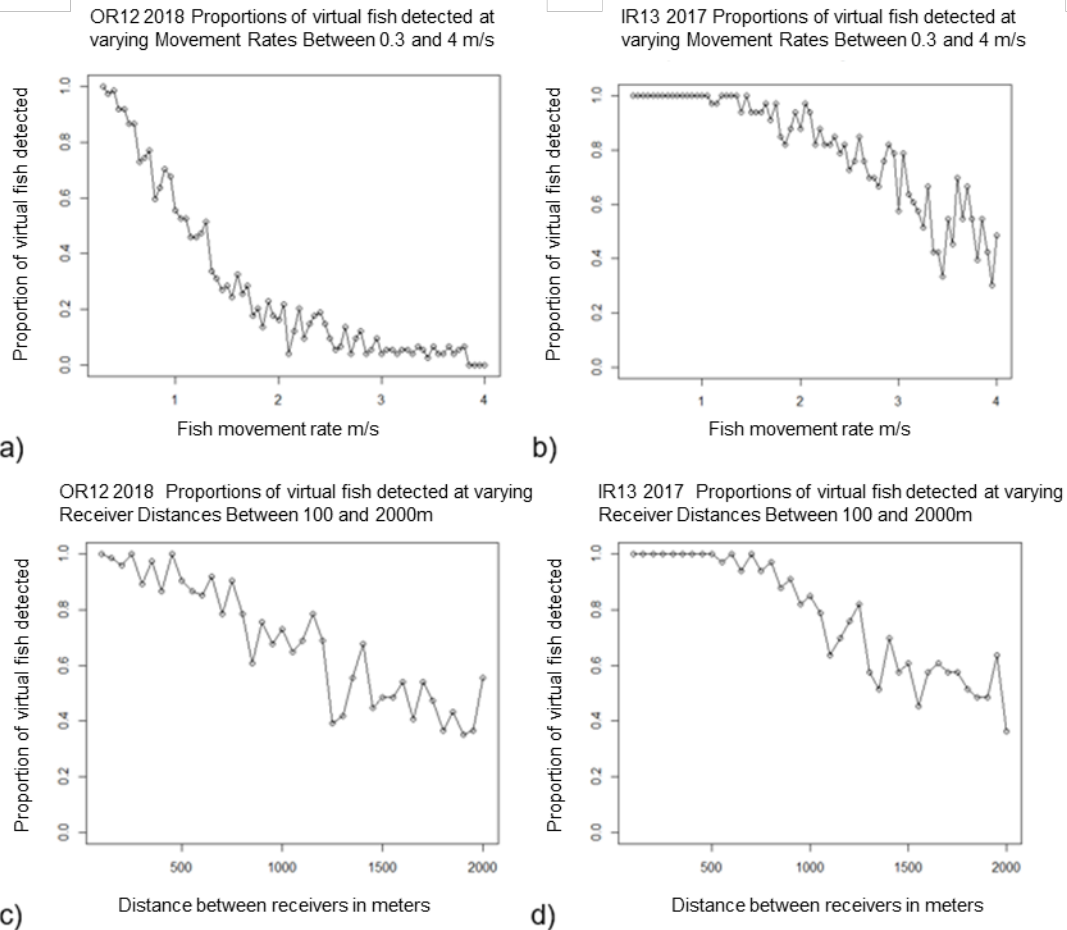


Figure 7.10: simulations of the probability of detecting a tagged fish based on the range test results showing fish detections probabilities at varying fish swimming speeds (a, b) and at differing receiver spacing (c and d).

Although simulation estimates predict good detection levels of passing fish, detection efficiency can change substantially both spatially and temporally. Thus if small drops in detection efficiency were to coincide with fish passing, the probability of detecting those fish reduces significantly.

7.5.1 Predation Events

Only one tag out of 45 depth and temperature tags deployed during 2017 and 2018 indicated a predation event by elevated temperature (Figure 7.11) readings. The tag recorded a spike in temperature for numerous detections at over 30°C, strongly suggesting predation by a mammal or a bird. This spike was detected within the harbour at the H2 gate.

Predation Events 2018

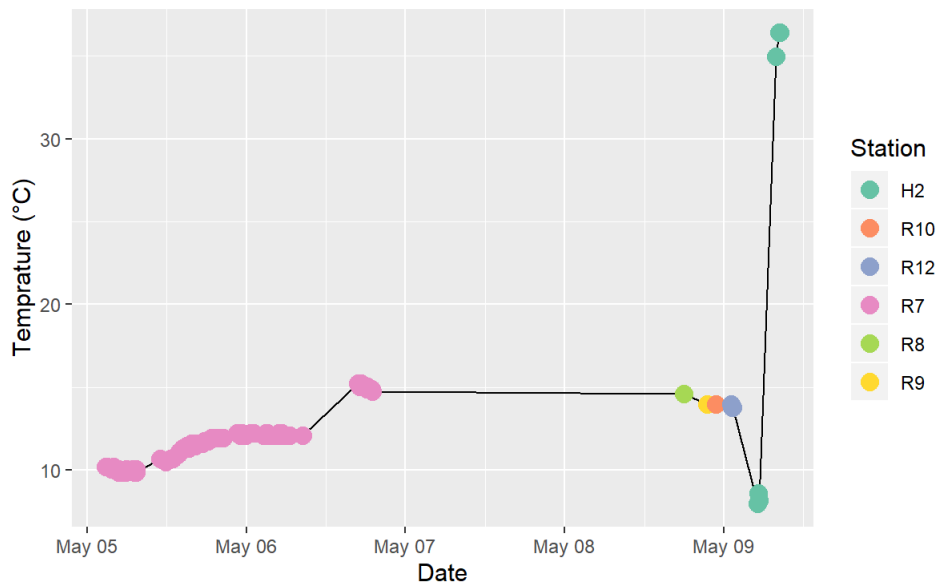


Figure 7.11: Temperature plot from transmitter (tag) serial number 20 in 2018 showing a drop in temperature followed by a rapid increase to 36.4°C. Coloured dots represent the ALS the tag was detected at.

Two other tags deployed in 2018 exhibited depth activity different to other tags in the study indicating possible predation events. One tag was detected at H2 at a depth of 10.2m and was not detected again on any ALS. A second tag was detected on curtain C at 14.7m although did return to the surface where it was subsequently detected numerous times between 1 and 5 metres deep (Figure 7.12). the remaining tags were never detected deeper than 7m below the surface in 2018 and 2017. Temperature data for these tags remained at ambient water temperature, thus it is not possible to confirm a predation event from these data alone.

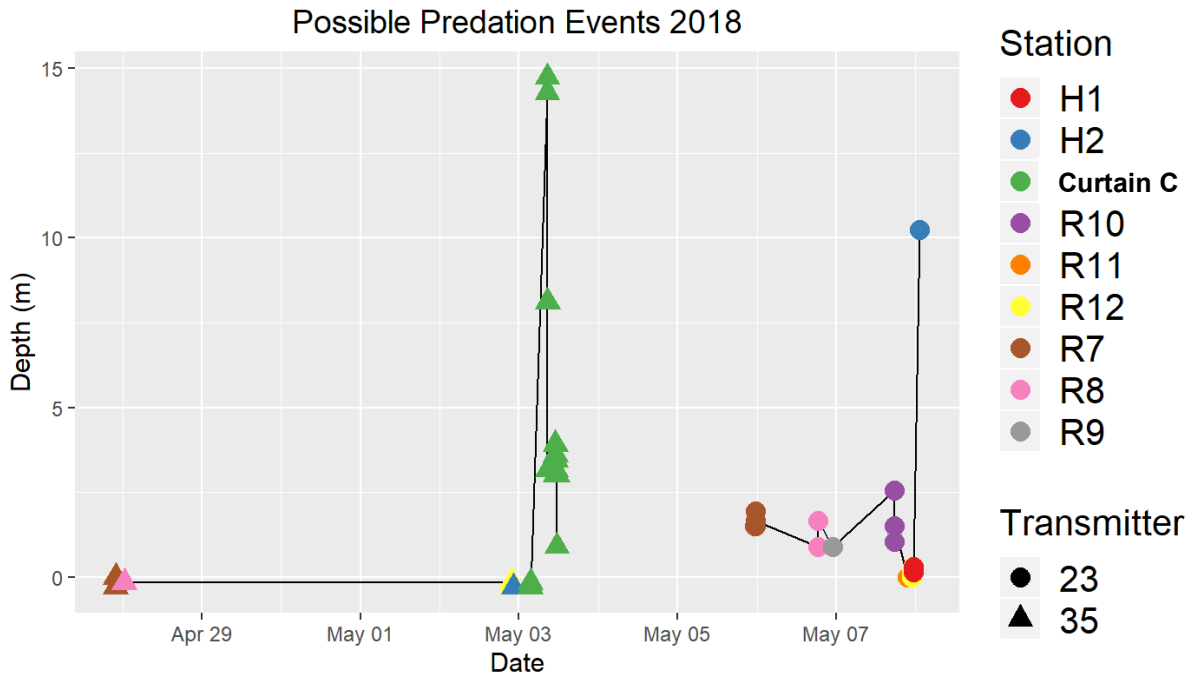


Figure 7.12: Depth plot from transmitter (tag) serial numbers 23 and 35 in 2018 showing an increase in swimming depth. Coloured shapes represent tag serial number 23 (round) and tag 35 (triangular) with the colour representing the ALS station number.

In 2019 and 2021, a number of fish were tagged with Vemco Predation tags. No predation events detected in 2019 on the Dee from 24 predation tags that were used. In 2021 predation events were detected on both the Dee and Don. In the Dee, one tag out of 5 predator tags deployed indicated a predation event within the estuary at R12. Within the Don, of a total 75 predator tags, two tags indicated a predation event high up in the river and a further two tags indicated a predation event in the lower river. Despite a predation event occurring it is not possible to determine exactly what the predator was.

7.6 Particle tracking

7.6.1 2018 near-field simulation spatial analysis

A total of 51 particles were released in near field simulations at the same times smolts were known to be exiting the harbour (last detection at H2 gate). A total of 51 particles were tracked and all these particles were 'detected' by curtain A (4km), for all swim speeds and behaviours. All 51 particles were also 'detected' at curtain C (10km) for all behaviours and swim speeds ([Appendix B](#))

The passive particles (fig 7.13a) tended to head south and then east with some north-south meandering due to the tide. The particles therefore tended to first cross the 4km Curtain (A) at the north and southern ends, and the southern end of the 10km Curtain (C). The negative rheotaxis particles (Figure 7.13b) again broadly headed south-east, following very similar trajectories to the passive particles, with more first crossings at eastern sectors of curtain C. The variable rheotaxis particles (Figure 7.13c) again cross curtain A predominantly at the northern and southern ends, due to the strong tidal oscillations, but then head predominantly east, crossing curtain C (10km) at a variety of locations at southern to eastern sectors of the array. The particles following a northerly bearing (Figure 7.13d), despite the swimming speed of 1.5 bl s^{-1} , still couldn't overcome the tide and first cross curtain A (4km) at the southern and northern ends, as well as eastern side, and then head north along the coast and cross curtain C (4km) at the northern end. The north-east bearing particles (Figure 7.13e) cross the curtain A at a variety of sectors, and curtain C (10km) predominantly in the easterly sector. First detections of actual tagged fish (Figure 7.13f) were made all along curtain A and were more dispersed at the curtain C, with most detections being made in the south-east sector of curtain C. No first detections were made by receivers close to the coast in either curtains, suggesting that the smolts were swimming away from the coast. In general the particle tracking behaviours that appear to most resemble the data are the two rheotaxis behaviours shown in Figure 7.13b and Figure 7.13c.

Faster swim speeds ([Appendix B – Near-field particle density plots for 2018 simulations with faster swim speeds – first detections](#)) had slightly differing results, but the broad picture stayed the same. The width of the particle fields under the constant bearing behaviours shrank with the particles crossing the curtains at even more well defined regions. Similarly, crossing points at curtain C (10km) under the rheotaxis behaviours tended to become more bimodal with first detections occurring more towards the northern and southern ends in general. The particle densities suggest the rheotaxis particles in general became more diffuse as the swim speed increased suggesting the particles are moving around a lot (with the tide) and crossing the

curtains at multiple locations over time (only the first crossing points are indicated in Figure 7.13 and Appendix B – Near-field particle density plots for 2018 simulations with faster swim speeds – first detections).

Figure 7.14 shows the same particle density plots, but with all (rather than the first) particle detections at each receiver location on the two arrays shown, for a swim speed of 1.5 bl s^{-1} . Faster swim speeds are shown in [Appendix C](#). These total detection results are broadly similar to the first detection results, with the results from the passive and rheotaxis behaviours showing more differences than the constant bearing behaviours. This is because the passive and rheotaxis behaviours follow the tidal velocities (to a greater or lesser degree) whereas the constant bearings ignore the tide completely and have a much more constant velocity vector. Thus, the constant bearing behaviours tend to cross the curtains once (or very few times), whereas the passive and rheotaxis behaviours meander much more and cross the curtains multiple times, potentially at multiple locations. The tidal influences appear to be higher at the curtain A (4km) because the curtain is more compact and the tidal deviation result in particles crossing at multiple locations along the array. Figure 7.14a shows that, when considering all particle crossing points, a higher frequency was seen at the south to east sectors in curtain A. Similarly, Figure 7.14 (b and c) a very wide spread of the curtain A crossing locations, compared with Figure 7.14 (b and c). Crossing locations at the curtain C (10km) of all particles broadly show much more similar results to the first detection results. The smolts tag data, for all detections, tells a very similar story to the first detections, and compared most closely with the variable rheotaxis result (Figure 7.14c).

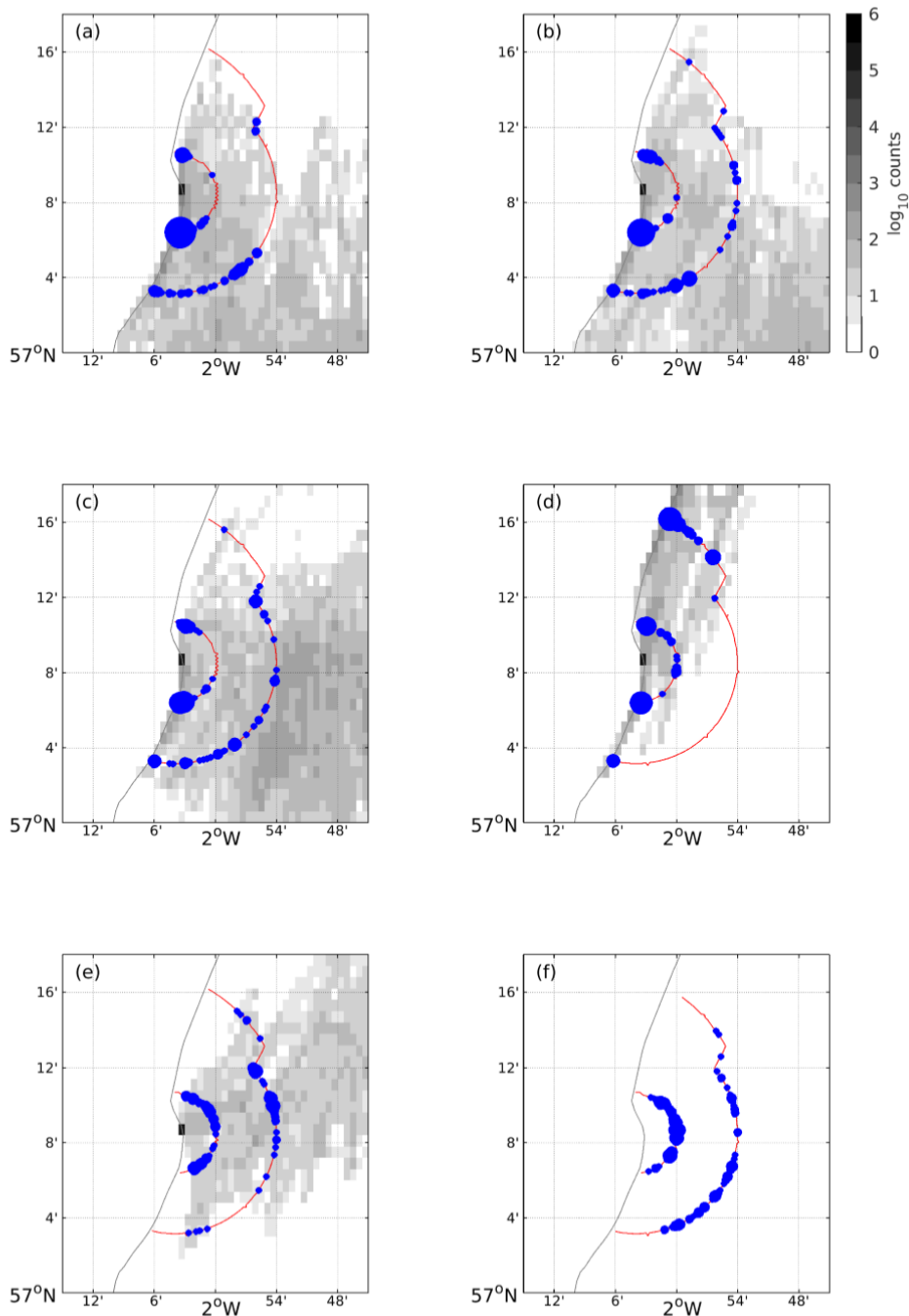


Figure 7.13: (a) – (e) show particle density plots for first detections of 2018 simulations around Aberdeen Bay for (a) passive (b) negative rheotaxis (c) variable rheotaxis (d) northerly bearing and (e) north-easterly bearing behaviours, with smolt swim speed set to 1.5 bl s⁻¹ for (b)-(e). Smolt body length was initially set to 0.14 m. The 2018 inner and outer arrays of acoustic receivers are indicated with red lines. The first detections of the particles on the arrays are shown by the blue dots, the size of which indicate the number of first particle detections at each receiver location. (f) shows the first detections of tagged salmon smolts at the two curtains (A and C), with the size indicating the number of unique detections at any one receiver.

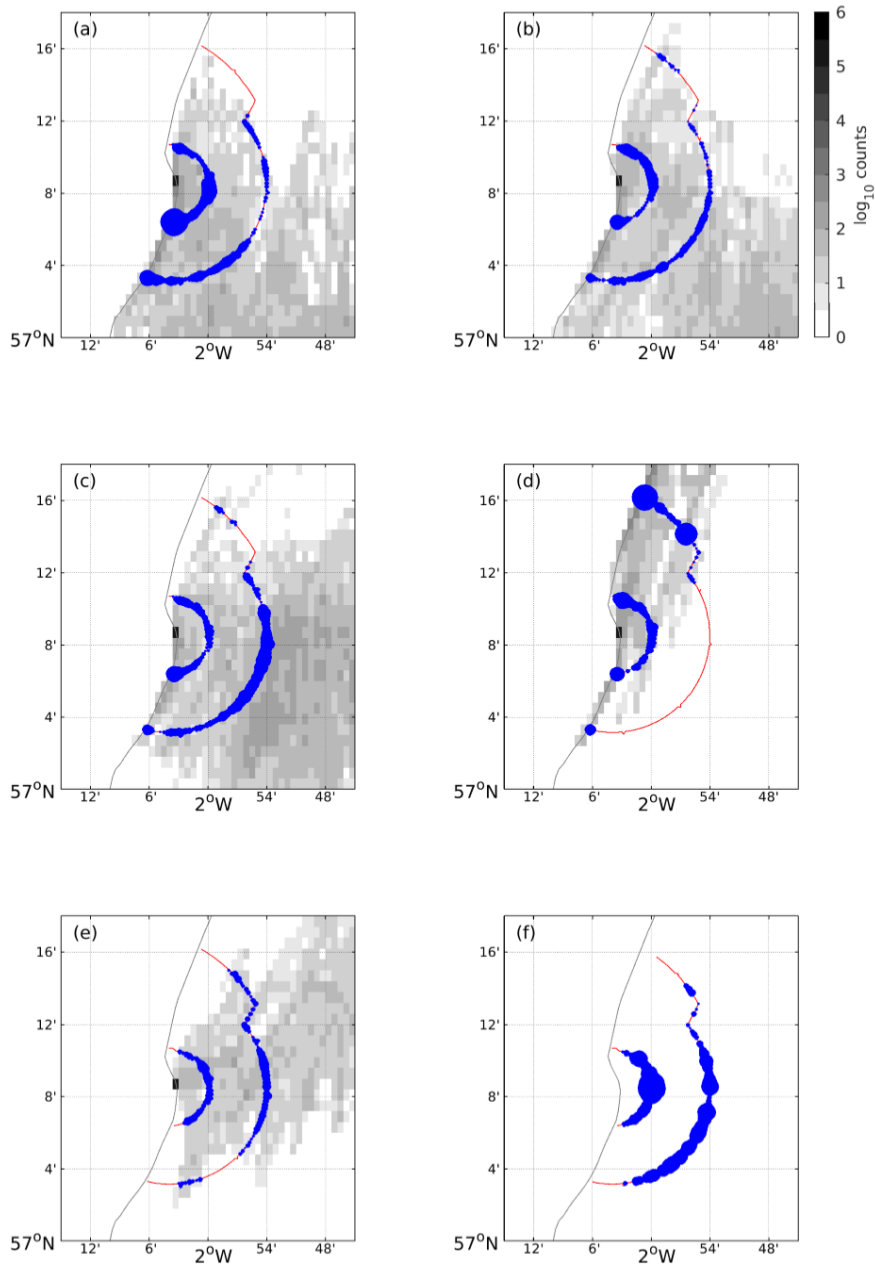


Figure 7.14: (a) – (e) show particle density plots for all detections 2018 simulations around Aberdeen Bay for (a) passive (b) negative rheotaxis (c) variable rheotaxis (d) northerly bearing and (e) north-easterly bearing behaviours, with smolt swim speed set to 1.5 bl s⁻¹ for (b)-(e). Smolt body length was initially set to 0.14 m. The 4km and 10km Curtains (A and C) are indicated with red lines. The detections of the particles on the arrays are shown by the blue dots, the size of which indicate the number of particle detections at each receiver location. (f) shows the detections of tagged salmon smolts at the two arrays, with the size indicating the number of detections at any one receiver.

7.6.2 2019 near-field simulations spatial analysis

For the 2019 simulations, 33 particles were released near the harbour mouth and tracked, and all these particles were 'detected' by curtain A (4km) and curtain D (20km), for all swim speeds and behaviours. The particle density plots and curtain A first detection points are very similar to the 2018 results, with the slight exception that the particles with the northerly heading tended to hug the coastline more in 2019 (due to differing hydrodynamic conditions in 2018 and 2019). First detection points at Curtain D (20km) differ a little to 2018 (curtain C, 20km) due to the curtain being further offshore. The tag data shown in Figure 7.15f show that smolts were first detected at a variety of locations along the curtain, but with clusters in the north-east and south-east sectors. In general the particle tracking behaviour that most resembles the tag first detection data shown in Figure 7.15f is the variable rheotaxis (Figure 7.15c).

The faster swim speed results (Appendix D – Near-field particle density plots for 2019 simulations with faster swim speeds – first detections) show very little difference in terms of first detection locations, with the only notable difference being that there are far fewer first detections at the south and south-east sectors of curtain D for the variable rheotaxis results with higher swim speeds. Tagged smolts were first detected on curtain D at these locations, suggesting that the slower swim speed of 1.5 bl s^{-1} may be more realistic.

As for the 2018 analysis, when comparing all detections of particles (Figure 7.16), the overall picture is unchanged with array crossing points all along the curtain A (4km) being revealed for the passive and rheotaxis results that follow the tide, rather than being limited to the north and south ends. Again, the simulation most resembling the tagged smolt data is the variable rheotaxis behaviour.

[Appendix E](#) shows the 2019 simulation results for faster swim speeds and all detection locations. As for the first detections, the results are broadly unchanged with the higher swim speeds with the only notable difference being the lack of detections of the south and south-east during the variable rheotaxis simulations with faster swim speeds.

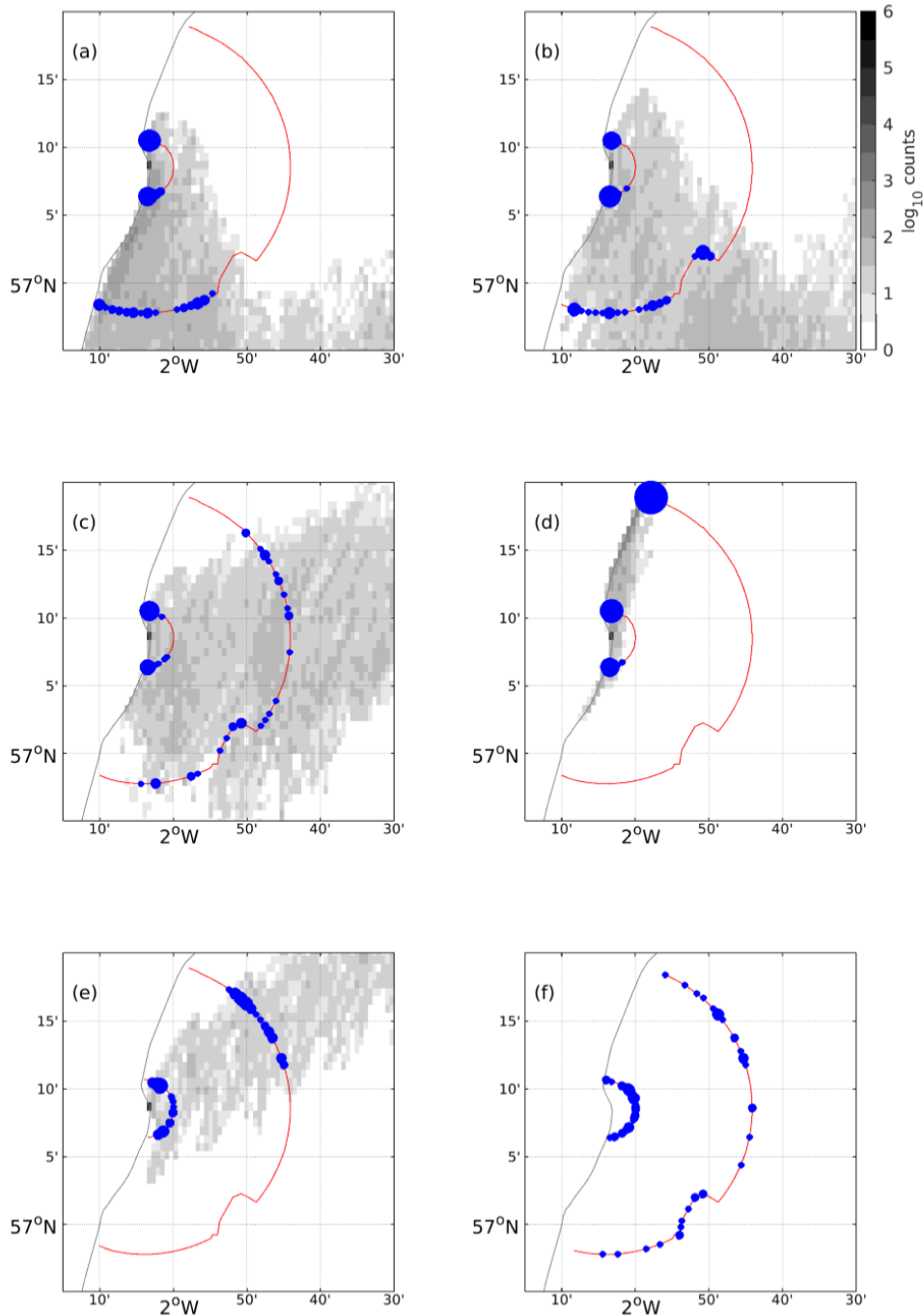


Figure 7.15: (a) – (e) show particle density plots first detection of particles in 2019 simulations around Aberdeen bay for (a) passive (b) negative rheotaxis (c) variable rheotaxis (d) northerly bearing and (e) north-easterly bearing behaviours, with smolt swim speed set to 1.5 bl s⁻¹ for (b)-(e). Smolt body length was initially set to 0.14 m. The 2019 4km (A) and 20km (D) Curtains of acoustic receivers are indicated with red lines. The first detections of the particles on the arrays are shown by the blue dots, the size of which indicate the number of first particle detections at each receiver location. (f) shows the first detections of tagged salmon smolts at the two curtains, with the size indicating the number of unique detections at any one receiver.

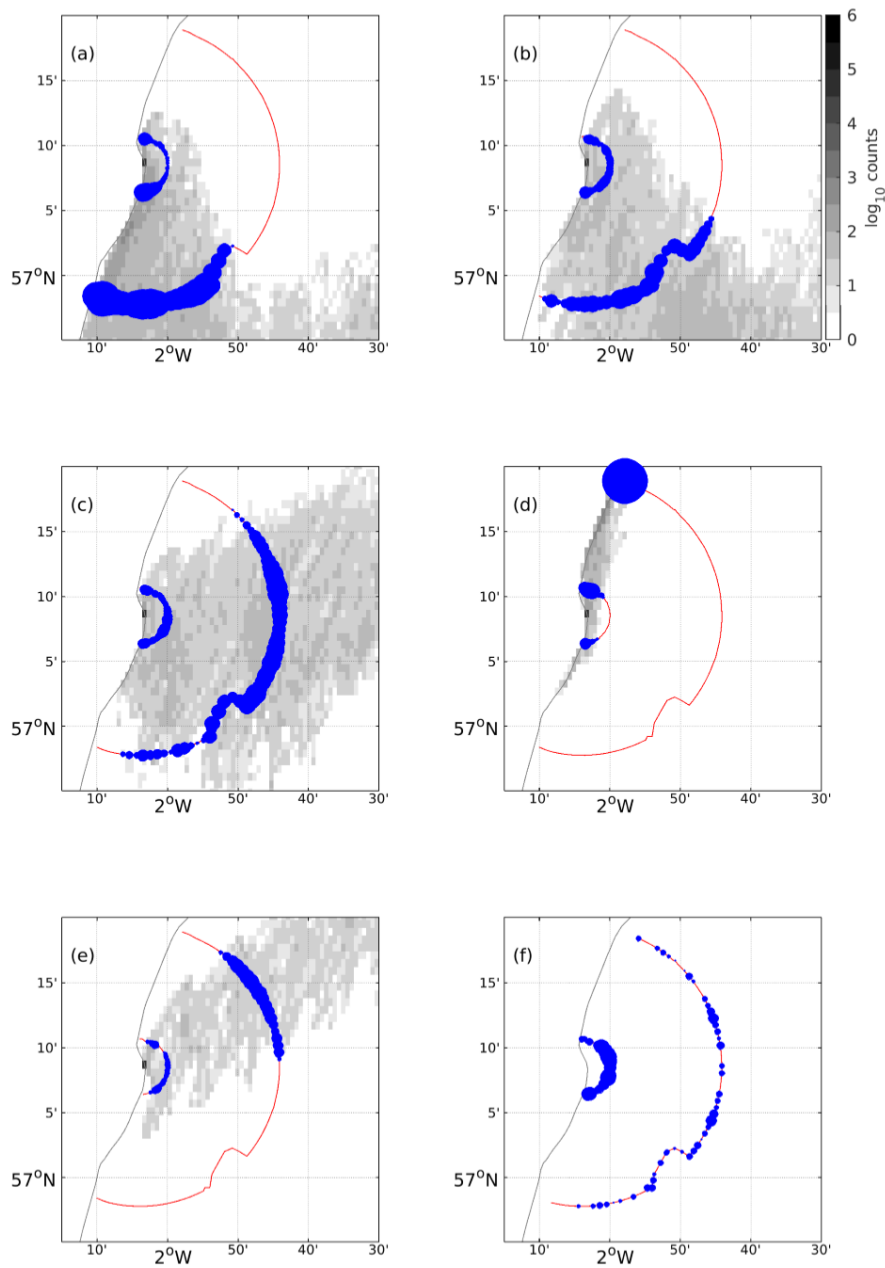


Figure 7.16: (a) – (e) show particle density plots for all detections in 2019 simulations around Aberdeen bay for (a) passive (b) negative rheotaxis (c) variable rheotaxis (d) northerly bearing and (e) north-easterly bearing behaviours, with smolt swim speed set to 1.5 bl s^{-1} for (b)-(e). Smolt body length was initially set to 0.14 m. The 2019 4km (A) and 20km (D) Curtains of acoustic receivers are indicated with red lines. The detections of the particles on the arrays are shown by the blue dots, the size of which indicate the number of particle detections at each receiver location. (f) shows the detections of tagged salmon smolts at the two Curtains, with the size indicating the number of detections at any one receiver.

7.6.3 Near-field simulation temporal analysis

The timing from the last harbour gate (H2) to both curtain A (4km) and the curtain D (20km) (D) was calculated for both transmitters and simulated particles (Figure 7.17 and Table 7.5). With the exception of the north-east bearing result, all simulated behaviours in 2018 appear to take longer to reach the curtain A than the tag data. This is not as pronounced for the 2019 results with negative rheotaxis and north-east bearing showing similar median values and spread to the tag data at curtain A. At the curtain (10km), the 2018 results show similar timings for all behaviours, other than passive, that compare well with the tag data. The only 2019 timing result, at the curtain D (20km) that is similar to the tag data is the north-east bearing result. All others take longer to reach curtain D (20km). As the simulated swim speeds increase, the time between harbour mouth, and marine curtains decreases. This is the case for all behaviours with a swim speed influence (all behaviours except passive).

[Appendix F](#) shows the timing data for faster swim speeds, 2.5 and 3.5 bl s⁻¹. The overall trends do not change a lot as the swim speed increases, but the rheotaxis timing results start to approach the tag observations with negative rheotaxis inner array actually being quicker on average than the tag data. For 1.5 bl s⁻¹, the north-east bearing timing results resemble the tag data but they become too fast at higher swim speeds.

Table 7.5: Time for particles to be detected for the first time at curtain A and C during the 2018 and curtain D 2019 simulations, under the different behaviours and smolt swim speeds in body lengths per second ($bl\ s^{-1}$). The array data shows the times derived from the detected tags. The initial smolt size was 0.14 m for all simulations. The mean, median and standard deviation (SD) for all particle, or detected tags for the array data, are shown.

Behaviour	year	swim speed ($bl\ s^{-1}$)	Time to first detection at Curtain A (hours)			Time to first outer curtain C or D (hours)		
			median	mean	SD	median	mean	SD
Array data	2018	-	2.20	2.42	0.90	9.19	9.58	5.51
Array data	2019	-	2.23	3.40	2.93	23.94	25.03	8.85
Passive	2018	-	4.88	5.15	3.05	22.97	26.43	16.42
Negative	2018	1.5						
Rheotaxis			2.63	3.77	2.59	16.97	17.81	10.34
Variable Rheotaxis	2018	1.5	2.81	4.05	2.61	15.19	17.59	10.07
Bearing North	2018	1.5	3.19	5.15	4.37	18.00	18.83	7.87
Bearing Northeast	2018	1.5	2.34	2.51	0.93	13.69	12.72	4.13
Passive	2019	-	3.19	4.00	2.12	63.19	84.93	42.90
Negative	2019	1.5						
Rheotaxis			2.34	2.47	1.15	48.38	51.10	13.41
Variable Rheotaxis	2019	1.5	2.63	3.26	1.67	66.84	69.98	21.89
Bearing North	2019	1.5	1.97	2.82	1.47	43.03	44.21	9.67
Bearing Northeast	2019	1.5	1.97	2.39	1.10	21.19	23.95	7.40
Negative								
Rheotaxis	2018	2.5	1.97	3.34	2.52	11.63	13.00	6.67
Variable Rheotaxis	2018	2.5	2.63	3.84	2.63	14.81	13.72	5.86
Bearing North	2018	2.5	2.53	3.08	1.84	14.81	14.78	5.42
Bearing North East	2018	2.5	1.97	1.92	0.48	7.31	7.87	2.19
Negative								
Rheotaxis	2019	2.5	1.88	2.15	1.12	49.50	50.65	14.44
Variable Rheotaxis	2019	2.5	2.53	2.74	1.07	48.66	52.44	22.73
Bearing North	2019	2.5	2.16	3.11	2.45	29.34	30.59	6.89
Bearing North East	2019	2.5	1.69	1.87	0.73	15.00	16.21	3.57
Negative								
Rheotaxis	2018	3.5	1.69	2.98	2.39	7.88	9.85	5.16

Variable Rheotaxis 2018	3.5	2.34	3.61	2.59	9.38	11.46	5.05
Bearing North 2018	3.5	1.97	2.73	1.88	14.53	13.87	4.01
Bearing North East 2018	3.5	1.50	1.53	0.37	5.34	5.72	1.38

Negative

Rheotaxis 2019	3.5	1.50	1.88	1.31	39.66	45.06	16.78
Variable Rheotaxis 2019	3.5	2.34	2.63	1.10	32.53	39.04	22.94
Bearing North 2019	3.5	1.88	2.55	1.74	22.50	22.80	6.13
Bearing North East 2019	3.5	1.31	1.49	0.49	11.34	9.96	3.15

Negative

Rheotaxis 2018	4.5	1.31	2.47	2.08	7.31	7.69	2.94
Variable Rheotaxis 2018	4.5	2.34	3.46	2.56	8.16	9.87	4.77
Bearing North 2018	4.5	1.97	2.42	1.70	11.81	11.67	4.51
Bearing North East 2018	4.5	1.31	1.19	0.28	4.31	4.61	1.07

Negative

Rheotaxis 2019	4.5	1.31	1.53	0.74	36.38	41.59	17.73
Variable Rheotaxis 2019	4.5	2.16	2.39	0.92	23.53	32.01	20.53
Bearing North 2019	4.5	1.69	2.24	1.70	15.84	16.21	3.40
Bearing North East 2019	4.5	1.13	1.22	0.40	8.16	7.69	2.25

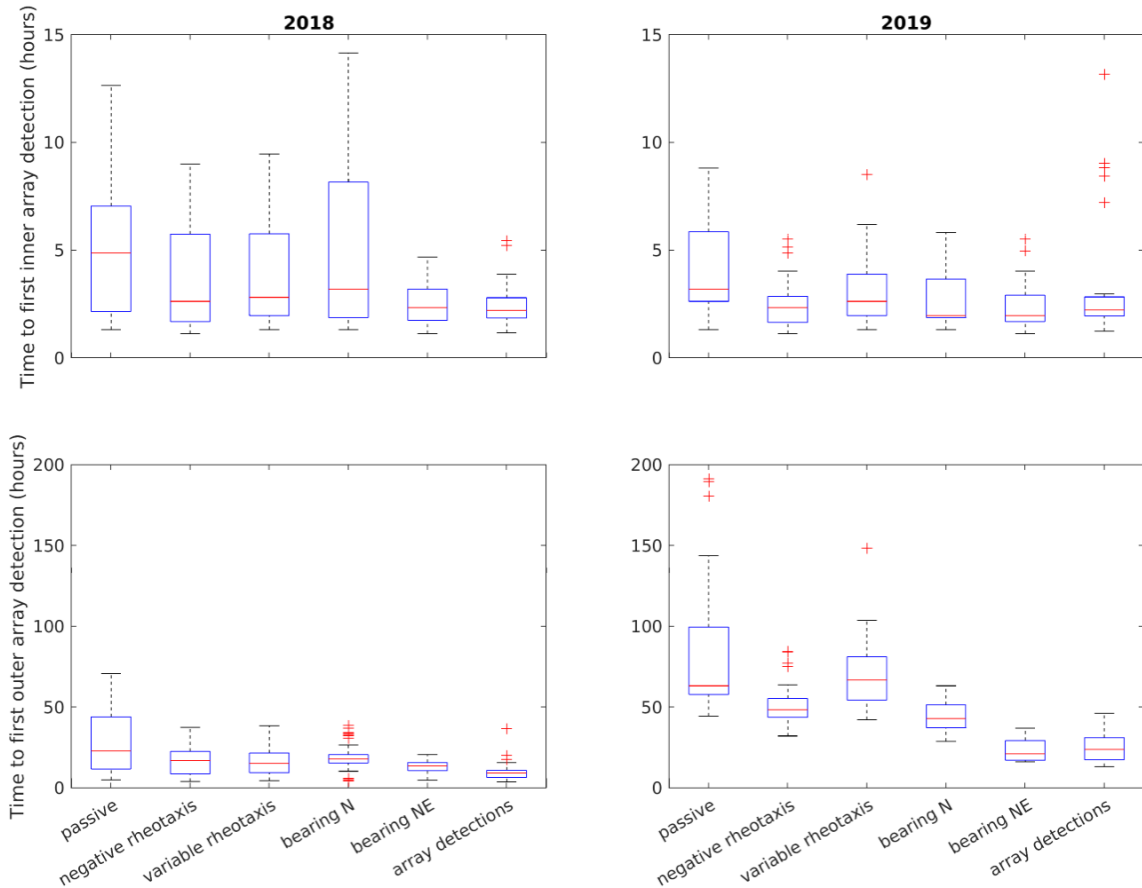


Figure 7.17: Boxplots showing the time for particles to be first detected at the inner (top) and outer (bottom) arrays for the 2018 (left) and 2019 (right) simulations, under the different behaviours with smolt swim speeds set to 1.5 bl s^{-1} . Red lines show median values for the particles tracked, or detections made, boxes show the 25th and 75th percentiles, the whiskers show the lower and upper adjacent values and the red crosses show any outliers.

7.6.4 Far-field simulations

Figure 7.18 shows particle density plots for each of the five smolt behaviours modelled for a 9 month period in 2018 only, with the smolt swim speed set to 1.5 bl s^{-1} . The particle densities were calculated on a 0.1° regular grid (approximately $11 \text{ km} \times 6 \text{ km}$ depending on latitude), are the number of particles that entered each grid element throughout the simulation, and indicate where the particles are found throughout the simulation. The passive particles (Figure 7.18a) tended to move to the south-east, then east around 56° N and then north-east towards Denmark and the Skagerrak. They then appear to split with some particles heading in to the Skagerrak and some into the Norwegian coastal current taking them north along the Norwegian coast. The particles with the negative rheotaxis behaviour (Figure 7.18b) broadly follow a similar trajectory to the passive particles, but move further into the Skagerrak and further north along the Norwegian coastline. The variable rheotaxis particles (Figure 7.18c)

follow an easterly trajectory across the North Sea, and again split into the Skagerrak and Norwegian coastal current. The trajectories of the particles following a bearing (Figure 7.18d and Figure 7.18e), go almost exactly on that bearing, with 20° variance, with a small amount of meandering due to the hydrodynamics.

Scottish east coast salmon tend to migrate to high latitudes and Haugland *et al.* (2006) estimated when smolts are likely to be found at latitudes $>56^\circ$ N. We investigated which simulated behaviour lead to particles going broadly north and used 61° N as an indicator that they had reached higher latitudes. Haugland *et al.* (2006) indicate that Scottish smolts are likely to be found around 61° N late May. Figure 7.19 shows the percentage of particles that were further north than 61° N during the 9 month simulation period, with the latter half of May indicated on the plots. The sub-plots (a, b, c) show the results from three swim speeds, 1.5, 2.5 and 3.5 bl s^{-1} . For all swim speeds, very few ($<2\%$) of the passive particles ever made it this far north during the 9 month simulation. All the other behaviours had more success with the constant bearing behaviours succeeding in getting particles this far north by May, with $>65\%$ before July for all swim speeds and higher percentages in May for the faster swim speeds. Despite using the coastal avoidance algorithm of Ounsley *et al.* (2020), a small percentage of the particles got stuck at the coastlines (e.g. Shetland in the case of the northerly bearing results) which is why the constant northerly bearing results never quite reach 100%. The two rheotaxis behaviours do lead to high percentages of particles (typically $>50\%$) heading north, but this is late in the year (Nov-Dec). The variable rheotaxis behaviour tends to lead to particles arriving north earlier in the year than the negative rheotaxis. This is because the particles are swimming more efficiently during the migration east across the north sea, i.e. only swimming with the current if it has an easterly component. This however is not more efficient once the particles are in the Norwegian coastal current, as this current has a small westerly component forcing the particles to become passive. This is why the negative rheotaxis result ultimately overtakes the variable rheotaxis result and leads to higher percentages of particles heading north. Surprisingly, the slower swim speeds lead to lower percentages of the variable rheotaxis particles heading north. This is because if they arrive in the region of the Skagerrak earlier in the year then a higher percentage get drawn into the Skagerrak by the residual currents. Appendix A – Far-field particle density plots for faster swim speeds shows the particle density plots for the results from the faster swim speeds (2.5 and 3.5 bl s^{-1}). The variable rheotaxis results exhibit a spikes in the percentage of particles $>61^\circ$ N, most notably around mid-December. This is because the particles enter a region of recirculation off Norway around 61° N at this time, and are briefly taken below 61° N and then back north again.

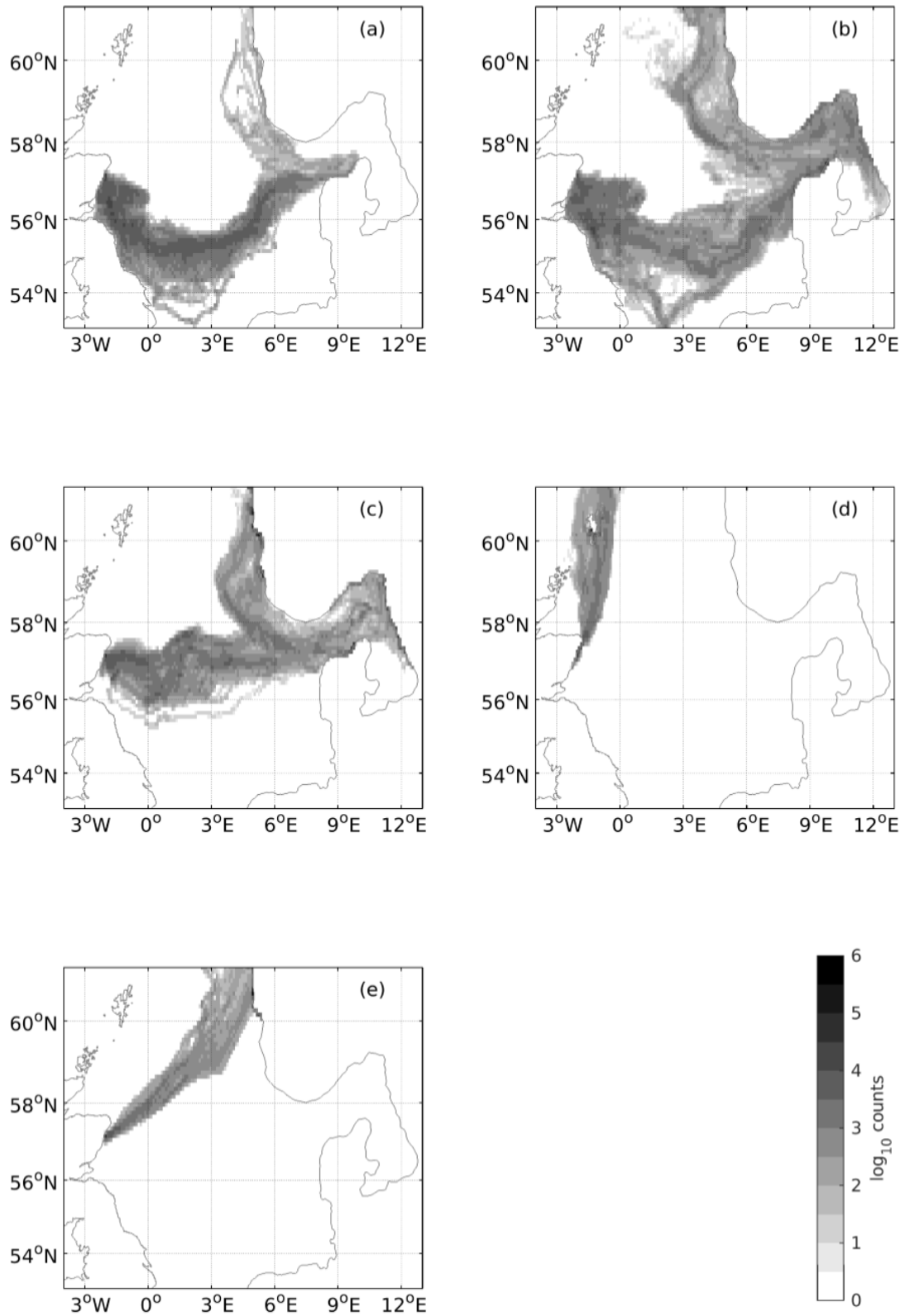


Figure 7.18: Particle density plots for (a) passive (b) negative rheotaxis (c) variable rheotaxis (d) northerly bearing and (e) north-easterly bearing behaviours for 2018, with smolt swim speed set to 1.5 bl s⁻¹ for (b)-(e). Smolt body length was initially set to 0.125m.

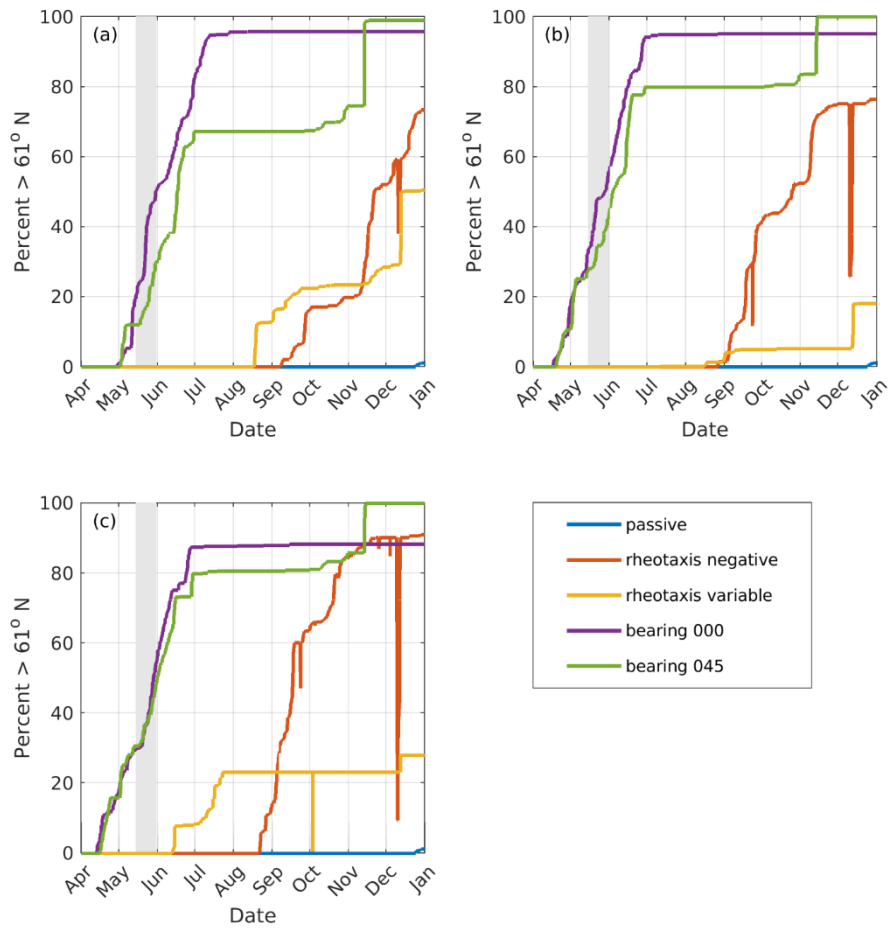


Figure 7.19: Percentage of particles further north than 61°N as a function of time for the five behaviours – passive, negative and variable rheotaxis and constant bearing to the north (bearing 000) and north-east (bearing 045), and three swim speeds 1.5, 2.5, and 3.55 bl s^{-1} , (a), (b) and (c), respectively. The vertical grey area shows the second half of May when smolts have been observed around 61°N (Haugland *et al.* 2006).

7.7 Discussion

The results presented in this study represent one of the few locations where emigrating salmon smolts are offered an un-interrupted 180 degree of expanse into marine waters of the North Sea. Smolts emigrate from the Dee in an Easterly to South Easterly direction, opposed to the predominant tidal currents which flow North South. Indeed further out from the coast salmon appear to be heading further south at an average bearing of 158° from North, 10km from the coast. This direction would not take smolts on a direct route north to feeding grounds within the Norwegian Sea. This counterintuitive directional swimming has been evidenced previously by Newton *et al.* (2021) where salmon smolts did not follow the prevailing currents within the Moray Firth (Scotland). However, Mcilvenny *et al.* (2021) suggested smolts emigrating from the Wick River (North East Scotland) were, to some extent following currents when current speed exceeded 2ms^{-1} although smolts in this study were much closer to shore (<2km) than in other studies. The general trajectories of smolts presented here seem counterintuitive as they do not directly lead towards the known Norwegian Sea feeding grounds, Ounsley *et al.* (2019) suggest a north or north easterly trajectory for east coast smolts would be most likely in their simulations. Despite slight differences between years the overall east, south easterly migration direction is maintained providing strong evidence that this is the regular migratory route of smolts emigrating from the Dee. These smolts must, at some point in their migration, make a course adjustment to allow for a more northerly trajectory to the feeding grounds in the Norwegian Sea this variation in direction during migration was also suggested by Ounsley *et al.* (2019).

The near-field simulation results were compared to the tagged smolt data obtained from curtains A and C, and can therefore more usefully be used to infer smolt behaviours in this nearshore environment. In this nearshore zone off the Scottish East Coast the constant bearings explored do not compare well with the tag observations. Repeatedly, the tagged smolt observations show detections at the east and southeast sectors of curtains C and D, whereas the constant bearing results all cross the outer arrays at more northerly sectors. The constant bearing results also all cross the arrays at very well defined, narrow, sectors, whereas the tag data reveal the wider dispersal nature of the smolts in the nearshore area. The modelled behaviour that compares most closely with the results from the tag data, in terms of array crossing locations, is the variable rheotaxis behaviour where particles/smolts *follow* the tide but only swim when the current is broadly heading away from the coast (has an easterly component). This current following behaviour reproduces the natural dispersal detected by

the arrays. The ability of migratory fish to determine directionality of currents without a spatial context, or a fixed point of reference remains unknown.

The spatial analysis suggests that the variable rheotaxis performs best for the swim speed of 1.5 bls^{-1} , but this does not agree with the timing data from the acoustic array, in that it takes too long for the particles to reach the 2019 outer array. This difference in timing reduces with higher simulated swim speeds, with 3.5 bls^{-1} agreeing with the tag data. It is however important to recognise that only 67% of the 33 smolts were detected by the outer acoustic array in 2019.

Only the passive and rheotaxis behaviours reproduce natural dispersal of the smolts. For this reason it is unlikely that the smolts are following a constant bearing when swimming in the nearshore zone close to their harbour mouth, or they are finding it hard to stick to this bearing in these high tidal environments. Nonetheless, the constant bearing is most successful in getting particle/smolts to high latitudes by May-Jun. The possible behaviour change, from a current following behaviour to a constant bearing (Ounsley *et al.* 2019), may occur as the fast tidal currents reduce away from the coast, or when the region of freshwater influence from the river reduces (salinity increases). Similarly, the variable rheotaxis behaviour explored here could be replaced with a modified one, e.g. where the smolts swim with the current only when it has a northerly component. Modelling behavioural changes such as these would be potentially interesting future work.

The hypothesis of a change in behaviour is supported by the far-field migration simulations where constant bearing behaviours were most successful at getting particles to high latitude ($>61^\circ \text{ N}$) earlier (May-June) in the year, this was also found by Ounsley *et al.* (2019). The negative and variable rheotaxis results did show some success however, and were always going to perform less well than a constant bearing as they take a more meandering route following the tide and residual currents. These two rheotaxis behaviours also successfully get particles away from the Scottish East Coast, but fail to get a high percentage of particles to head north once they arrive in the east of the North Sea where they experience different hydrodynamic conditions to those off the Scottish East Coast (Western North Sea).

The simulations performed here use extremely simple behaviours that do not adapt or change with time or the conditions experienced by the smolts. In reality the smolts are likely to be more adaptable and may seek to swim in the most optimal or efficient manner. For example, they are likely to vary their swim speed during their migration rather than using the constant speeds simulated here. This change in swim speed could account for the discrepancy between the simulated and observed times difference (between harbour and acoustic arrays), e.g. the

smolts may have sped up, or changed their behaviour, somewhere between the 2018 (Curtain C) and 2019 (Curtain D) ALS positions.

The results presented here attempt to compare the simulated particle trajectories with the acoustic tag data. Two approaches comparing first detections and all detections were used, and the timing results only used first detection results/data. Whilst these methods (comparing particle tracking with observations) were designed to be as compatible as possible, there are uncertainties associated with the analysis. For example, all the simulated particles tracked are accounted for at the inner and outer arrays whereas not all (67-88%) were detected in reality. Similarly, only the tags that were detected at the harbour were simulated and their release times were taken as the last detections. In reality, more tagged post-smolts left the harbour and their departure times may have been different to those simulated (i.e. a different time in the tidal cycle). The time analysis was only conducted using first detection times at the inner and outer arrays and a further analysis using the last detection times could potentially give some insight to the uncertainty between the two methods.

The underlying hydrodynamics heavily influence the particle trajectories, especially the passive and rheotaxis results. The constant bearings are less affected by the hydrodynamics, especially for the faster modelled swim speeds which dominate over the background currents. Any uncertainty in the hydrodynamics will therefore propagate through to the particle tracking results. This work used flow fields from the Scottish Shelf Model, SSW-RS, which has a spatial resolution of around 500-1000 m in the nearshore zone. Offshore this resolution is more than appropriate, but accurate hydrodynamic modelling of the nearshore zone typically requires high spatial (and often temporal) resolution. Marine Scotland Science is developing a higher resolution model of this region, as part of their Scottish Shelf Model (<https://marine.gov.scot/themes/scottish-shelf-model>) suite of models, and future work could utilise these high resolution model outputs. The precise timing of the particle releases could potentially influence their subsequent near-field trajectories. This uncertainty was minimised using the harbour mouth detection times, but future work could investigate this sensitivity.

The direction of migration for smolts from the Dee suggests a likelihood of encounter with planned offshore wind developments to the South (e.g. Scot Wind E3 and E1). The result of this encounter remains unknown. However it has been hypothesised that congregations of marine predators have the potential to prey on emigrating smolts. Friedland *et al.* (2016) suggest that shifts in the distribution and intensity of predators in the Baltic has reduced post-smolt survival, primarily as a result of change in Cod (*Gadus morhua*) distributions.

Aggregations of predators (mainly cod) have resulted in mortality of up to 24.8% for the Rivers Surna and Orkla in Norway (Hvidsten and Mokkalgjerd, 1987; Hvidsten and Lund, 1988). However no such predatory effects were reported in the Tana (Northern Norway) despite predators being present, this was likely due to the large abundance of lesser sandeels as an alternative food source (Svenning *et al.* 2005). There is a key requirement to understand the effects of renewable developments on salmon smolts, these are likely to be indirect potentially through changes in predator and prey distributions. In the current study, predation events were detected in the estuaries and lower river of both the Dee and Don but not on any marine curtains, providing a baseline should developments in the area cause a shift in predator prey dynamics. Similarly, the lower river appears to be a key spot for predation of smolts thus changes in predatory behaviour or increase in densities here may also negatively affect the numbers of successful migrants.

The relative few missing fish between the end Aberdeen harbour (H2) and the outer Curtains (C and D) in this study suggest data collection was robust and that the number of tagged fish detected most likely represents the wider population. Had many fish entering the marine environment not been detected on the outer Curtains this would have been cause for concern, however this was not the case. Around 80% of those fish detected at the lower River Dee (R12) were detected on the outer most curtains. Although the numbers of fish missed in 2019 and 2021 was likely slightly higher due to the wider spacing of marine ALS in curtain C and D.

The only detected predation events within the River Dee occurred within the lower river and harbour, no confirmed predation events were identified outwith the harbour area. However, caution should be applied here in that it is not always possible to determine if a tag has been consumed by a predator or not, this is only possible where tags have predation sensors or where marine mammals or birds consume a tag that can record temperature, thus estimates of predation in this study should be treated as a minimum estimate. Within the Don, predation events were also recorded further upriver within the freshwater sections of the study. Predation pressures are likely to vary between specific locations and future studies are required to identify the causes of this predation and determine if it is heightened by tagging, or other anthropogenic means or if the level observed is simply natural predation.

This study provides further evidence to that presented in Newton *et al.* (2021) that salmon smolts are located primarily in the top few metres of the water column directly addressing needs outlined in the ScotMER evidence maps ([Streamlined ScotMER evidence map - gov.scot \(www.gov.scot\)](https://www.gov.scot/evidence-maps)). Diving has been reported within adult Atlantic salmon (Hedger *et*

al. 2022) and it is not certain when such diving behaviour is initiated, it is possible that acoustic telemetry is not adequately suited to detecting such behaviour. However the tendency of surface layer occupation of smolts suggests there is further potential for interaction with offshore marine renewable developments, such as floating tidal, wave and wind installations, the effect of which remains largely unknown.

The data presented here have shown how the near shore (< 20km) movement of Atlantic salmon smolts is not simple to predict. The insights seen in these data suggest that developments further to the south east of the River Dee have potential for interaction with migrating smolts from the Dee and Don should their trajectory be continued. The emerging evidence supports the hypothesis that different migration trajectories are employed by salmon populations emigrating from different regions along the coast, with fish in this study heading south east yet migrating smolts from the Moray Firth region migrating due east (Newton *et al.* 2021) and highlights the need for further studies determining the connectivity between salmon populations and potential renewable development areas.

7.8 Conclusion (Salmon)

The aims of the salmon smolt work were:

- a) What is the predicted spatial distribution of salmon smolts from the Rivers Dee, Don and Ythan upon leaving their rivers?
- b) How does the distribution of smolts vary depending on variation in smolt size (and hence swimming speed), weather and date of sea entry?
- c) Is there evidence of narrow or wide dispersal of smolts from each river? This question is important for establishing whether a development might be encountered by a large or small proportion of the fish from a given river.

Atlantic salmon smolts emigrating from the Aberdeenshire Dee in the east of Scotland migrate in a south easterly direction within the first 20km from shore, a pattern which is maintained throughout each study year. There is therefore potential for connectivity of salmon populations on the east coast of Scotland to marine renewable developments further south than previously thought. The initial south easterly migration direction is counterintuitive to the known feeding grounds of these salmon populations in Norwegian waters, and further highlights the challenges in predicting the early marine migrations of salmonids. To reach Norwegian feeding grounds the emigrating smolts are required to migrate north. Identifying the location at which this transition occurs is a critical component in determining connectivity with marine

developments, and in the assessment of potential cumulative effects on populations should they migrate through multiple marine development sites. This study has demonstrated the value of acoustic telemetry in determining migration routes of tagged fish. However, the methodology has significant logistical and resource constraints further offshore, where epipelagic trawling may be a more appropriate method for determining spatial distribution of salmon. This method has been successfully used for both Pacific and Atlantic salmon populations, and integration of the two is likely to provide a tractable route to further inform spatial distribution of salmon within the North Sea.

Telemetry studies across multiple rivers within a larger geographic region would provide valuable information on determining migration routes in the near shore environment and provide more robust inputs for simulations of migration routes. As seen in this study, some salmon from the Don migrated in a more northerly direction as opposed to south east, suggesting that there may be slight differences between populations in close proximity. The grid array deployed in 2021 would have provided added information on the nearshore trajectories, however the Covid pandemic severely restricted fieldwork and thus relatively few fish were tagged in the River Dee.

Fish were relatively well dispersed across the study with no evidence of aggregation but were generally heading in the same south easterly direction. However, it is important to note that the tagged individuals represent only a fraction of the total population migrating each spring, thus despite being apparently dispersed these fish may well be within larger concentrations of untagged migrating salmon smolts. There was no evidence to suggest smolt size was related to the migration direction, though due to the tag size, fish in this study were limited to larger individuals within the population. Where fish size effects have been shown to be significant in other studies, extremely large sample sizes are required for such effects to be detected.

The outward salmon smolt migration was relatively fast with fish predominantly detected within the top 3m of the water column, and thus potentially at risk of predation from surface feeding avian species as well as predators within the water column. Despite the relatively low sample size and rapid migration, a number of tags identified predation events within Aberdeen Harbour, suggesting a considerable risk of predation in nearshore environments.

In conclusion, salmon emigrating from the River Dee and Don migrate in a south easterly direction, the migration is relatively rapid and undertaken within the top few meters of the water column. No evidence of aggregation along nearshore migration lines was apparent, but only

a very small proportion of the population were tracked. Future acoustic telemetry work would provide further insights into the complex migrations of Atlantic salmon smolts.

8 Sea Trout

8.1 Introduction

Salmo trutta have a widespread distribution across the globe (MacCrimmon and Marshall, 1968) and the species as a whole is considered to be of “least concern” by the IUCN (Wilson and Veneranta, 2019). Although most stocks are not formally assessed, Wilson and Veneranta (2019) note that some populations, such as those found in Portugal, are vulnerable and that other countries including the UK are reporting reduced rod catches of sea trout (sea trout is a general term that can include both anadromous and semi-anadromous *Salmo trutta*). A report from Marine Scotland Science (2015) showed that sea trout rod catches across Scotland’s districts have been variable but overall have shown a steady decline since 1952, suggesting that sea trout are experiencing increased pressures. Moore (2020) has shown that the decline was more pronounced on the West than the East coast.

It is unclear what is causing the decline in sea trout rod catches within Scotland. Moore (2020) reports that environmental effects such as greater winter rainfall had a negative correlation with sea trout catches. However, Wilson and Veneranta (2019) suggest that sea trout rod catch decline could be due to migratory obstacles such as dams and weirs, aquaculture pens with their associated pathogens, and development in estuaries, such as ports. It is possible that environmental factors, such as an increase in winter rainfall, coupled with increased anthropogenic effects are responsible for their decline (Moore, 2020; Wilson and Veneranta, 2019).

Depending on a combination of environmental and genetic factors trout can follow a range of life history strategies: remaining within their natal waterbody (resident), migrating between different freshwater bodies within a river system (potamodromous), or migrating to and from brackish or marine environments (anadromous) (Ferguson *et al.* 2019). Fish that migrate to sea are commonly called ‘sea trout’ while the fish that remain in fresh water are known as ‘resident’ or ‘brown’ trout. Within this categorisation of strategies there is a further range of life history options. Some anadromous trout migrate into estuarine areas or brackish water but migrate no further and are thus referred to as semi-anadromous whereas trout that make it to marine water are commonly referred to as anadromous (Chapman *et al.* 2012; Ferguson *et al.* 2019).

Within Scandinavian countries, estuaries have been found to be crucial habitat for *Salmo trutta* with specific emphasis on fjords and fjards, (Aldvén and Davidsen, 2017). This may be

because estuaries can be nutrient rich habitats, as they have freshwater and marine inputs, meaning that they can be rich in species and abundance (Dobson and Frid, 2009). However, Aldvén and Davidsen (2017) note that few studies have investigated *Salmo trutta* within different estuarine habitats such as those found in the UK. Fjords and fjards together cover only 7% of total area of estuaries within the UK, Aldvén and Davidsen (2017) suggest that further research should be conducted in other estuary types to investigate how *Salmo trutta* differ from their Scandinavian counterparts. To date, few studies have investigated whether variation in migration strategies exhibited by *Salmo trutta* also exist in river systems where there is little estuary and no sea loch or fjord. Fjords and sea lochs create a diverse range of intertidal habitats which may promote differentiation in migration strategies (Aldvén and Davidsen, 2017). However, what is yet to be seen is if these strategies still exist in a coastal plain estuary, where a river discharges into the open sea with an unconstrained coastline.

The study presented here uses acoustic telemetry to track smolts naturally emigrating from the River Dee (North East Scotland) out into the marine environment. The River Dee has very little estuary habitat and discharges directly into the North Sea providing smolts with an unconstrained coastline of 180°.

8.2 Methods

8.2.1 *Tag Specifications*

In 2018, two types of tags were used: Nineteen trout smolts were tagged with the Thelma Biotel ADTT-LP-7,3 (69Khz, 22mm length, 7.3mm diameter, 2g in air 139 dB re 1 μ Pa at 1m) with sensors for depth and temperature. The depth calibration for these tags were set at 0 to 290m with a precision of 0.5m. The temperature was set at 0 to 25.5°C with a precision of 0.1°C and a battery life of 101 days. Thirty four trout smolts were tagged with the second type of tag the Thelma Biotel ATID-LP-7,3 (69khz, 18mm length, 7.3mm diameter, 1.9g in air, 139 dB re 1 μ Pa at 1m) and a battery life of 87 days.

Twenty six trout smolts were tagged in 2019 using Vemco V7D-2x-069k-1. (69khz, 22mm length, 7mm diameter, 1.7g in air with a sound volume of 139 dB re 1 μ Pa at 1m and with an estimated tag life of 93 days). This model of tag is classed as a predation tag which sends a different signal when a biopolymer switch dissolves in acid of animals' stomachs (Halfyard et al., 2017).

8.2.2 Study Array for 2018 and 2019

Harbour and marine ALS locations are described in section 6.4 Receiver Locations. In addition, in 2018, 12 ALS were deployed in the River Dee (R1 to R12) (Figure 8.1). R1-R11 are in fresh water, R12 is 2.7km below the maximum tidal reach where, due to the increase in sea level, the river starts backing up at high tide. Seaward of this the marine curtains are the same for the rest of the study as described in section 6.4 Receiver Locations.

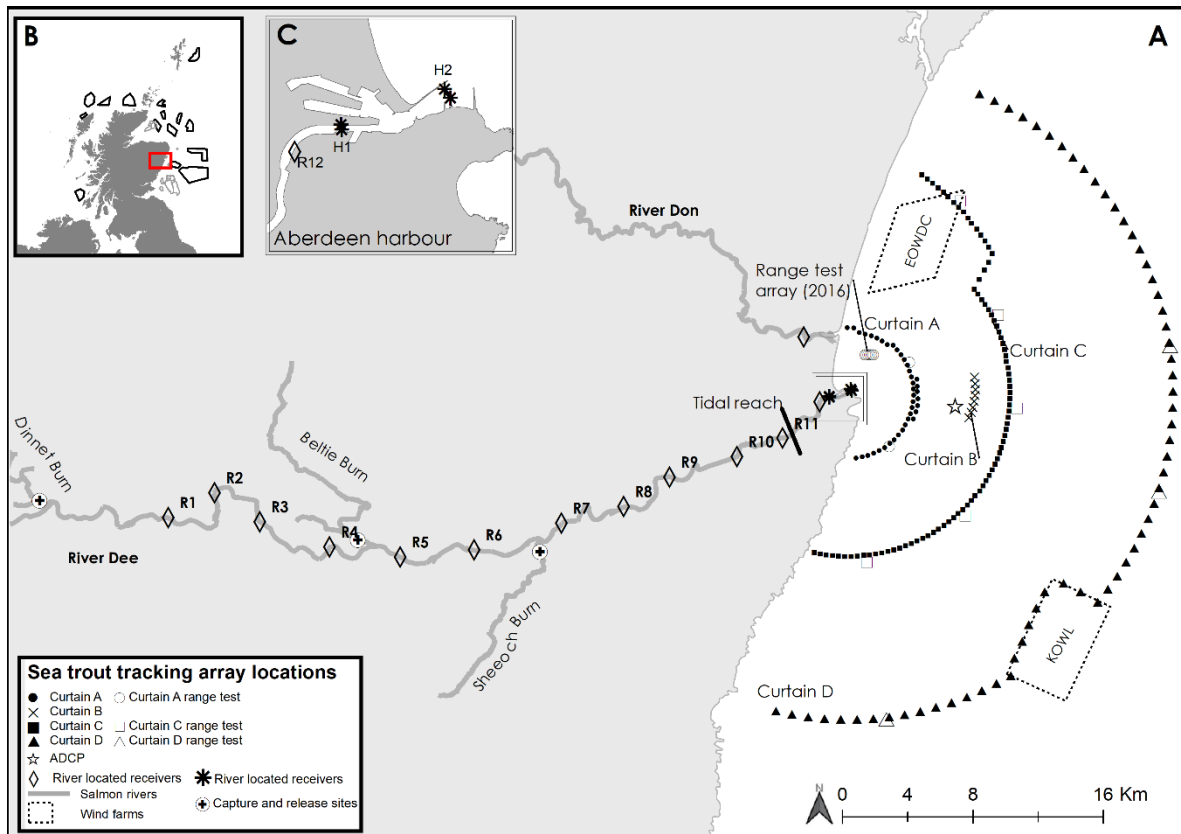


Figure 8.1: The study site with the location of ALS and release locations, curtain A, B and C in 2018, curtains A and D 2019. Vattenfall's European Offshore Wind Deployment Centre (EOWDC) and Kincardine Offshore Wind Farm (KOWL) are denoted by a dashed boarder. Insert B: study site within larger geographic area including built (outlined in grey) and planned (outlined in Black) windfarm locations. Insert C: Harbour ALS locations.

8.2.3 Defining habitat at ALS locations

ALS R1 to R11 were classed as river habitat receivers, as they were all above the tidal reach and therefore above the estuarine area. ALS R12, H1 and H2 were all classed as estuary habitat as they were below the tidal reach and before the harbour break walls, which can exhibit brackish salinity under the Venice system (1959), with the mixing of the river fresh water and full marine water depending on the tidal cycle. All ALS seaward of H2 had a salinity of more than 30 parts per thousand (ppt). The marine ALS on curtain A were separated into

three habitat classifications based upon chart datum depths: littoral waters less than 10m, shallow water 10m to 25m and pelagic water depths of 25m or greater (Figure 8.2), as adapted from Eldøy *et al.* (2015) and Flaten *et al.* (2016).

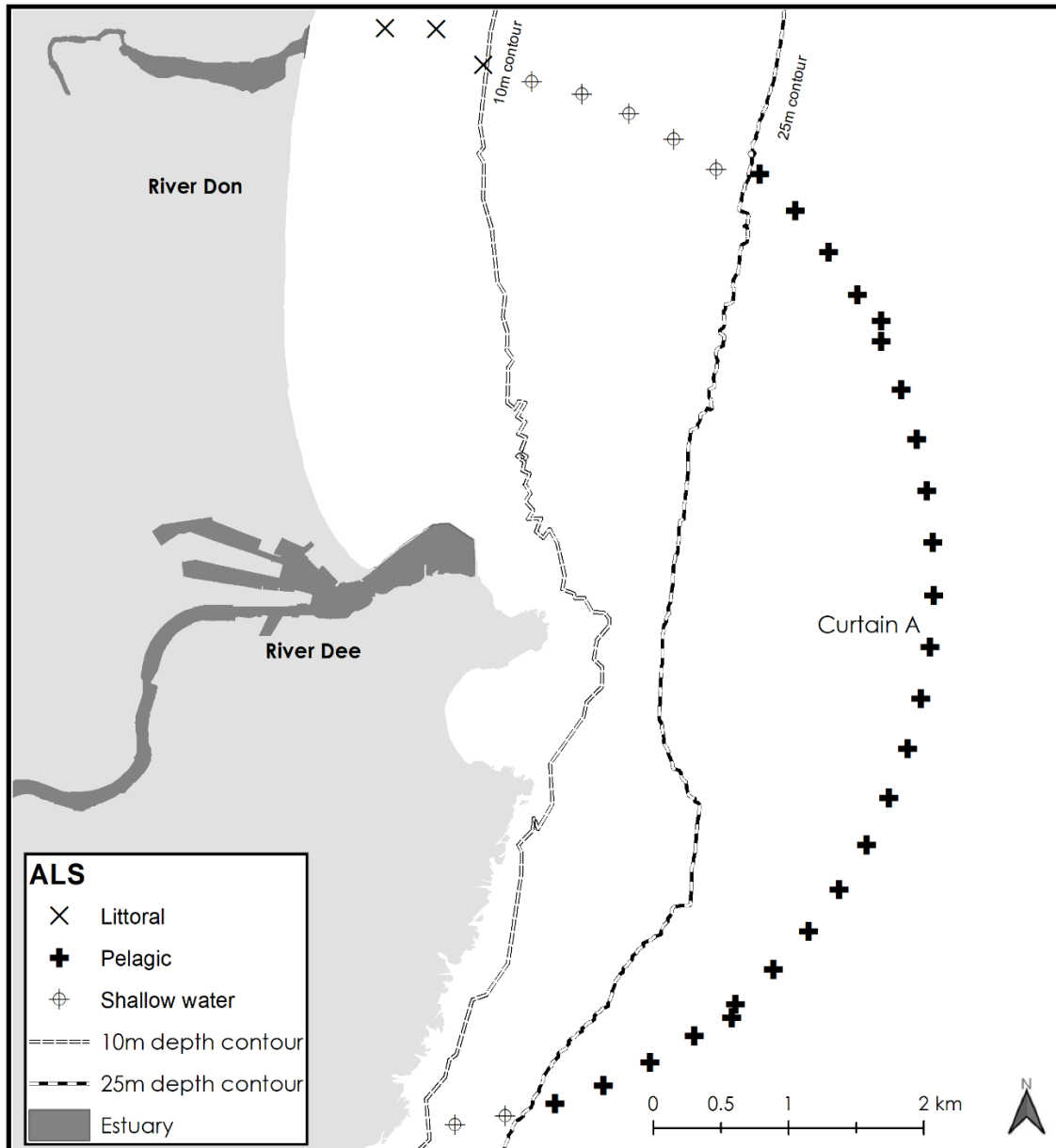


Figure 8.2: Marine habitat classification where ALS were deployed were; littoral ($\leq 10\text{m}$, black X), shallow water ($>10 - 25\text{m}$, circle bisected with black plus and), pelagic ($>25\text{m}$, bold black plus)

8.2.4 Data Handling

All raw data exported from Vemco's VUE software was initially screened for predation events using R software and the Actel package (Flávio and Baktoft, 2020). Actel was used to identify tag detections which were suspected to have undergone ingestion by predation and inactive

tags by either increased temperature or an activated predation tag (Halfyard *et al.* 2017). After suspected predated tags were removed, the data were screened for false positive detections (a single detection of a tag within 30mins) from the estuarine ALS, which is a method used by Eldøy *et al.* (2015) and Flaten *et al.* (2016). In 2018, this method identified a total of 588 (0.6%) possible false positive detections, these were thus removed from the original 100,340 detections. In 2019, 242 (0.58%) possible false positive detections were removed from the original 42,546.

8.2.5 Categorising of migration strategies.

The observed migration of each *Salmo trutta* smolt in this study was allocated to one of five groups. Three of these are migration strategies based upon discrete patterns of behaviour and the basis of habitat use. Two categories were assigned as “predated” and “No data”. The group “No data” were smolts that were never detected after release from tagging. Predated were smolts identified as being predated as described in data handling section 8.2.4 and in Table 8.1. Examples of predated smolts can be seen in Figure 8.4.

The three migration strategies were: potamodromous, semi-anadromous and anadromous. Potamodromous consisted of smolts that were detected on ALS R1 to R11. Within the potamodromous group it was not always possible to determine the tags’ fate, thus it cannot be confirmed that migration ceased due to a biological decision to stop migrating, predation, the smolt died naturally, or battery life of tag ceased prior to completion of migration.

Smolts were assigned to the semi-anadromous group if they successfully migrated to, and were detected by, any ALS in the estuary (R12, H1 and H2) and not detected on any of the marine ALS. The anadromous group is defined as any smolt that was detected at least once on any of the marine ALS. Definitions and rules for placing smolts into each category can be seen in Table 8.1.

Table 8.1: The allocation of migration outcomes and their definitions.

Group (Migration Strategy)	Rules for placing smolts in the group
Potamodromous (2018 only)	<p>Smolts that were detected at least once on any of the ALS R1 to R11 in 2018</p> <p>Smolts were not detected on R12, H1, H2 gates or any marine ALS.</p> <p>This category was not possible in 2019, as R1-R11 ALS were not in place. Smolt migration may have ceased prior to the ultimate migration strategy being identified, for example if predation occurred between ALS and no subsequent detections of the tag occurred.</p>
Semi-anadromous	<p>Smolts that were detected at least once on ALS R12, H1, and H2 in 2018 and 2019</p> <p>Not detected on any marine ALS</p> <p>Smolt migration may have ceased prior to the ultimate migration strategy being identified, for example if predation occurred between ALS and no subsequent detections of the tag occurred.</p>
Anadromous	<p>Smolts in 2018 and 2019 that were detected at least once on a marine ALS.</p>
Predated	<p>When temperature exceeded the ambient water temperature (Strøm <i>et al.</i> 2019)</p> <p>When the predation tag exhibited a signal of four to 255 (Halfyard <i>et al.</i> 2017)</p> <p>Confirmed predated tags are not included in migration analyses as end migration point cannot be determined.</p>
No data	<p>Smolts that had no detections on any ALS in the study period (2018/2019)</p> <p>In 2019 this may have included smolts that would have been classed as potamodromous. However due to no ALS in the river above the tidal reach it is not possible to determine their migration end point.</p> <p>Smolts were not classed as potamodromous as the reason for them not reaching the estuary could not be determined.</p>

8.2.6 Statistical analysis

To test if potamodromous, semi-anadromous and anadromous migration strategies, (defined in Table 8.1), were dependent upon their stream origin (Hypothesis 1) a chi squared goodness of fit test was used to compare observed migration strategies against expected, for each capture location.

To test if there was any statistical difference between; fork length, body weight, Fulton's body condition ($100 * (\text{Smolt weight in air (g)} / (\text{Fork Length (cm)})^3)$), tag burden, and stream origin (Hypothesis 2), a one-way ANOVA was run for each continuous response variable against the explanatory factor variable the stream origin.

To test if there was any statistical difference between the groups of smolts outlined in Table 8.1, potamodromous, semi-anadromous, anadromous and no data, (predated smolts were excluded as the sample size is too small) the response variables: fork length, body weight, Fulton's body condition, Julian day of release, tag burden and their group were used (Hypothesis 3). A one-way ANOVA was run for each response variable against the explanatory factor group. Smolts with no data were tested in case they were significant in other ways which might explain why they were never detected.

Multiple regression ANCOVA was used to test which factors influence mean migration ground speed through the river between anadromous and semi-anadromous smolts (Hypothesis 4/Model 1). Mean ground speed was the dependent variable and used as an indicator of how much smolts utilise riverine environments. Mean ground speed was calculated as time between release and first detection at R12, divided by distance between stream origin and R12. Mean ground speed was tested for a normal distribution using a Shapiro-Wilk test, which significantly differed from normal distribution ($W=0.601$, $p= 3.26^{-9}$) and therefore the smolts ground speed was log transformed to enable normalising of the data, and retested to confirm normality ($W=0.956$, $p= 0.123$). Explanatory variables in the model were: migration strategy (anadromous or semi-anadromous), stream origin, year of study, Fulton body condition, fork length. This model was then subjected to likelihood ratio test (LRT), with the least significant explanatory variables being removed until the simplest model remained.

Model 1: Ground speed through the river (m/s): Multiple regression/ANCOVA

Log (mean migrating ground speed through river(m/s)) ~ Migration Strategies (Semi-anadromous and anadromous) + stream origin+ year of study + Fulton's body condition + fork length (cm)

To test whether the estuary is a staging post, the anadromous smolts speed should significantly decrease from their in-river migration to effectively utilise the resources within the estuary (Hypothesis 5). Anadromous smolt mean ground speed was calculated through the river from tagging location. The initial detection on R12 and migration through the estuary is from R12 to their last detection on any of the following ALS H1 and H2. A Wilcoxon signed rank test was used to determine difference in mean ground speed between fish migrating in fresh water and those migrating through the estuary.

Multiple regression ANCOVA was used to test which factors influence the total time in the estuary for anadromous and semi-anadromous smolts (Hypothesis 6/Model 2). Total occupancy time in the estuary was calculated as the total time a fish was detected on and between ALS R12, H1, and H2. Total time in the estuary differed from normality (Shapiro Wilks test $W=0.712$, $p=1.569 \times 10^{-7}$) and was therefore log transformed. Explanatory variables in the model were: migration strategy (anadromous or semi anadromous), stream origin, Fulton body condition, fork length, Julian day of release, year of study, Julian day of arrival at R12. This model was then subjected to likelihood ratio test (LRT) with the least significant explanatory variable being removed until the simplest model remained.

Model 2, The time spent in the estuary: Multiple regression/ANCOVA

$\text{Log (Total Occupancy Time in Estuary (days))} \sim \text{Migration Strategies (Semi-anadromous and anadromous)} + \text{Stream origin} + \text{Smolts Fulton's body condition} + \text{Fork Length (cm)} + \text{Julian day of release} + \text{Year of study} + \text{Julian day of arrival at R12}$

Table 8.2: showing models 1 and 2, variables, their description, and the model they were used in

Response or explanatory variable	Variable	Description of Variable	Model used in
Response	Log (Mean ground speed of anadromous smolts in river) (m/s) (Numeric)	The natural log of (the time it took for anadromous and semi-anadromous smolts to swim from their stream origin to R12)	1
Response	Log (Total occupancy time in Estuary) (Numeric)	The natural log of (The sum of all residency events at ALS R12, H1 and H2 and the time spent between these ALS. Time is per smolt)	2
Explanatory	Semi-Anadromous and Anadromous Migration Strategies (Factor)	Semi-Anadromous, Anadromous smolts as per Table 8.1	1,2
Explanatory	Stream origin (Factor)	The sites the smolts were tagged and released: Beltie, Dinnet and Sheecho	1,2
Explanatory	Fork Length (cm) (Numeric)	Smolts length from nose to the fork in the caudal fin	1,2
Explanatory	Smolts Fulton's body condition (Numeric)	$100 * (\text{Smolt weight in air (g)} / (\text{Fork Length (cm)}))^3$	1,2
Explanatory	Year of study (Factor)	The year study took place	1,2
Explanatory	Julian day of release (Integer)	Julian date of the smolt being released	2
Explanatory	Julian day of arrival at the last river ALS (R12) (Integer)	Julian date of the smolt arriving at the last river ALS. (first detection on ALS R12)	2

The estuary habitat of the Dee was further subdivided into two separate sub-habitats; the last river ALS (R12), which maintains many natural features of a river and at low tide is completely fresh water, and the harbour, which exhibits a salt wedge and is artificially modified (Hypothesis 7). To test whether smolts significantly differed their habitat occupancy time usage between the last river ALS (R12) and the harbour, the smolt's total time in each habitat was

tested with a paired sample Wilcoxon test (Nonparametric). Total occupancy time for lower river ALS is the sum of residency events on ALS R12. Total occupancy time in harbour is the sum of all smolts residency events on and between ALS H1 and H2.

To test how anadromous smolts from the River Dee use this distinctive marine geography in both years (Hypothesis 8) occupation time between littoral, shallow and pelagic habitats were compared, using Kruskal-Wallis rank sum test. Occupation time was calculated as the total time spent within each habitat on Curtain A. This was standardised for the number of receivers within each habitat by dividing total time by the total number of ALS within that habitat; a method used in Eldøy *et al.* (2015) and Flaten *et al.* (2016). Curtains B, C and D were not used as they were not present in both years (Figure 6.1).

A chi squared test of independence was used to determine if there was a difference in space use between the two study years. Space use was determined by the number of detections per habitat per year. Totals were divided by the number of anadromous smolts, to account for variation of smolts tagged between years (2018=7, 2019=15). Only detections on marine ALS, which were present in the same location for both 2018 and 2019 were used. Number of detections was used as a proxy for time spent in the habitat

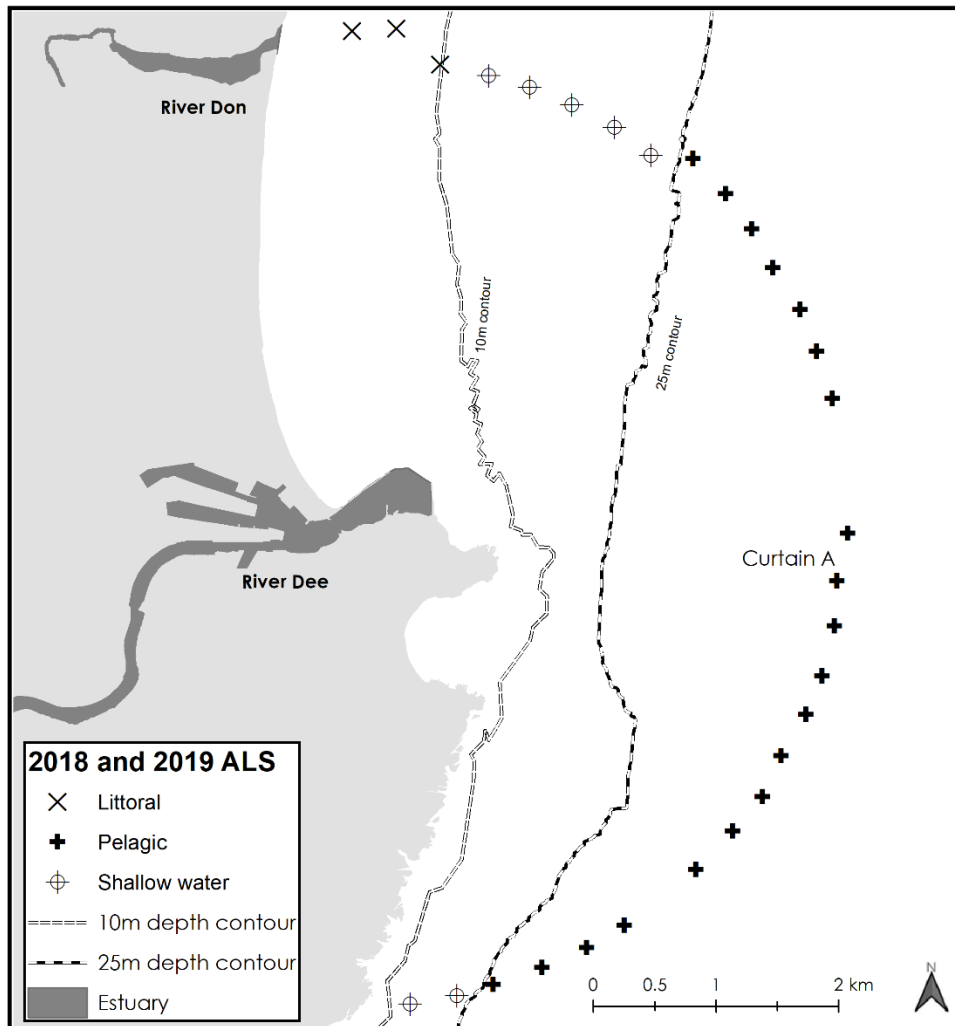


Figure 8.3: Map of the ALS on curtain A. Notes: The ALS were positioned in the same place in 2018 and 2019 for yearly comparison. Habitat where ALSs were deployed was split into littoral (black cross), pelagic (bold plus sign) and shallow water (circle bisected with plus sign). Gaps in the marine curtain are where ALS were lost in one year and therefore cannot be compared to the other year.

8.2.7 A framework to describe the continuum of behaviours available to anadromous trout with the marine environment

Here, an anadromous trout can be any trout that enters the marine environment (salinity of >30ppt) for any length of time, thus, any trout that is detected at least once on a marine ALS is anadromous. Due to the variation of behaviour that *Salmo trutta* exhibit, it may not be possible to split anadromous smolts into two or three distinct migration categories based on location, duration, and distance. Therefore, a framework was created consisting of four criteria to describe the variation of migration behaviours that anadromous smolts could exhibit whilst in the marine habitat.

The four criteria were used to describe behaviours based on location, duration and migration distance, which will objectively place anadromous smolts into one of 36 possible unique marine migration behaviours (Table 8.1). The four criteria will describe:

- Length of time anadromous smolts initially spent in the estuary before their first foray into the marine habitat
- Number of times anadromous smolts moved between the marine habitat and estuary habitat
- How long anadromous trout spend within the marine study area, whether the anadromous trout go undetected for a 48hours while in the marine study area.
- The probable area anadromous smolt would be at the end of the tag battery life

To describe the length of time anadromous smolts initially spent in the estuary before moving into the marine habitat (Criterion one), the smolts were classed as anadromous when they spent less than 48 hours in the estuary as 'non-stager'. Anadromous smolt that stayed with the estuary for more than 48 hours was classed as a 'stager'. 48 hours was chosen as it would give the smolt ample time to migrate out with the estuary on an ebb tide, independent of arrival time. Time initially spent in the estuary was calculated by the difference in time from initial to final detection in the estuary, prior to entering the marine environment.

To describe how many times the anadromous smolts moved between the marine habitat and the Dee estuary (Criterion two), smolt that did not return to the Dee estuary during the period of tag's estimated battery life were classed as a 'non-returner'. Any anadromous smolts that returned to the estuary after being in the marine habitat once and stayed in the estuary or river was classed as 'returner'. Any anadromous smolts that moved between the Dee's estuary and the marine habitats more than once was classed as an estuarine 'oscillator'. Estuarine oscillators can return and stay in the estuary after being in the marine habitat multiple times.

To describe whether the anadromous smolts resided in the marine study areas or migrated straight through it (Criterion three), an anadromous smolt that resided within the marine study area for at least 48 hours was classed as a 'local marine occupant'. Any anadromous smolt that was detected for less than 48 hours in the marine study area and not detected again was classed as a 'local marine migrant'. 48 hours was chosen, as it would give the smolt ample time to migrate through the marine study area no matter when they exited the harbour into the sea.

The location of anadromous smolts at the end of the study period, was defined by one of three categories: natal estuary, local marine, and distant marine (criterion four). An anadromous smolt that was last detected on any ALS (R12, H1 and H2) in the estuary was assigned to the 'natal estuary'. Any anadromous smolt that was last detected on any of the ALS in the marine study 48 hours before the tag battery life was 95% consumed, was assigned to 'local marine'. Alternatively, an anadromous smolt that was not detected within 48 hours of when the tag battery life had consumed by 95% was presumed to have migrated out the study area and was classed as 'distant marine'. However, it is possible that distant marine anadromous trout were unable to complete their migration and potentially return to the study area due to being predated, or their tags may have been ejected from their body cavities as they continued their journeys.

The above framework for harbour and marine assessments makes some assumptions:

- No anadromous smolt died during the study period. This is difficult to determine, thus if an anadromous smolt did die within the marine zone, it would have been unable to complete its migration strategy (e.g., return to the estuary). Hence the following data may have been affected.

Criterion 1 – Cannot add to the overestimation, time spent in estuary is accurately calculated for each individual.

Criterion 2 - Over estimation in non-returner and underestimation of returner and oscillator groups.

Criterion 3 - Over estimation in smolts migrated straight through and underestimation for smolts that resided in the marine study area.

Criterion 4 - Over estimation in distant marine and underestimation local marine and natal estuary.

The changing of the marine array design between 2018 and 2019 had no effects on category placement

Criterion 4 - This may have led to an over estimation in 2018 for local marine and underestimation in 2019 in local marine

8.3 Results

8.3.1 *Detected Predation Events*

In this study, there were four confirmed predation events on brown trout smolts, two in 2018 and two in 2019. The two in 2018 were confirmed predated because the temperature sensor recorded 25.5 °C (maximum reading of the tag), which is greater than ambient water temperature (Figure 8.4). One smolt that recorded a reading of 25.5 °C was in the harbour, there were then no further detections (Figure 8.4). The second smolt (21st May) was recorded at 25.5 °C over two days, during which the tag was recorded on all ALS within the estuary. Over this period the tag recorded depths greater than 9m multiple times. After the two days the tag was continually recorded in the harbour at ambient water temperature of 10 °C, increasing to 12.5°C and at a depth of greater than 6m. The tag remained here for 37 days whilst the depth changed with the tidal cycle (Figure 8.4), suggesting the tag had been excreted by a predator.

In 2019, two predator tags were triggered, confirming predation events. the first was triggered in the lower river (R12) and then had subsequent detections in both the Harbour and lower river (R12). The second was triggered in the harbour and then, after its initial predation event, was never detected again (Figure 8.4).

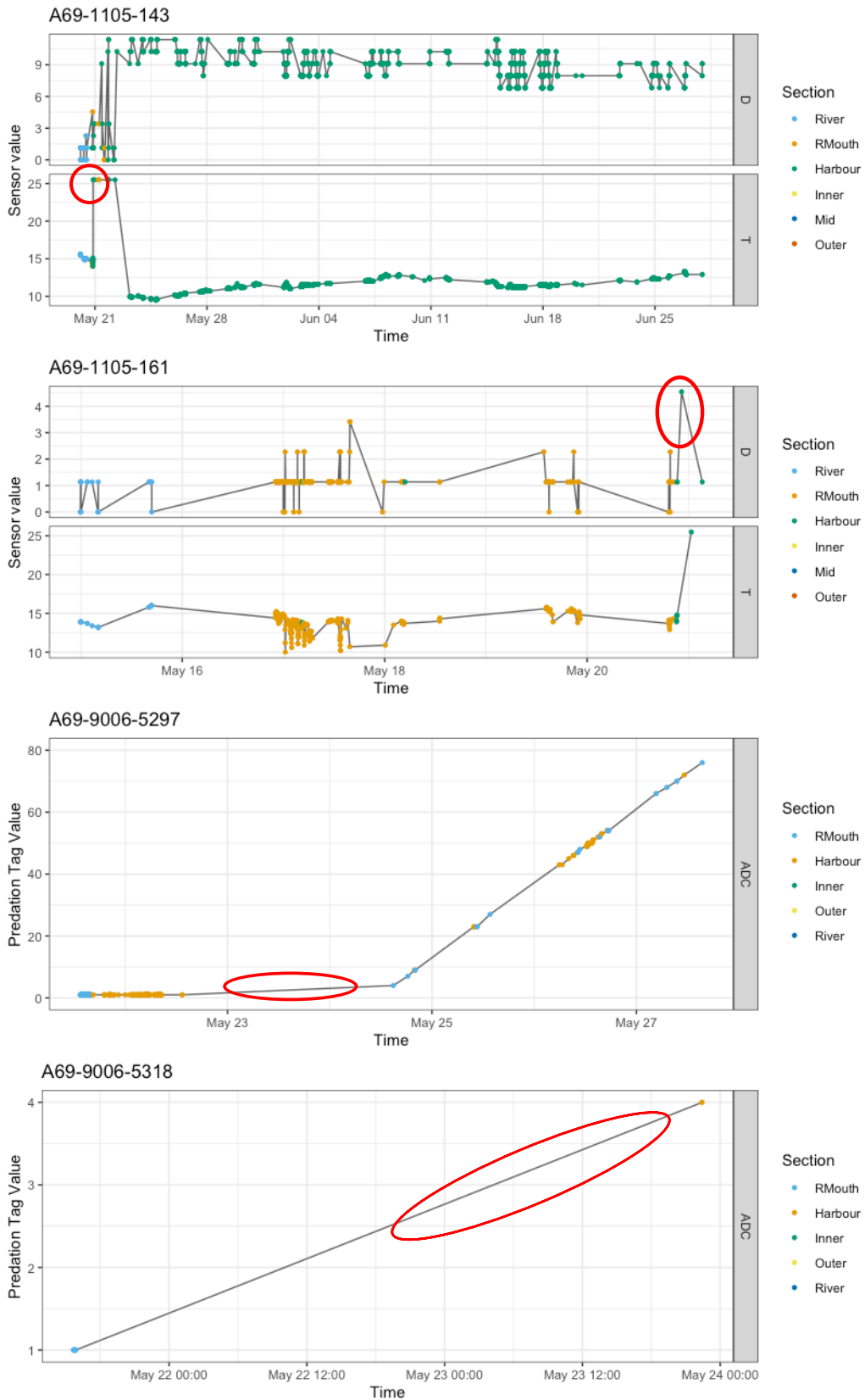


Figure 8.4: Detection plots of the four smolts that were classed as predated. Red circles indicate when predation could have taken place. Tags A69-1105-143 and A69-1105-161 are of smolts from 2018 with Thelma biotel temperature and depths tags. Tags A69-9006-5297 and A69-9006-5218 were smolts of 2019 with Vemco predation tags. Using D = Depth (m), T = ($^{\circ}$ C), ADC = Digestion sensor. RMouth is the ALS R12

In addition to the confirmed predation events, in 2018, one potamodromous smolt was recorded moving back upstream from R11, 23 km to R7 (Figure 8.5). This behaviour is abnormal for salmon smolts but not for *Salmo trutta* (Birnie-Gauvin *et al.* 2019). No other smolts exhibited this behaviour or were seen migrating back up-stream past the closest ALS to their stream origin. This behaviour was not considered confirmation of a predation event, as it was biologically plausible behaviour for a *Salmo trutta* and consequently was classed as potamodromous instead of predated.

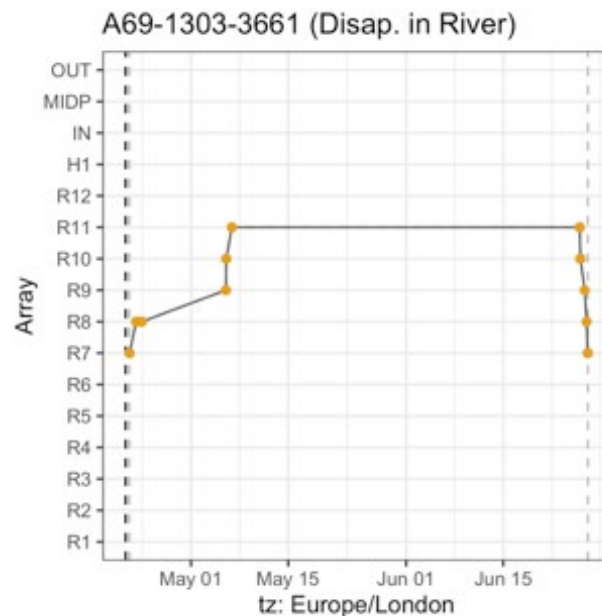


Figure 8.5: The smolt that migrated downstream then swam back 23km upstream to the area that the smolt was released. The black-hashed line is the date time of smolts release. The First vertical (grey) line is date time of first detection. The last vertical (hashed) line is the last known detection. Orange dots are detections on an ALS within the river.

8.3.2 Hypotheses test results

A chi squared goodness of fit for each smolt's stream origin found that the allocated migration strategy was not affected by smolt stream origin (Hypothesis 1). There was no statistical significance between Beltie (chi-square, df = 2, n = 19, test statistic = 0.973, p=0.61), Dinnet, (chi-square, df = 2, n = 6, test statistic = 1.33, p=0.51) and Sheechoch stream origin, and the migration strategy adopted (chi-square, df = 2, n = 24, test statistic = 2.00, p=0.36). This may have been attributed by the low number of samples at each release location.

Table 8.3: Allocation of tagged sea trout smolts into each of the five categories by tagging site and year, using definitions as described in Table 9.1. Note: N/A for potamodromous 2019 as there were no ALS within the freshwater part of the River Dee in 2019.

Group (Migration)	Location						Totals
	Beltie		Dinnet		Sheeoch		
	2018	2019	2018	2019	2018	2019	
Potamodromous	4	N/A	1	N/A	4	N/A	9
Semi Anadromous	7	2	0	1	4	4	18
Anadromous	4	2	4	0	7	5	22
Predated	1	0	0	1	1	1	4
No data	9	2	3	1	4	7	26

To test if the groups outlined in Table 8.1 (predated smolts were excluded from the test due to only four samples) significantly differed from one another in body length, Fulton's body condition, weight, or tag burden a one-way ANOVA was used for each response variable (Hypothesis 3). There was no significant difference between the smolts' group and fork length (ANOVA, $F_{(3,71)}=0.958, p = 0.417$), body weight (ANOVA, $F_{(3,71)}=1.005, p = 0.396$), tag burden (ANOVA, $F_{(3,71)}=0.802, p = 0.497$), body condition (ANOVA, $F_{(3,71)}=0.206, p = 0.892$) or day of release (ANOVA, $F_{(3,71)}=0.204, p = 0.116$).

Table 8.4: Biological differences between smolts in the four different migration groups, 2018 and 2019 data combined.

		No Detections	Predated	Potamodromous	Semi Anadromous	Anadromous	Total
Number (%)		26 (32.9%)	4 (5.06%)	9 (11.39%)	18 (22.78%)	22(27.8%)	79(100%)
Body Length (cm)	Mean	15.33	17.05	16.14	15.82	15.52	15.69
	SD	±1.29	±1.65	±2.30	±1.16	±1.13	±1.41
	Rang e	13.7-18.3	15.8- 19.3	13.8-21.3	14-17.8	14-17.7	13.7- 21.3
Fulton's Body conditio n	Mean	1.021	0.973	1.018	1.032	1.036	1.025
	SD	±0.087	±0.069	±0.069	±0.068	±0.075	±0.076
	Rang e	0.84-1.20	0.90- 1.06	0.88-1.10	0.89-1.14	0.90-1.16	0.84- 1.20
Weight (g)	Mean	37.76	48.75	45.00	41.38	39.22	40.37
	SD	±11.17	±12.60	±20.83	±8.99	±8.41	±11.67
	Rang e	25-69	39-67	29-94	27-58	28-59	25-94
Day Release d (Julian)	Mean	118.50	119.00	111.22	117.27	117.77	117.21
	SD	±8.12	±10.3	±2.22	±9.02	±7.70	±8.02
	Rang e	109-129	110- 128	109-115	102-129	109-129	109-129
Tag burden (%)	Mean	5.19	3.93	4.91	4.66	4.91	4.89
	SD	±1.26	±0.78	±1.58	±0.84	±0.97	±1.13
	Rang e	2.74-7.6	2.98- 4.76	2.02-6.55	3.03-6.29	3.22-6.78	2.02- 7.60

To test what factors most influence overall swimming speeds through the river to the last river ALS (R12), (Hypothesis 4) it was found that the best fitting model was

$\text{Log}(\text{Mean ground speed migrating through river}) \sim \text{Stream origin} + \text{Fork Length (cm)} + \text{Year of study.}$

Smolt fork length had a significant positive relationship with ground speed, with larger smolts moving faster ($p=0.0403$) (Figure 8.6). The year of tagging had significant impact, with smolts in 2019 swimming faster than smolts tagged in 2018 ($p=0.026$). Smolts' mean ground speed in 2018 was 0.23ms^{-1} , with a SD $\pm 0.29\text{ms}^{-1}$ and a range of 0.04ms^{-1} to 1.18ms^{-1} . Smolts'

mean ground speed in 2019 was 0.23 ms^{-1} , with a SD $\pm 0.07 \text{ ms}^{-1}$ and a range of 0.05 ms^{-1} to 0.34 ms^{-1} . The smolts' Fulton body condition, stream origin and the migration strategies they adopted had no correlation to their swimming speeds downriver (Table 8.4).

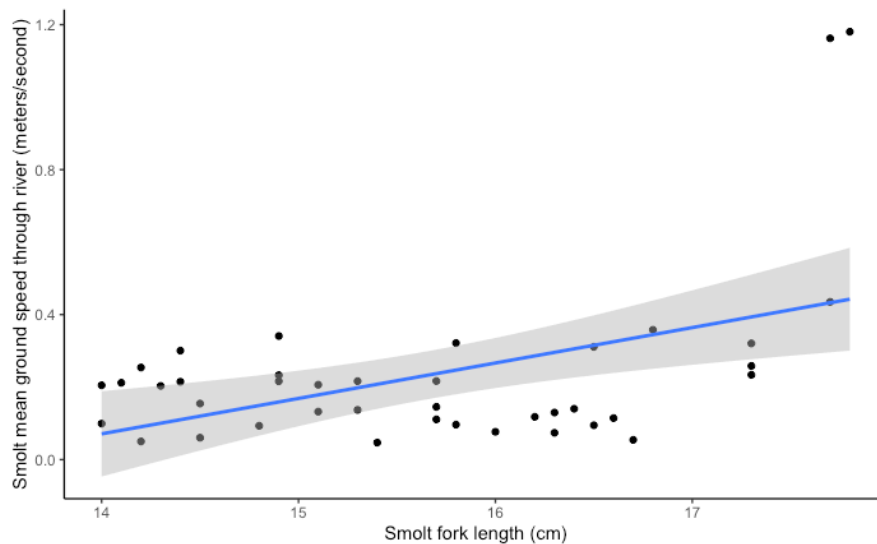


Figure 8.6: Semi-anadromous and anadromous smolts' mean ground speeds down the river, in relation to their fork length. The blue line indicates the smolts' mean ground speed though river. The grey area denotes 95% confidence intervals. Black dots are individual smolts.

To test whether anadromous smolts stage in the estuary before moving into the marine environment, smolt speeds were compared between the river and the estuary (Hypothesis 5). The comparison of speed was tested for significant difference using a Wilcoxon signed rank test. Smolts did not significantly alter their speed between the river and their initial migration through the estuary ($V=140$ $p=0.67$).

The best fitting model to determine time spent in estuary between semi-anadromous and anadromous smolts was:

$$\text{Log (Total Occupancy Time in Estuary (days))} \sim \text{Migration Strategy} + \text{Julian day of arrival at the ALS R12}$$

The smolts' migration strategy best explained the occupancy time in the estuary ($p=0.0017$), with anadromous smolts spending on average 18 days (SD of ± 19.90 , range of 0.012 to 58.034) in the estuary, and semi-anadromous smolts' mean of 3.5 days (SD of ± 8.07 , range of 0.006 to 34.89). The time the smolts arrived at the last river ALS (R12) also had a significant effect ($p < 0.001$), with smolts that had arrived earlier staying longer within the estuary (Figure

8.7). The smolts' body condition, body length, Julian day of release, year of the study or their stream origin did not contribute to the model's strength.

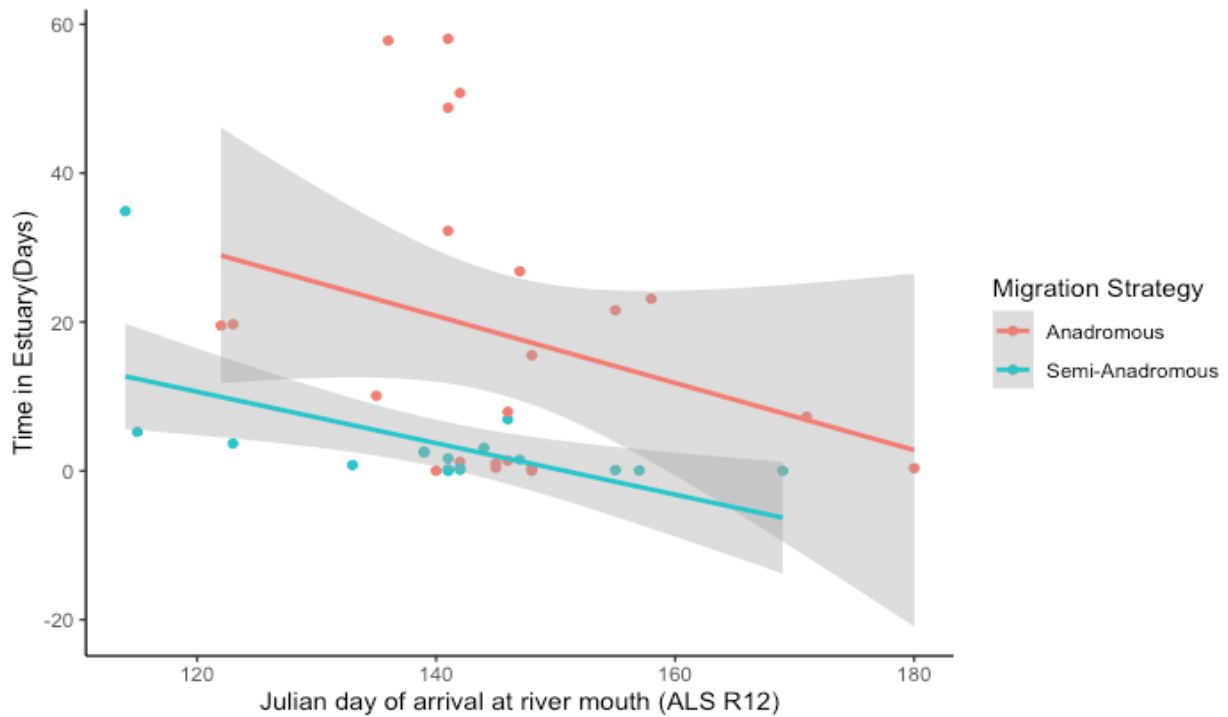


Figure 8.7: Smolts' occupancy time in the estuary in relation to their migration strategy (Semi-anadromous in blue and anadromous in red) and time of arrival at the estuary. Grey areas are 95% confidence intervals of the mean. Dots are individual smolts

To test whether both semi-anadromous and anadromous smolts spent their time equally in the harbour and lower river (ALS R12), a paired sample Wilcoxon test was used. A significant difference was found between occupancy time spent in the harbour and time spent at the last river ALS (R12, $W=115$ $p<0.001$), with smolts spending longer at lowest river ALS R12 (median 1.32 days, IQR 0.17-11.9 days and a max of 55.78 days) than within harbour (6.72 hours, IQR 2.88 minutes to 2.23 days, with a max of 11.82 days) despite the harbour covering a larger area (Figure 8.8).

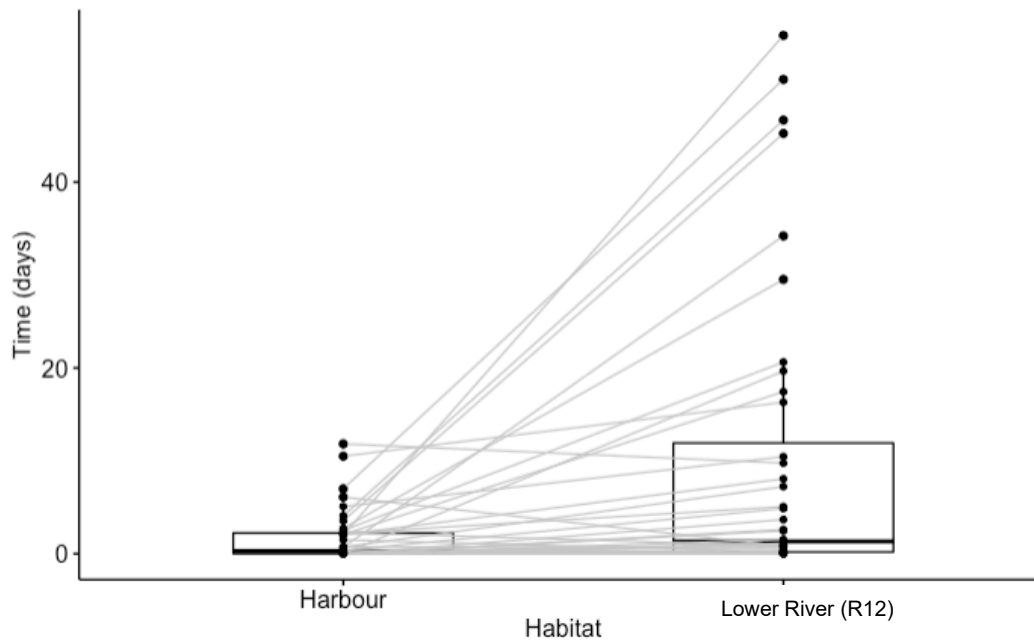


Figure 8.8: Time difference between both semi-anadromous and anadromous smolts in the two estuarine habitats (river mouth was ALS R12, harbour was H1 and H2b). Notes: The black horizontal line is the median; the box is the interquartile range, and the vertical lines are minimum and maximum values. The grey lines between black dots denote the difference in time between individuals in the habitats.

A Kruskal Wallance rank sum test was used to determine habitat occupancy in the marine environment. This showed that there was no significant difference in occupancy across zones (Littoral, Shallow water and Pelagic) ($df = 2$, p -value = 0.8113).

To test the difference in number of detections per habitat for individual smolts between each year, a chi-squared test was used, which showed the p -value is 0.3062 (chi-square statistic is 6, df 5, $N=742$), this suggests that the number of smolt detections within the habitat was independent of the year (Table 8.5).

Table 8.5: Table showing the mean number of detections per smolt within a year and within each habitat

Marine Habitat	Year of study	
	2018	2019
Littoral	262	288
Shallow Water	32	33
Pelagic	34	93

8.3.3 *Anadromous smolts use on marine curtains A, B, C and D*

Due to the differential placement of ALS between years, no statistical test could be performed, to compare habitat use between years, on the outer marine curtains (curtains C and D). However, the data from these curtains provide an insight to how smolts used the local marine area. The largest number of detections were around the harbour, on curtain A and to the north-north-east, within the shallow and pelagic waters on curtain C and D. It is unknown whether the anadromous smolts used the littoral areas in these areas as there were no ALS in the littoral zones on these curtains (Figure 8.9).

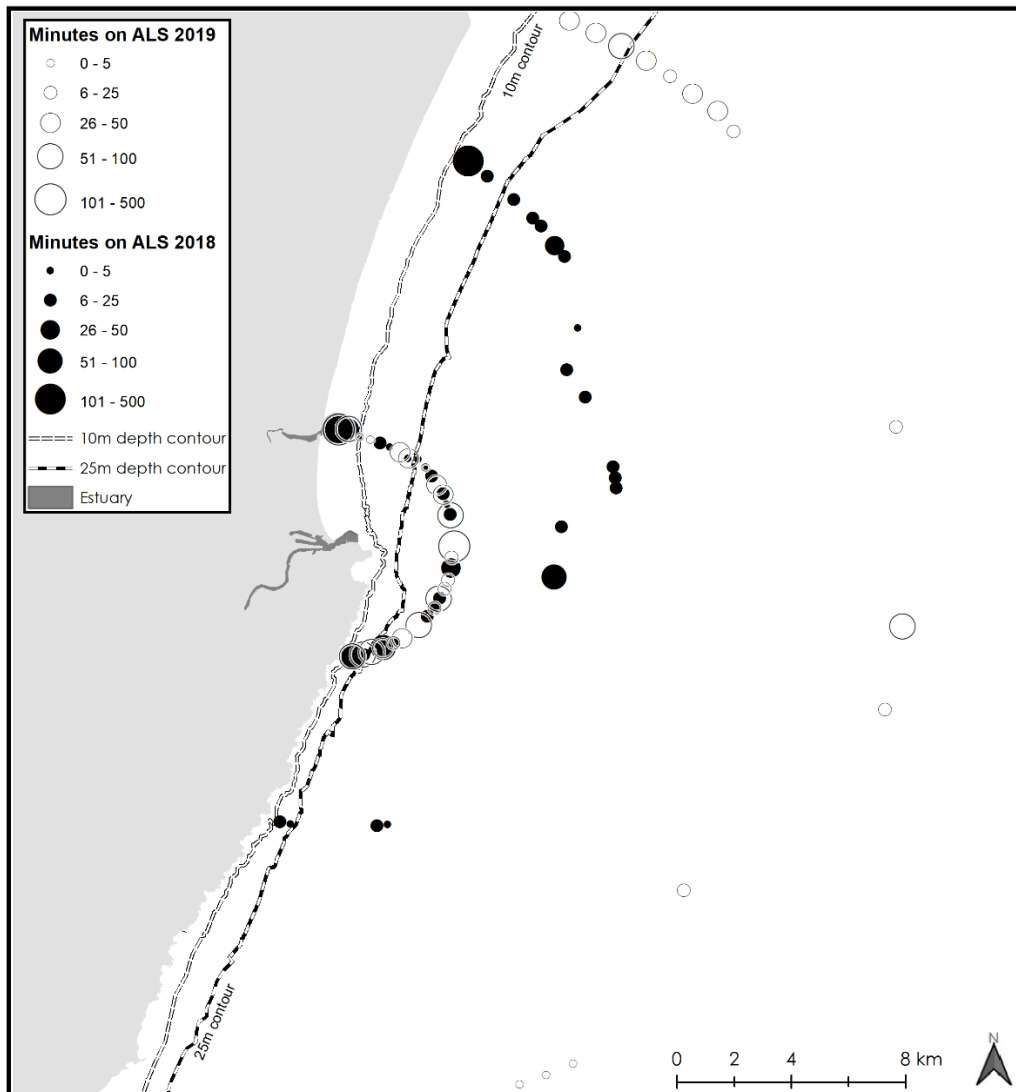


Figure 8.9: Map of the study area with white dots indicating a residency event for 2018 and the black dots indicating a residency event for 2019. The dot size indicates the total time the anadromous smolts spent on the ALS. Residency times in estuary and river are not shown

It should be noted that once the smolts from the River Dee entered the marine habitat, none were detected on the ALS within the neighbouring River Don. Most of the detections in the marine habitats are within 0.5km to 3.45km from shore, however one smolt was detected 27.9km from shore (Figure 8.10). In 2018, anadromous smolts had a median swimming distance from shore of 0.88km IQR 0.5-3.45 km, with a maximum distance of 11.9 km. In 2019, the median swimming distance from shore was 1.16km IQR 0.77-3.12km with a maximum distance of 27.9km

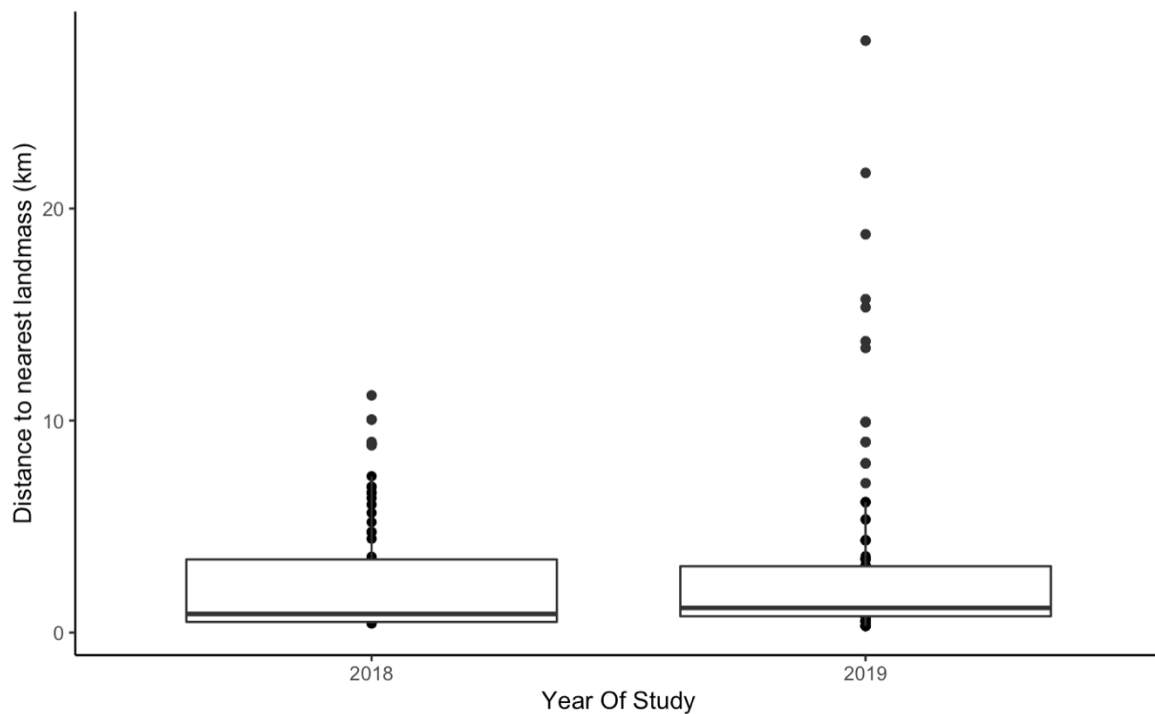


Figure 8.10: Distance from shore the anadromous smolts were detected from the nearest landmass. Note: Black horizontal line is the median, the box is the interquartile range, and the vertical lines are minimum and maximum values. Black dots beyond vertical lines are outliers.

8.3.4 Temperature and Depth

No quantitative analysis could be undertaken for temperature and depth use due to the small number of individuals fitted with temperature and depth tags in each migration strategy group; Potamodromous (3), Semi Anadromous (7), Anadromous (4), Predated (2), No data (4). In 2018, there were temperature and depth recordings on all curtains (Curtain D was not deployed in 2018). The use of temperature sensors was primarily to identify rates of mammal predation, however in general, the further smolts migrated from the river, the colder and more stable (lower SD) the water temperature they experienced (Table 8.6).

Table 8.6: Temperature the smolts experienced during their migration to marine curtain C in 2018

	River	Last ALS in River (R12)	Harbour	Marine Curtain A	Marine Curtain C
Mean	13.7°C	12.8°C	11.8°C	10.4°C	8.43°C
SD	±2.2	±2.06	±1.43	±1.4	±0.206
Range	6.5-18.9	6.9-18.6	8.7-17.4	8.7-14.1	8.2-8.6

Smolts exhibiting different migration strategies did not differ in depth use when in the river, however this may be due to the narrow range of depths in the river (a few metres at ALS deployment sites). Both semi-anadromous and anadromous smolts used a wide range of the water column in the river mouth and harbour (river mouth 0.00-5.69m, harbour 0.00-7.96) although they remained primarily within the top three metres. As anadromous smolts migrated into the marine habitat, their depth use decreased relative to the river mouth and harbour. The deepest recordings on curtain C were 3.4m, despite maximum potential depths of 70m (±4m for tides) being available (Table 8.7).

Table 8.7: Swimming depths (m) recorded of smolts within each habitat, using Thelma Biotel temperature and depth tags

		River	Last ALS in River (R12)	Harbour	Marine Curtain A	Marine Curtain C
Potamodromous	Median	1.14	NA	NA	NA	NA
	IQR	1.14-1.14	NA	NA	NA	NA
	Max	2.27	NA	NA	NA	NA
Semi anadromous	Median	1.14	1.14	1.14	NA	NA
	IQR	0.00-1.14	1.14-1.14	1.14-1.14	NA	NA
	Max	2.27	4.55	3.41	NA	NA
Anadromous	Median	1.14	1.14	2.27	0.00	1.14
	IQR	1.14-2.27	0.00-1.14	1.14-3.41	0.00-1.14	0.85-1.70
	Max	2.27	5.69	7.96	6.82	3.41

Within the marine habitat, the anadromous smolts stayed near the water surface regardless of the potential swimming depths available. There is some evidence to suggest that the closer the smolts were swimming to the shore, the deeper they swam. There was no evidence of diving behaviour in the marine habitat (Figure 8.11).

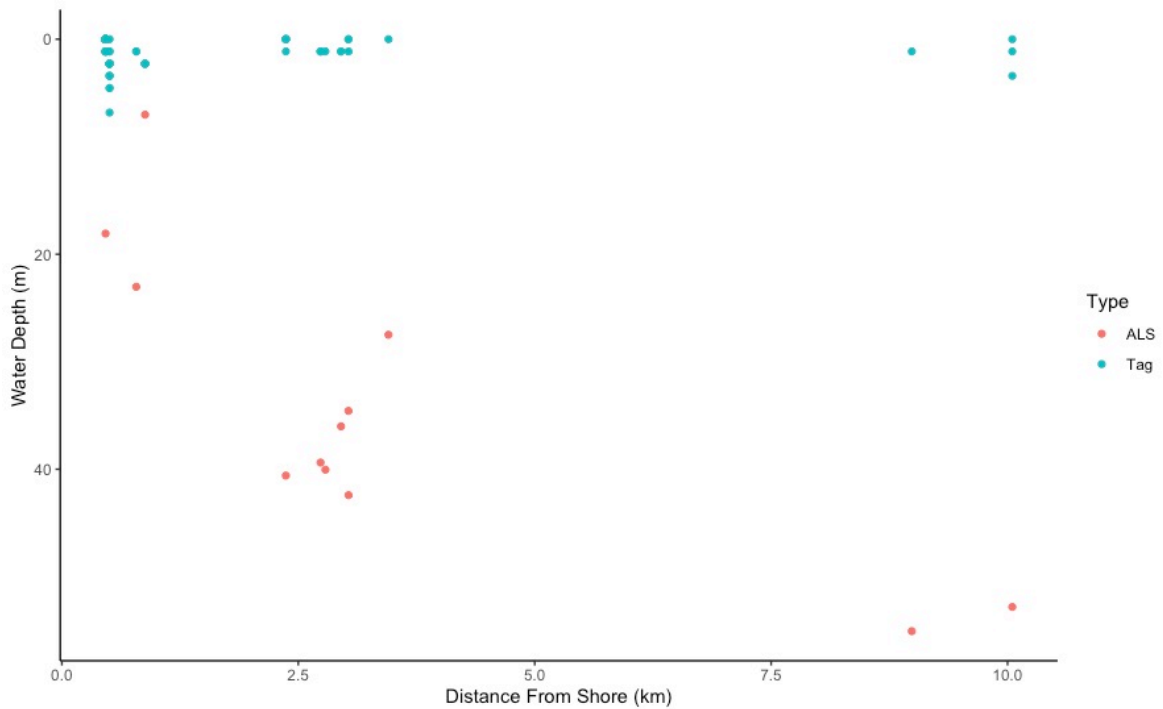


Table 8.8: The various migration strategies exhibited by the River Dee anadromous sea trout smolts

Stager or Non-Stager	Returner, Non-Returner, Oscillator	Spent more than 48 hours in the study area	Probable area smolt would be at the end of the tag battery life	Number of individuals
Stager	Non-Returner	Non-local Occupant	marine Distant marine	5
Stager	Oscillator	Local occupants	marine Local marine	1
Stager	Returned	Local occupants	marine Estuary	2
Stager	Non-Returner	Local occupants	marine Distant marine	1
Stager	Oscillator	Local occupants	marine Distant marine	5
Stager	Oscillator	Local occupants	marine Estuary	1
Non-Stager	Non-Returner	Non-local occupant	marine Distant marine	3
Non-Stager	Returned	Local occupants	marine Estuary	1
Non-Stager	Non-Returner	Local occupants	marine Distant marine	2
Non-Stager	Oscillator	Local occupants	marine Local marine	1

Seven smolts stayed within the estuary for less than 48 hours, they migrated through the harbour within a mean time of 20.64 hours with a SD of ± 15.36 hours, one individual took 33 minutes to migrate through, while the maximum length taken was 45.12 hours. The other 15 anadromous smolts stayed in the estuary for longer than 48 hours, with a mean time of 19.18 days, SD ± 15.83 days and range 5.68 to 52.38 days. There was a mean gap of 17.33 days between stagers and non-stagers. Of the eight oscillator smolts, five returned to the estuary twice, two returned to the estuary and back to the marine habitat three times, one individual oscillated between the estuary and marine habitat four times.

The four smolts that returned to the estuary had a mean battery life left of 33.19 days SD ± 22.28 and a range of 10.69 - 56.67 days. It is assumed these smolts stayed within the estuary

or migrated back upriver and were not predated. The 16 smolts that were predicted to have left the study area altogether had tags with a mean battery life left of 38.36 days, (SD± 17.85 and range 11.31 to 67.11 days). It is assumed these smolt had left the study area and had the ability to come back but choose not to. Of the two local marine anadromous smolts, one had 5.53 days of tag battery left and the other smolt had exceeded its predicted battery life of 101 days by 7.85 days; it is assumed that these smolt batteries died, hence there were no further detections. It is possible that these fish may have returned to the estuary or river after this time but that they would not be detected.

8.4 Discussion

This study has shown the highly variable migration strategies exhibited by *Salmo trutta* in the marine environment. It is potentially the first such study which has examined trout at sea in an area unconstrained by natural borders, such as sea lochs or fjords. *Salmo trutta* from the Aberdeenshire Dee exhibit both anadromous and semi-anadromous migrations strategies.

River Dee smolts exhibited considerable individual variation in the anadromous migration strategies. The observed marine behaviours in this study suggest that anadromous migration is far more varied than simply migrating out to a marine habitat, feeding and then returning to overwinter or spawn (Jonsson *et al.* 2011). There is evidence to suggest that the behaviours observed here are even beyond the scope of the strategies set out previously by Birnie-Gauvin *et al.* (2019) and Eldøy *et al.* (2015). Despite the wide variety of behaviours exhibited, some combinations of specific behaviours were used more than others, suggesting that there is an optimum combination specific strategies and behaviours used.

This study is not, however, the first study to observe the variety of anadromous trout migration strategies on the east coast of Scotland. Nall (1930) and Pratten and Shearer (1983) observed that anadromous smolts often returned to their natal river as finnock (immature sea trout), within 5 to 6 weeks after being tagged with Carlin and Floy tags. Migration out to sea as smolts and back into the estuary/riverine habitat before winter is called premature returning by Nevoux *et al.* (2019). 50% (n=11) of the anadromous smolts in this study were observed exhibiting premature returning behaviour. Premature returning can be a prevalent behaviour in populations; Jonsson and Jonsson (2009), Davidsen *et al.* (2014), del Villar-Guerra *et al.* (2014) and Flaten *et al.* (2016) have all observed between 38% to 65% of their anadromous smolts exhibiting this behaviour. The main finding from Nall (1930) and Pratten and Shearer (1983) was that anadromous smolts from Scottish East coast rivers migrated to other river

estuaries on Scotland's eastern coastline. In the study reported here, despite there being an automated listening station (ALS) in the River Don (3.5km north from the River Dee's mouth) in 2019, not one of the seven anadromous smolts that year were detected there. From this study, it is not possible to determine why different smolts exhibit different patterns for return migration. Davidsen *et al.* (2014) hypothesised that premature returning trout move back into the estuary as it may be providing ample feeding opportunities to offset the risks of predation staying within the estuary. An alternative hypothesis, by Jensen *et al.* (2014), Rikardsen *et al.* (2007) and Kristensen *et al.* (2018) is that trout may move back into the warmer estuary to elevate their body temperature up to a preferred temperature of 12°C as observed in their studies or for osmotic relief in smolts that have not fully adapted to sea water.

Within a population of *Salmo trutta*, the spectrum of migration strategies is maintained by the population's phenotypic plasticity (Wysujack *et al.*, 2009). This often leads to differences in migration strategies between individuals from different stream origins, years, sexes, body length, body weight and body condition (Bergman *et al.* 2013; Dahl *et al.* 2004; Jonsson and Jonsson, 1993, 2011; Olsson and Greenberg, 2004; Wysujack *et al.* 2009). The results in this study show that there was no significant difference in migration strategies adopted by smolts from the different stream origins. This may be because there was no significant difference between smolts length, weight, and tag burden from different stream origins. Bohlin, Pettersson and Degerman (2001) showed altitude and other environmental conditions can influence a population of trout adopted migration strategies. Despite the streams in this study being different distances from the sea it had no effect on migration strategies adopted. Rodger *et al.* (2020) also found both non-anadromous and anadromous life history tactics in the same geographic population and despite there being genetic differences over a small spatial scale this did not convert to different populations adopting alternative life histories. Rodger *et al.* (2020) did however find a different ratio between sexes and life histories, but this wasn't consistent between the different genetic populations. This suggests that life history strategies may depend on individual physiology.

Despite the estuary in this study having relatively smaller surface area (2.6km²) than some fjords in studies (such as del Villar-Guerra *et al.* (2014) (144km²) and Flaten *et al.* (2016) (60 km²)), the estuary appeared to be an important location for both semi-anadromous and anadromous *Salmo trutta* to reside. The results from the present study concur with del Villar-Guerra *et al.* (2014), in that the estuary is a valuable habitat, with some smolts (semi-anadromous) migrating into the estuary and no further. del Villar-Guerra *et al.* (2014) suggested that fjord residency was a viable alternative to migrating to sea due to the food availability and the stable, low salinity of the fjord. Although food availability and salinity were

not measured in this study, it is feasible that the estuary area could provide preferred environmental conditions for smolts. Estuaries seem to be an important habitat for anadromous *Salmo trutta* in the UK, as seen by Honkanen *et al.* (2020) and Pemberton (1976a).

This study identified that tagged trout spent more time within the natural river mouth than the artificial harbour area, despite the harbour being approximately 10 times larger in surface area. The reasons for this may be the disturbance and sound pollution created by shipping creating a barrier or unfavourable conditions for fish to reside there (European Offshore Wind Deployment Centre (EOWDC), 2011; Nevoux *et al.* 2019). However, it may also coincide with the change in temperature or salinity between the river mouth and harbour (Jensen *et al.* 2014). Kristensen, Birnie-Gauvid and Aarestrup (2018) found that a single population of *Salmo trutta* with a choice of seas to migrate to, preferred to migrate to the more brackish Kattegat sea as opposed to the more saline North Sea. Larsen *et al.* (2008) and Wynne *et al.* (2021) showed that the choice to stay in lower salinity waters was genetic and thus this could be the reason for the divergence between semi-anadromous and anadromous migration strategies and could be why trout in the study by Kristensen, Birnie-Gauvid and Aarestrup (2018) migrated east. As this study highlights a difference between trout residing in the natural estuary more than the harbour, understanding the reason for the difference in space use warrants further investigation, as Nevoux *et al.* (2019) noted that little is known about the role of manmade structures on the movements and survival of sea trout.

Another possibility for smolts residing more in the river mouth is predator avoidance, as the lower parts of estuaries generally exhibit higher instances of freshwater, marine and avian predators (Jepsen *et al.* 2006; Jonsson and Jonsson, 2009; Koed *et al.* 2006; Schwinn *et al.* 2018). Within this study, 4 predation events were detected, equating to 5.06% loss of the total tagged population. As migration is not conducive to predation-avoiding behaviours, smolt exposure to predators is increased (Aldvén *et al.* 2015). Smolts are also exposed to new predators, as they enter habitats where learned predator avoidance behaviours may not be suitable to new predator tactics (Koed *et al.* 2006; Lyse *et al.* 1998). As all detected predation events occurred within the estuary it strongly suggests that this is a zone of heightened predation risk, as seen by Jepsen *et al.* (2006), Jonsson and Jonsson (2009), Koed *et al.* (2006) and Schwinn *et al.* (2018).

Anadromous smolts from the River Dee did not differ in their use of the littoral, shallow water, and pelagic habitats. This differs from other studies, which were predominantly conducted in deep rocky fjords or sea lochs and which found that post-smolts use the littoral habitats

significantly more than pelagic habitats (Flaten *et al.* 2016; Jensen *et al.* 2014; Johnstone *et al.* 1995; Lyse *et al.* 1998; Middlemas *et al.* 2009; Pemberton, 1976a). However, Eldøy *et al.* (2015) and Flaten *et al.* (2016) observed that that sea trout preferred littoral habitats without steep cliffs rather than littoral areas with a steep cliff. This could suggest that depth may not be the only factor in habitat preference, and that substrate and shoreline composition play an important role in marine habitat choice.

The most prevalent hypothesis, proposed by Eldøy *et al.* (2015) and Flaten *et al.* (2016), is that habitat preference is related to feeding opportunities. Studies on sea trout prey choice in marine areas note that sea trout that feed in littoral areas are more generalist and those that are pelagic are more piscivorous (Knutsen *et al.* 2001; Rikardsen *et al.* 2006). However, these studies were conducted in deep rocky areas, which may have a different composition of prey choice to the sandy coasts. There is some evidence the anadromous smolts from the River Dee in the littoral habitat used a greater proportion of the water column which may point to benthic feeding. While anadromous smolts in the shallow and pelagic zones stayed near the surface suggesting pelagic feeding, as seen in Knutsen *et al.* (2001) and Rikardsen *et al.* (2006).

8.5 Conclusion Sea Trout

The aim of this study was

- a) What is the predicted spatial distribution of sea trout smolts from the Rivers Dee, Don and Ythan

This study has demonstrated that sea trout within the River Dee exhibited a wide range of migration strategies and the species is highly plastic in its nature. Sea trout within the Dee exhibit both anadromous and semi-anadromous behaviour, spending periods of time within the lower river and harbour areas of the River Dee.

For those fish that entered the marine environment, despite access to potential depths of up to 70m, anadromous and semi-anadromous smolts were only recorded to a maximum depth of 3.4m. There was also no difference in the use of littoral, shallow water, or pelagic habitats, suggesting sea trout were not preferring a particular habitat. This may be a result of the study design and future investigations should consider differences in ALS deployment to adequately monitor sea trout given their behavioural differences with salmon. For example a grid array maybe more appropriate to determine habitat use as opposed to the curtain design used here.

This study has shown how important the nearshore and estuarine habitats are to sea trout and how this may increase the likelihood of them being present during developments in these areas, e.g. harbour developments. The range of migration strategies combined with the wide spatial and temporal distribution of sea trout smolts suggests that new harbour, coastal and near-shore developments as well as ongoing activities in these areas should consider the potential interactions of their development on sea trout, although there is evidence of some sea trout migrating further afield. As with salmon, sea trout are of high conservation concern at present reflecting population numbers continuing to decline.

9 Overall Conclusions

This study has collected novel data on both Atlantic salmon and sea trout smolts behaviour in the Rivers Dee and Don as well as the near shore environment (up to 20km from shore). Additionally, this study investigated movements of salmon post-smolts further from shore on the way to Norwegian Sea feeding grounds using model simulations. Such information is highly valuable in informing future EIA for offshore wind as the connectivity between potential developments and specific populations is relatively unknown.

With the current decline in the numbers of returning adult salmon to Scottish rivers (Marine Scotland, 2022) and the planned expansion of the Renewable Energy (RE) industry in Scottish waters, care needs to be taken to ensure offshore development and associated activities do not negatively impact populations of these iconic species of fish. The particle simulation modelling for salmon smolts leaving the River Dee in this study, predicts a wide sweep of particles dispersing in band across the North Sea. If the model was to be expanded to cover more rivers, the distribution of particles will widen potentially covering much of the North Sea. Data gathered by Marine Scotland Science (and in the process of being written up for publication) during post-smolt trawling surveys suggest that Atlantic salmon post-smolts are present at some point in time in many of the proposed windfarm locations in the Scottish North Sea. The implications for Atlantic salmon migrating through these windfarms should be given careful consideration during both the post-smolt and adult migration phase of their life cycle.

Several potential impact pathways have been identified as having particular relevance for Renewable Energy (RE) and salmon interactions. These include predation at novel locations, underwater noise from activities such as pile driving, collision with tidal devices and behavioural changes caused by electromagnetic fields (EMF). These may not be relevant to every type of RE (wind or tidal) or only have potential for impact at certain salmonid lifecycle stages. The lack of knowledge and gaps in our understanding of diadromous fish movements and behaviour are detailed in Malcolm *et al.* 2010 and the potential impact pathways in the ScotMER Diadromous Fish Evidence Map ([Diadromous Fish Specialist Receptor Group - gov.scot \(www.gov.scot\)](http://www.gov.scot)). For example, in shallow inshore areas salmon post-smolts or returning adults may encounter export cables emitting EMF in a small local inshore area. EMF nearshore alone might not cause a significant issue to salmon post-smolts, however, from the data presented in this study sea trout may be more vulnerable as they show a more coastal migratory pattern if EMF were shown to impact salmonid migration and behaviour. This may be the total opposite in a large scale floating offshore windfarm which has many cables

suspended in the water over a large geographic area that may increase the risk of salmon post-smolt losing their way to feeding grounds or adults to natal rivers, for example. Another potential impact pathway is the aggregation of predators such as cod or haddock around new offshore structures and the impact this might have on survival of migrating post-smolts. Much more investigative work needs to be carried out to ensure these potential issues are fully understood.

10 References

- Aldvén, D., Davidsen, J.G., 2017. Marine migrations of sea trout (*Salmo trutta*). Sea Trout: Science & Management: Proceedings of the 2nd International Sea Trout Symposium 288–297.
- Barry, J., Kennedy, R., Rosell, R., Roche, W. (2020). Atlantic salmon smolts in the Irish Sea: First evidence of a northerly migration trajectory. Fisheries Management and Ecology. 27. 10.1111/fme.12433.
- Booker D. J., Wells N. C., Smith I. P. 2008. Modelling the trajectories of migrating Atlantic salmon (*Salmo salar*). Canadian Journal of Fisheries and Aquatic Sciences, 65: 352–361.
- Byron C. J., Burke B. J. 2014. Salmon ocean migration models suggest a variety of population-specific strategies. Reviews in Fish Biology and Fisheries, 24: 737–756.
- Chapman, B.B., Skov, C., Hulthén, K., Brodersen, J., Nilsson, P.A., Hansson, L.A., Brönmark, C., 2012. Partial migration in fishes: Definitions, methodologies and taxonomic distribution. Journal of Fish Biology 81, 479–499. DOI:10.1111/j.1095-8649.2012.03349.x
- Chaput, G., 2012. Overview of the status of Atlantic salmon (*Salmo salar*) in the North Atlantic and trends in marine mortality. ICES Journal of Marine Science 69, 1538–2548. <https://doi.org/10.1093/icesjms/fss013> Overview
- Cooke S. J., Thorstad E. B. 2011. Is Radio Telemetry Getting Washed Downstream? The Changing Role of Radio Telemetry in Studies of Freshwater Fish Relative to other Tagging and Telemetry Technology, American Fisheries Society Symposium. 76: 349–369
- Cooke, S.J., Midwood, J.D., Thiem, J.D., Klimley, P., Lucas, M.C., Thorstad, E.B., Eiler, J., Holbrook, C., Ebner, B.C., 2013. Tracking animals in freshwater with electronic tags: Past, present and future. Animal Biotelemetry 1, 1–19. <https://doi.org/10.1186/2050-3385-1-5>
- Dobson, M., Frid, C., 2009. Ecology Of Aquatic Systems, 2nd ed. Oxford University Press.
- Eldøy, S.H., Davidsen, J.G., Thorstad, E.B., Whoriskey, F., Aarestrup, K., Næsje, T.F., Rønning, L., Sjørnsen, A.D., Rikardsen, A.H., Arnekleiv, J.V., 2015. Marine migration and

habitat use of anadromous brown trout (*Salmo trutta*). Canadian Journal of Fisheries and Aquatic Sciences 72, 1366–1378. DOI:10.1139/cjfas-2014-0560

Ferguson, A., Reed, T.E., Cross, T.F., McGinnity, P., Prodöhl, P.A., 2019. Anadromy, potamodromy and residency in brown trout *Salmo trutta*: the role of genes and the environment. Journal of Fish Biology 95, 692–718. DOI:10.1111/jfb.14005

Flaten, A.C., Davidsen, J.G., Thorstad, E.B., Whoriskey, F., Rønning, L., Sjørnsen, A.D., Rikardsen, A.H., Arnekleiv, J. V., 2016. The first months at sea: marine migration and habitat use of sea trout *Salmo trutta* post-smolts. Journal of Fish Biology 89, 1624–1640. DOI:10.1111/jfb.13065

Flávio, H., Baktoft, H., 2020. actel: Standardised analysis of acoustic telemetry data from animals moving through receiver arrays. Methods in Ecology and Evolution 2020, 1–8. DOI:10.1111/2041-210x.13503

Friedland KD, Dannewitz J, Romakkaniemi A, Palm S, Pulkkinen H, Pakarinen T, Oeberst R (2017) Post-smolt survival of Baltic salmon in context to changing environmental conditions and predators. ICES J Mar Sci 74:1344–1355

Gill, A., Bartlett, M., Thomsen, F., 2012. Potential interactions between diadromous fishes of U.K. conservation importance and the electromagnetic fields and subsea noise from marine renewable energy developments. Journal of Fish Biology 81, 664–695.

Green, A., Honkanen, H.M., Ramsden, P. et al. Evidence of long-distance coastal sea migration of Atlantic salmon, *Salmo salar*, smolts from northwest England (River Derwent). Anim Biotelemetry 10, 3 (2022). <https://doi.org/10.1186/s40317-022-00274-2>

Halfyard, E.A., Webber, D., Del Papa, J., Leadley, T., Kessel, S.T., Colborne, S.F., Fisk, A.T., 2017. Evaluation of an acoustic telemetry transmitter designed to identify predation events. Methods in Ecology and Evolution 8, 1063–1071. DOI:10.1111/2041-210X.12726

Halttunen, E., Rikardsen, A.H., Davidsen, J.G., Thorstad, E.B., Dempson, J.B. (2009). Survival, Migration Speed and Swimming Depth of Atlantic Salmon Kelts During Sea Entry and Fjord Migration. In: Nielsen, J.L., Arrizabalaga, H., Fragoso, N., Hobday, A., Lutcavage, M., Sibert, J. (eds) Tagging and Tracking of Marine Animals with Electronic Devices. Reviews:

Methods and Technologies in Fish Biology and Fisheries, vol 9. Springer, Dordrecht.
https://doi.org/10.1007/978-1-4020-9640-2_3

Scottish Government (2022) Scottish Wild Salmon Strategy. Available at: [Scottish Wild Salmon Strategy \(www.gov.scot\)](https://www.gov.scot)

Hayden T. A., Holbrook C. M., Binder T. R., Dettmers J. M., Cooke S. J., Vandergoot C. S., Kruegar C. C. 2016. Probability of acoustic transmitter detections by receiver lines in Lake Huron: results of multi-year field tests and simulations. *Animal Biotelemetry*, 4: 19.

Haugland, M., Holst, J. C., Holm, M., and Hansen, L. P. 2006. Feeding of Atlantic salmon (*Salmo salar* L.) post-smolts in the Northeast Atlantic. *ICES Journal of Marine Science*, 63: 1488–1500. <https://doi.org/10.1016/j.icesjms.2006.06.004>.

Hoar W. S. 1988. The physiology of smolting Salmonids. *Fish Physiology*, 11(B): 275–343.

Hodder K. H., Masters J. E. G., Beaumont W. R. C., Gozlan R. E., Pinder A. C., Knight C. M., Kenward R. E. 2007. Techniques for evaluating the spatial behaviour of river fish. *Hydrobiologia*, 582: 257–269.

Hvidsten, N.A., Lund, R.A. 1988. Predation on hatchery-reared and wild smolts of Atlantic salmon, *Salmo salar* L., in the estuary of River Orkla, Norway

Hvidsten, N.A., Møkkelgjerd, P.I. 1987 Predation on salmon smolts (*Salmo salar* L.) in the estuary of the River Surna, Norway *J. Fish. Biol.*, 30, pp. 273-280

ICES (2020): North Atlantic salmon stocks. ICES Advice: Recurrent Advice. Report. <https://doi.org/10.17895/ices.advice.6010>

ICES, 2019. Working group on North Atlantic Salmon (WGNAS). ICES Scientific Reports 1, 368.

Liu, C., Cowles, G. W., Churchill, J. H., and Stokesbury, K. D. E. 2015. Connectivity of the bay scallop (*Argopecten irradians*) in Buzzards Bay, Massachusetts, U.S.A. *Fisheries Oceanography*, 24: 364–382. <http://doi.wiley.com/10.1111/fog.12114>.

Lucas M. C., Baras E. 2000. Methods for studying spatial behaviour of freshwater fishes in the natural environment. *Fish and Fisheries*, 1: 283–316.

MacCrimmon, H.R., Marshall, T.L., 1968. World Distribution of Brown Trout . *Canadian Journal of Fisheries and Aquatic Sciences* 25, 2527–2548.

Malcolm, I.A., Godfrey, J., Youngson, A.F., 2010. Review of migratory routes and behaviour of atlantic salmon, sea trout and european eel in scotland's coastal environment: implications for the development of marine renewables. *Scottish Marine and Freshwater Science Volume 1 No 14* .

Marine Scotland Science, 2015. Status of Scottish Salmon and Sea Trout Stocks 2014, Report 01/15.

Mcilvenny, J., Youngson, A., Williamson, B. J., Gauld, N., Goggijin-Murphy, L., Villar-Guerra, D.D., (2021) Combining acoustic tracking and hydrodynamic modelling to study migratory behaviour of Atlantic salmon (*Salmo salar*) smolts on entry into high-energy coastal waters. *ICES J mar Sci fsab111*. <https://doi.org/10.1093/icesjms/fsab111>

Moore, I., 2020. Factors impacting sea trout *Salmo trutta* populations in changing marine environments (Doctoral thesis). Available from [2020MoorePhD.pdf \(gla.ac.uk\)](#)

Moriarty P. E., Byron C. J., Pershing A. J., Stockwell J. D., Xue H. 2016. Predicting migratory paths of post-smolt Atlantic salmon (*Salmo salar*). *Marine Biology*, 163: 74.

Mork, K.A., Gilbey, J., Hansen, L.P., Jensen, A.J., Jacobsen, J.A., Holm, M., Holst, J.C., Ó Maoiléidigh, N., Vikebø, F., McGinnity, P., Melle, W., Thomas, K., Verspoor, E., Wennevik, V., 2012. Modelling the migration of post-smolt Atlantic salmon (*Salmo salar*) in the Northeast Atlantic. *ICES Journal of Marine Science* 69, 1616–1624. <https://doi.org/10.1093/icesjms/fss108>

Newton M, Barry J, Lothian A, Main R, Honkanen H, Mckelvey S, Thompson P, Davies I, Brockie N, Stephen A, Murray RO. Counterintuitive active directional swimming behaviour by Atlantic salmon during seaward migration in the coastal zone. *ICES J Mar Sci*. 2021. <https://doi.org/10.1093/icesjms/fsab024>.

Ounsley, J.P., Gallego, A., Morris, D.J., Armstrong, J.D., 2019. Regional variation in directed swimming by Atlantic salmon smolts leaving Scottish waters for their oceanic feeding grounds—a modelling study. *ICES Journal of Marine Science* 77, 315–325. <https://doi.org/10.1093/icesjms/fsz160>

Pawlowicz, R., Beardsley, B. and Lentz, S. 2002. Classical tidal harmonic analysis including error estimates in MATLAB using T_TIDE. *Computer and Geosciences*. 28:8.

Rikardsen A. H., Dempson J. B. 2011. Dietary life-support: the food and feeding of Atlantic salmon at sea. In *Atlantic Salmon Ecology*, pp. 115–143. Ed. by Oystein A., Einum S., Klemetsen A., Skurdal S.. Blackwell, Oxford

Strøm, J.F., Thorstad, E.B., Hedger, R.D., Rikardsen, A, H. (2018) Revealing the full ocean migration of individual Atlantic salmon. *Anim Biotelemetry* 6, 2. <https://doi.org/10.1186/s40317-018-0146-2>

Svenning M.-A., Borgstrøm R., Dehli T. O., Moen G., Barrett R. T., Pedersen T., Vader W. 2005. The impact of marine fish predation on Atlantic salmon smolts (*Salmo salar*) in the Tana estuary, north Norway, in the presence of an alternative prey, lesser sandeel (*Ammodytes marinus*). *Fisheries Research*, 76: 466–474.

Tang, J., Wardle, C.S., 1992. Power Output of Two Sizes of Atlantic Salmon (*Salmo Salar*) at their Maximum Sustained Swimming Speeds. *Journal of Experimental Biology* 166, 33 LP – 46.

Team, R.C., 2021. R: A language and environment for statistical ## computing. R Foundation for Statistical Computing, Vienna, Austria.

The Scottish Government (2022) *Scottish Wild Salmon Strategy*. The Scottish government ISBN: 978-1-80201-645-1

Thorstad, E.B., Whoriskey, F., Uglem, I., Moore, A., Rikardsen, A.H., Finstad, B., 2012. A critical life stage of the Atlantic salmon *Salmo salar*: Behaviour and survival during the smolt and initial post-smolt migration. *Journal of Fish Biology* 81, 500–542. <https://doi.org/10.1111/j.1095-8649.2012.03370.x>

Venice system, 1959. The final resolution of the symposium on the classification of brackish waters. *Archo Oceanogr.limnol* 346–347.

Wilson, K., Veneranta, L., 2019. Data-limited diadromous species – review of European status. ICES Cooperative Research Report 348, 1–273. DOI:10.17895/ices.pub.5253

11 Appendix A – Far-field particle density plots for faster swim speeds

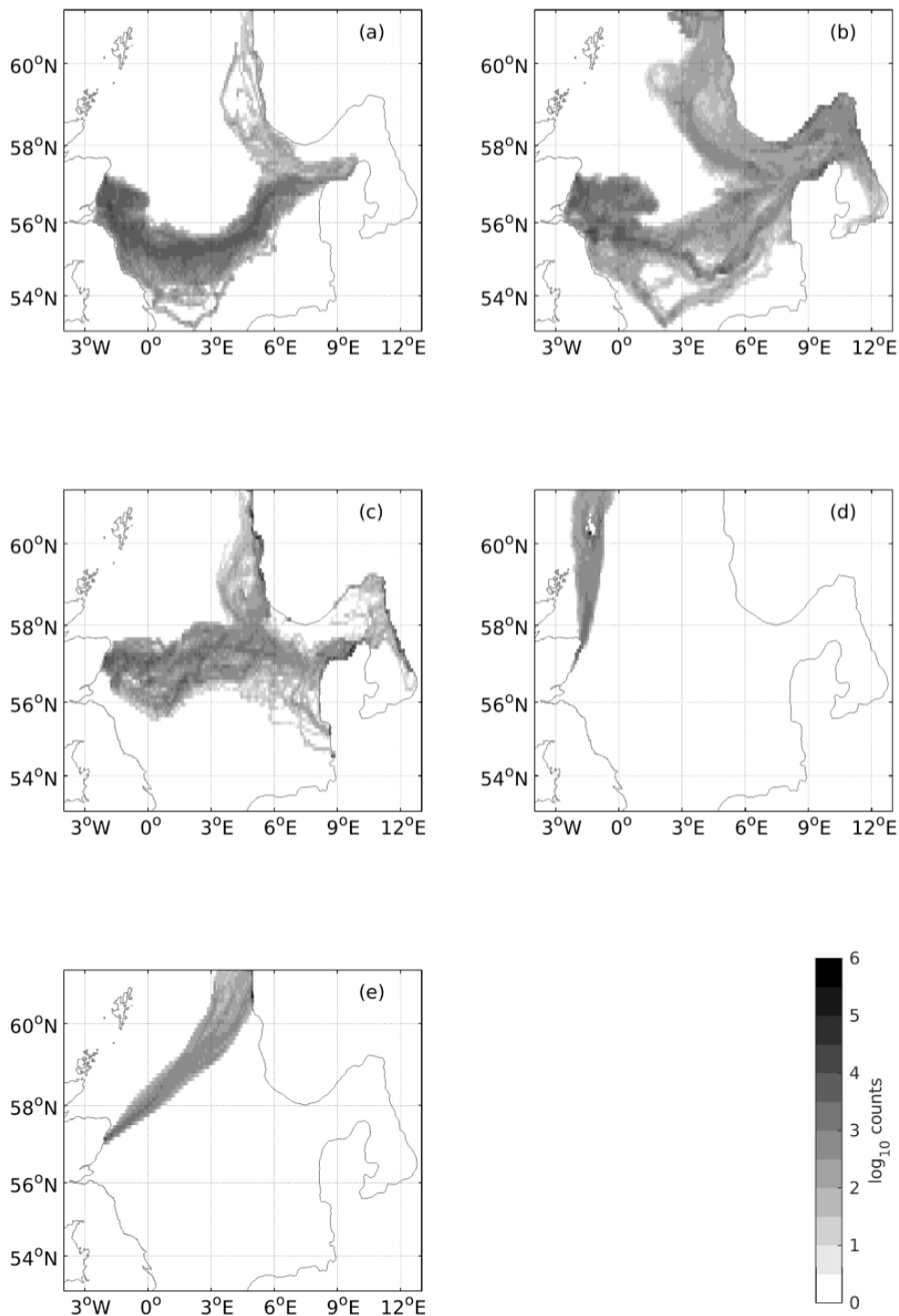


Figure 11.1 Particle density plots for (a) passive (b) negative rheotaxis (c) variable rheotaxis (d) northerly bearing and (e) north-easterly bearing behaviours for 2018, with smolt swim speed set to 2.5 bl s⁻¹ for (b)-(e). Smolt body length was initially set to 0.125m

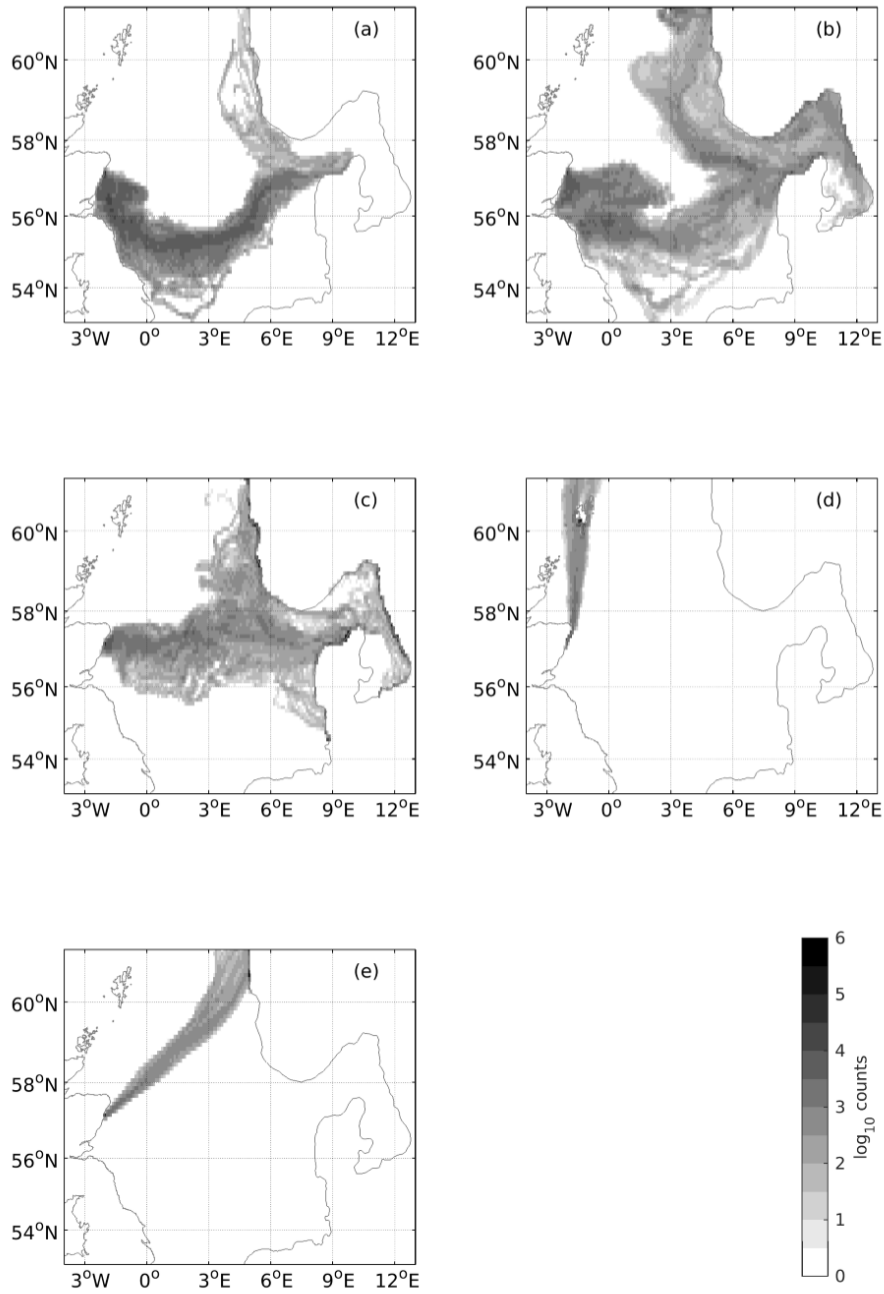


Figure 11.2 Particle density plots for (a) passive (b) negative rheotaxis (c) variable rheotaxis (d) northerly bearing and (e) north-easterly bearing behaviours for 2018, with smolt swim speed set to 3.5 bl s⁻¹ for (b)-(e). Smolt body length was initially set to 0.125m

12 Appendix B – Near-field particle density plots for 2018 simulations with faster swim speeds – first detections

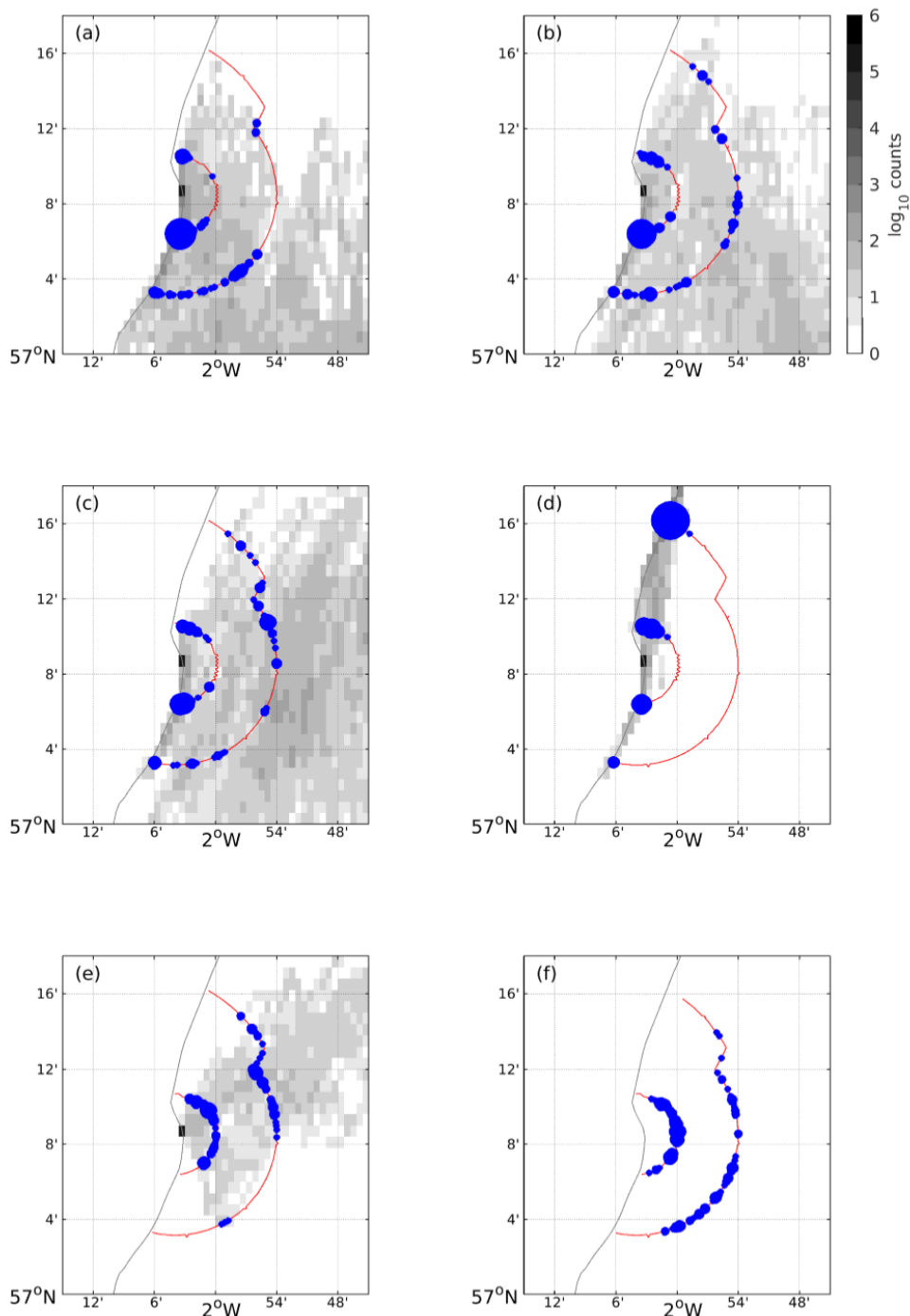


Figure 12.1 (a) – (e) show particle density plots for 2018 simulations around Aberdeen bay for (a) passive (b) negative rheotaxis (c) variable rheotaxis (d) northerly bearing and (e) north-easterly bearing behaviours, with smolt swim speed set to 2.5 bl s⁻¹ for (b)-(e). Smolt body length was initially set to 0.14 m. The 2018 inner and outer arrays of acoustic receivers are indicated with red lines. The first detections of the particles on the arrays are shown by the blue dots, the size of which indicate the number of first particle detections at each receiver location. (f) shows the first detections of tagged salmon smolts at the two arrays, with the size indicating the number of unique detections at any one receiver.

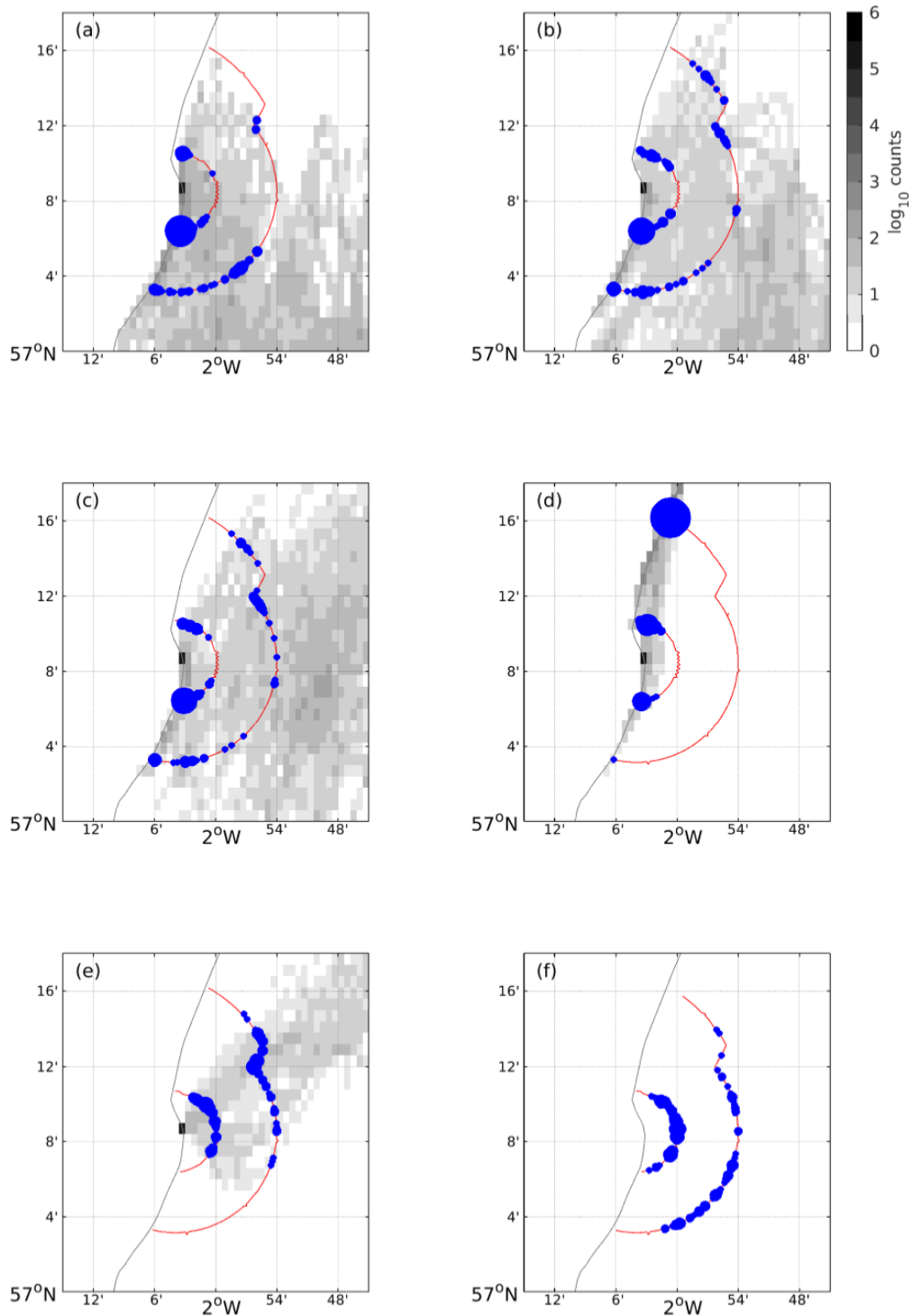


Figure 12.2 (a) – (e) show particle density plots for 2018 simulations around Aberdeen bay for (a) passive (b) negative rheotaxis (c) variable rheotaxis (d) northerly bearing and (e) north-easterly bearing behaviours, with smolt swim speed set to 3.5 bl s⁻¹ for (b) –(e). Smolt body length was initially set to 0.14 m. The 2018 inner and outer arrays of acoustic receivers are indicated with red lines. The first detections of the particles on the arrays are shown by the blue dots, the size of which indicate the number of first particle detections at each receiver location. (f) shows the first detections of tagged salmon smolts at the two arrays, with the size indicating the number of unique detections at any one receiver.

13 Appendix C – Near-field particle density plots for 2018 simulations with faster swim speeds – all detections

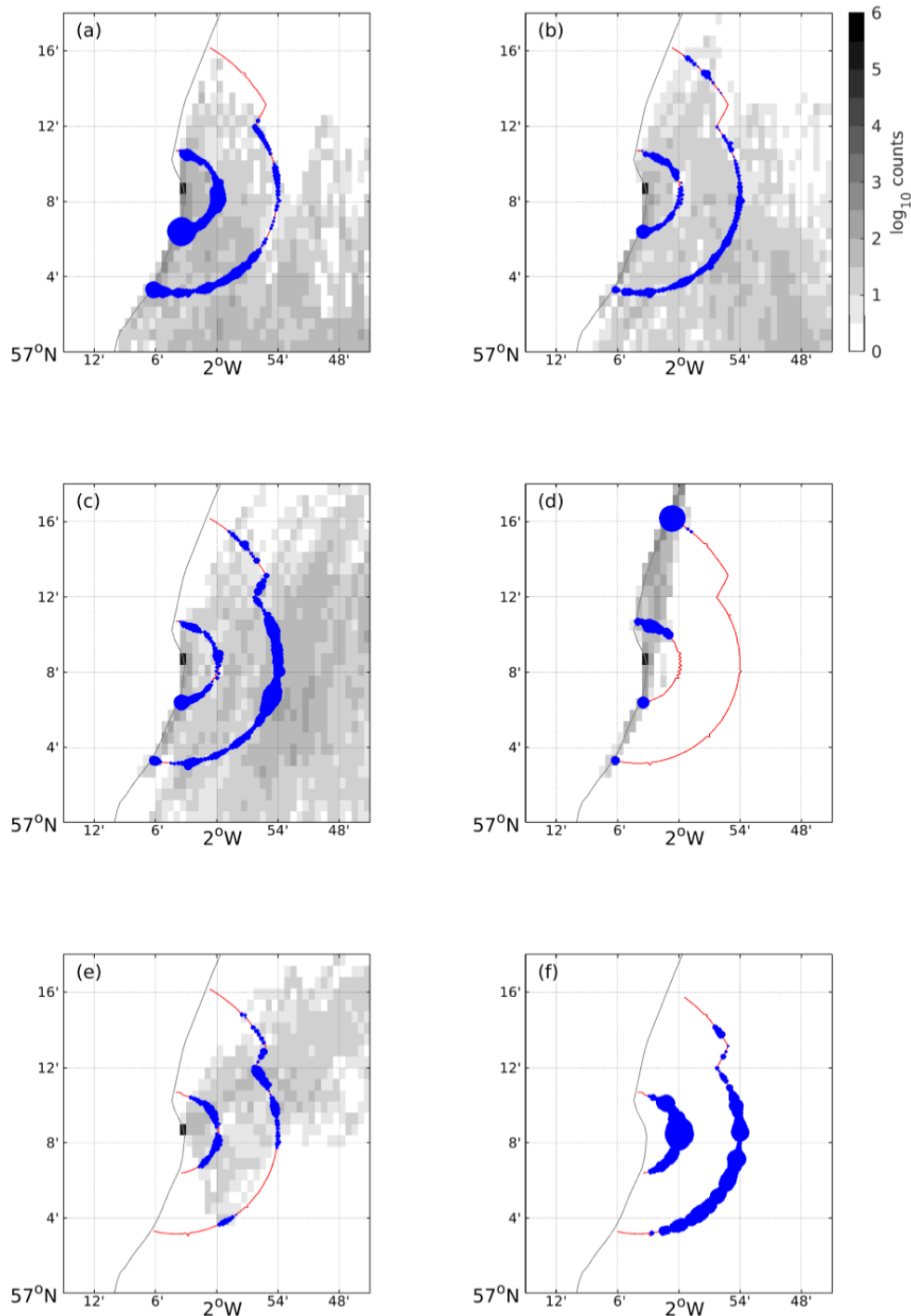


Figure 13.1 (a) – (e) show particle density plots for 2018 simulations around Aberdeen bay for (a) passive (b) negative rheotaxis (c) variable rheotaxis (d) northerly bearing and (e) north-easterly bearing behaviours, with smolt swim speed set to 2.5 bl s⁻¹ for (b)-(e). Smolt body length was initially set to 0.14 m. The 2018 inner and outer arrays of acoustic receivers are indicated with red lines. The detections of the particles on the arrays are shown by the blue dots, the size of which indicate the number of particle detections at each receiver location. (f) shows the detections of tagged salmon smolts at the two arrays, with the size indicating the number of detections at any one receiver.

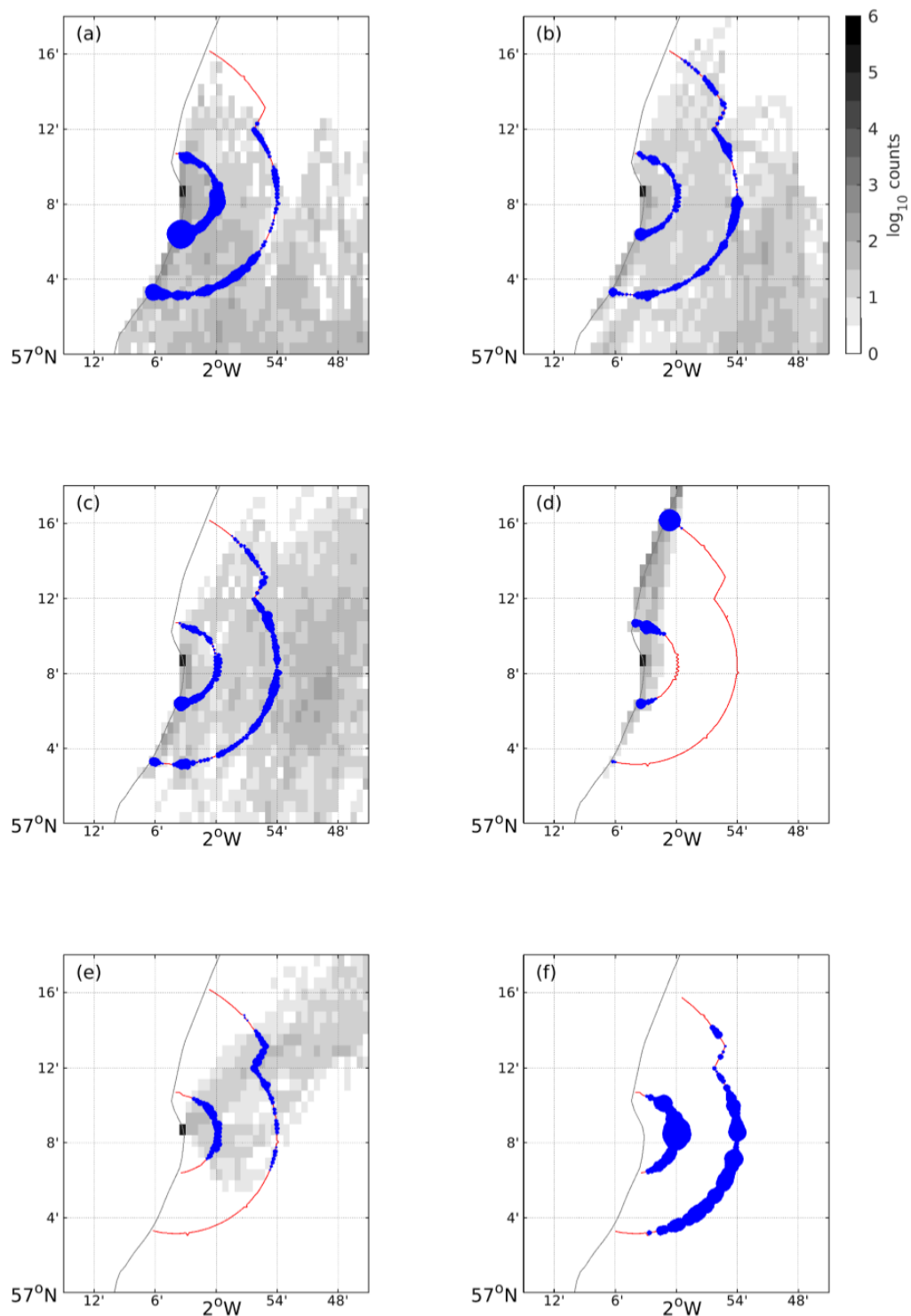


Figure 13.2 (a) – (e) show particle density plots for 2018 simulations around Aberdeen bay for (a) passive (b) negative rheotaxis (c) variable rheotaxis (d) northerly bearing and (e) north-easterly bearing behaviours, with smolt swim speed set to 3.5 bl s⁻¹ for (b) – (e). Smolt body length was initially set to 0.14 m. The 2018 inner and outer arrays of acoustic receivers are indicated with red lines. The detections of the particles on the arrays are shown by the blue dots, the size of which indicate the number of particle detections at each receiver location. (f) shows the detections of tagged salmon smolts at the two arrays, with the size indicating the number of detections at any one receiver.

14 Appendix D – Near-field particle density plots for 2019 simulations with faster swim speeds – first detections

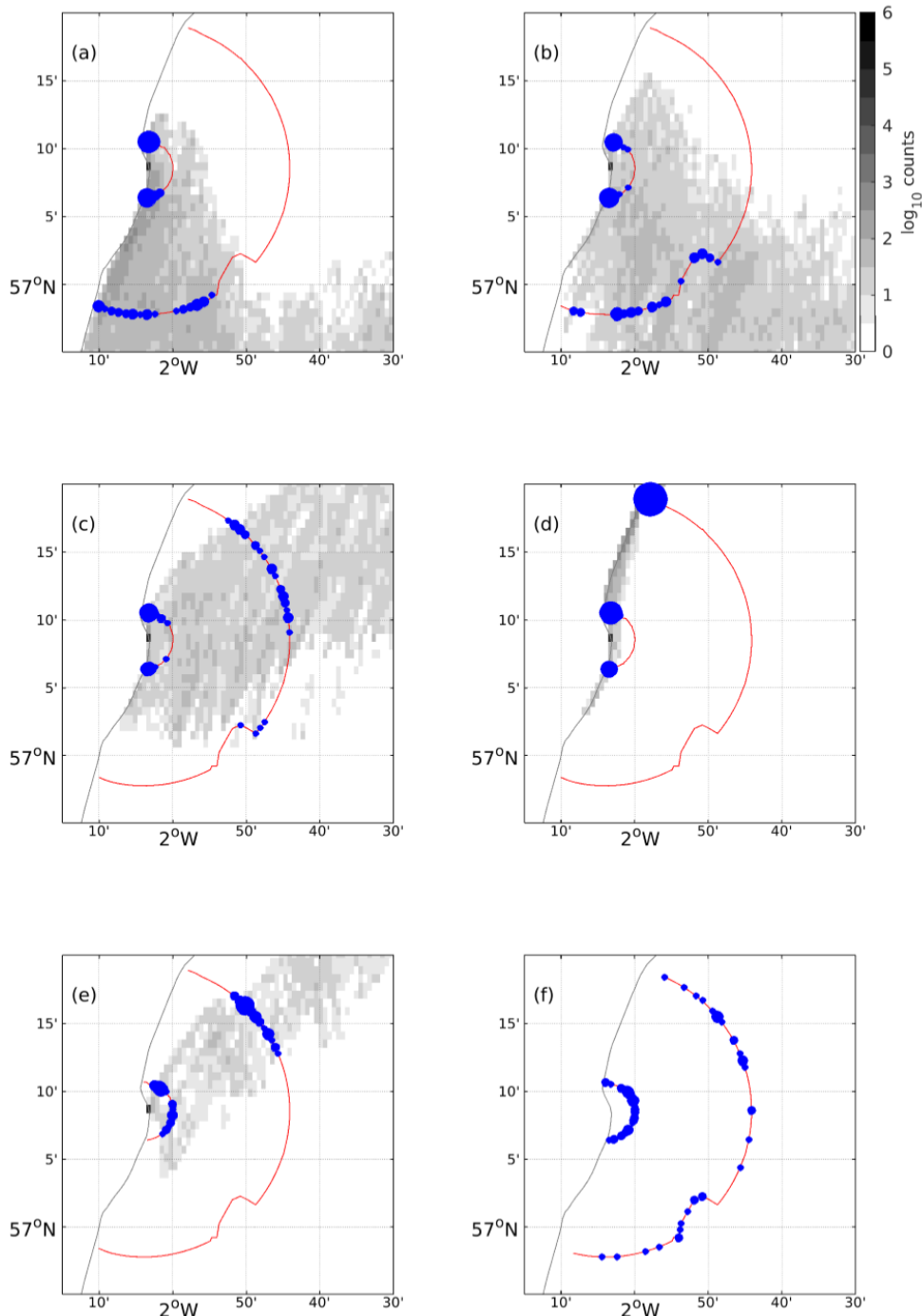


Figure 14.1 (a) – (e) show particle density plots for 2019 simulations around Aberdeen bay for (a) passive (b) negative rheotaxis (c) variable rheotaxis (d) northerly bearing and (e) north-easterly bearing behaviours, with smolt swim speed set to 2.5 bl s⁻¹ for (b) -(e). Smolt body length was initially set to 0.14 m. The 2019 inner and outer arrays of acoustic receivers are indicated with red lines. The first detections of the particles on the arrays are shown by the blue dots, the size of which indicate the number of first particle detections at each receiver location. (f) shows the first detections of tagged salmon smolts at the two arrays, with the size indicating the number of unique detections at any one receiver.

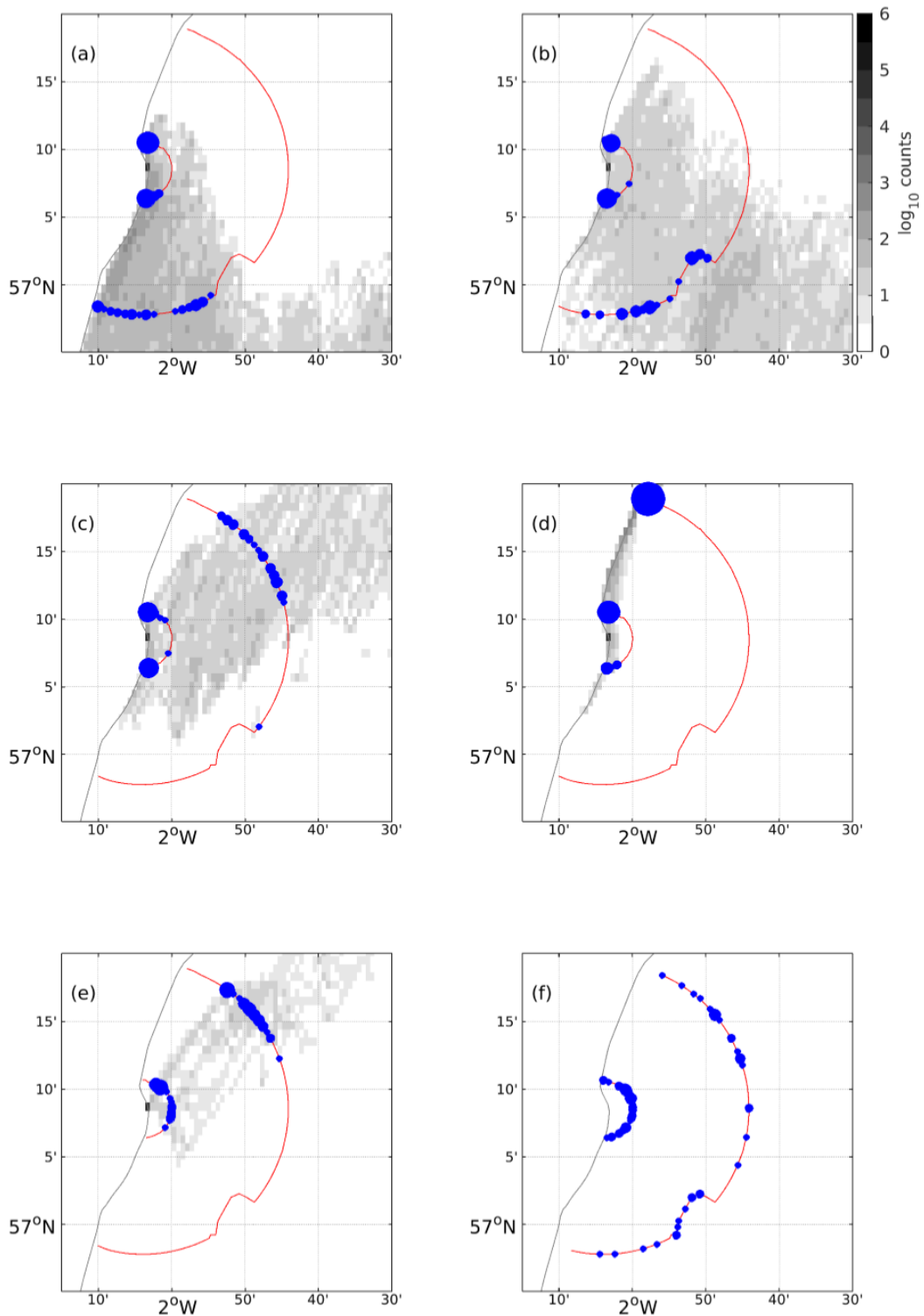


Figure 14.2 (a) – (e) show particle density plots for 2019 simulations around Aberdeen bay for (a) passive (b) negative rheotaxis (c) variable rheotaxis (d) northerly bearing and (e) north-easterly bearing behaviours, with smolt swim speed set to 3.5 bl s⁻¹ for (b)-(e). Smolt body length was initially set to 0.14 m. The 2019 inner and outer arrays of acoustic receivers are indicated with red lines. The first detections of the particles on the arrays are shown by the blue dots, the size of which indicate the number of first particle detections at each receiver location. (f) shows the first detections of tagged salmon smolts at the two arrays, with the size indicating the number of unique detections at any one receiver.

15 Appendix E – Near-field particle density plots for 2019 simulations with faster swim speeds – all detections

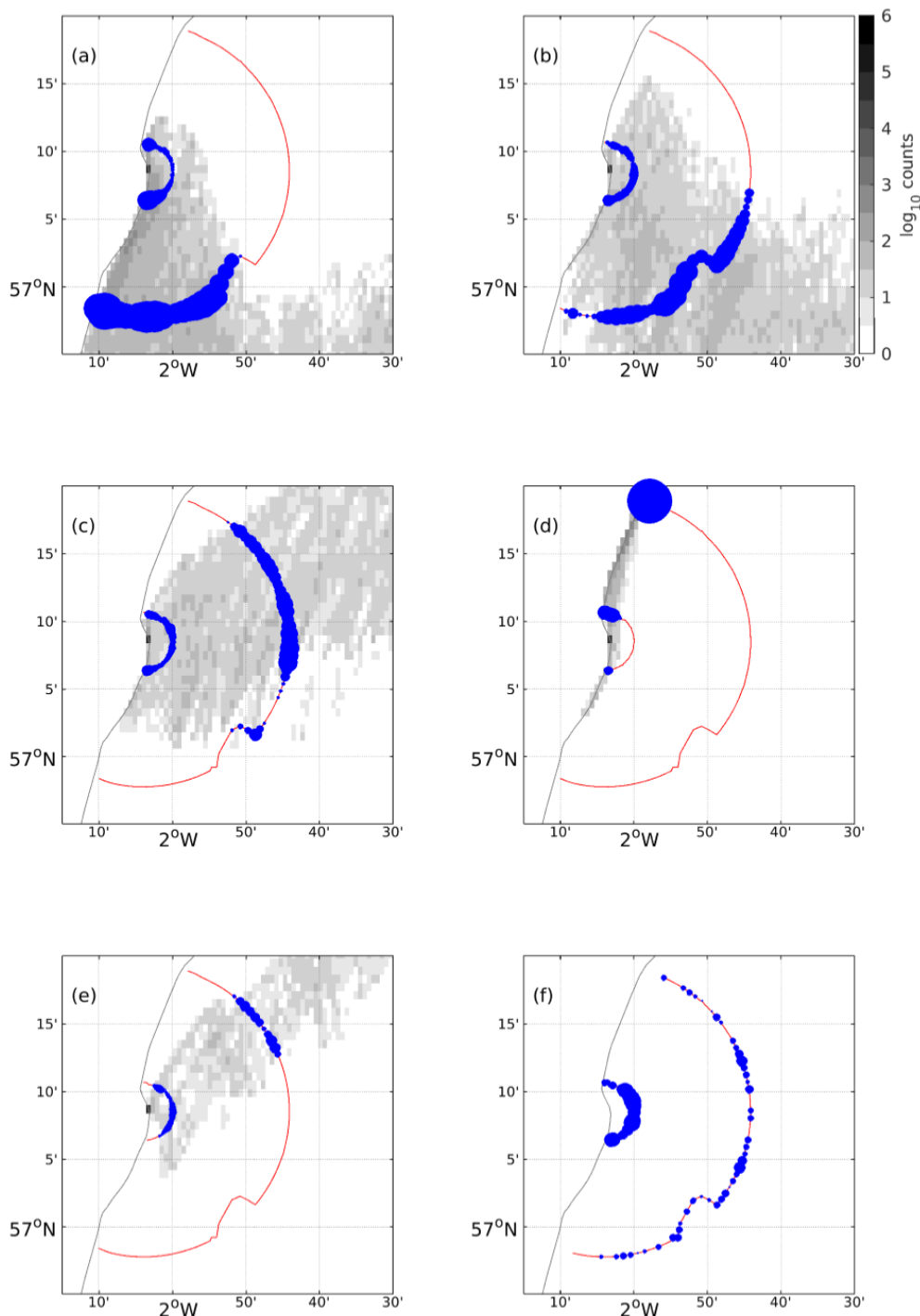


Figure 15.1 (a) – (e) show particle density plots for 2019 simulations around Aberdeen bay for (a) passive (b) negative rheotaxis (c) variable rheotaxis (d) northerly bearing and (e) north-easterly bearing behaviours, with smolt swim speed set to 2.5 bl s⁻¹ for (b)-(e). Smolt body length was initially set to 0.14 m. The 2019 inner and outer arrays of acoustic receivers are indicated with red lines. The detections of the particles on the arrays are shown by the blue dots, the size of which indicate the number of particle detections at each receiver location. (f) shows the detections of tagged salmon smolts at the two arrays, with the size indicating the number of detections at any one receiver.

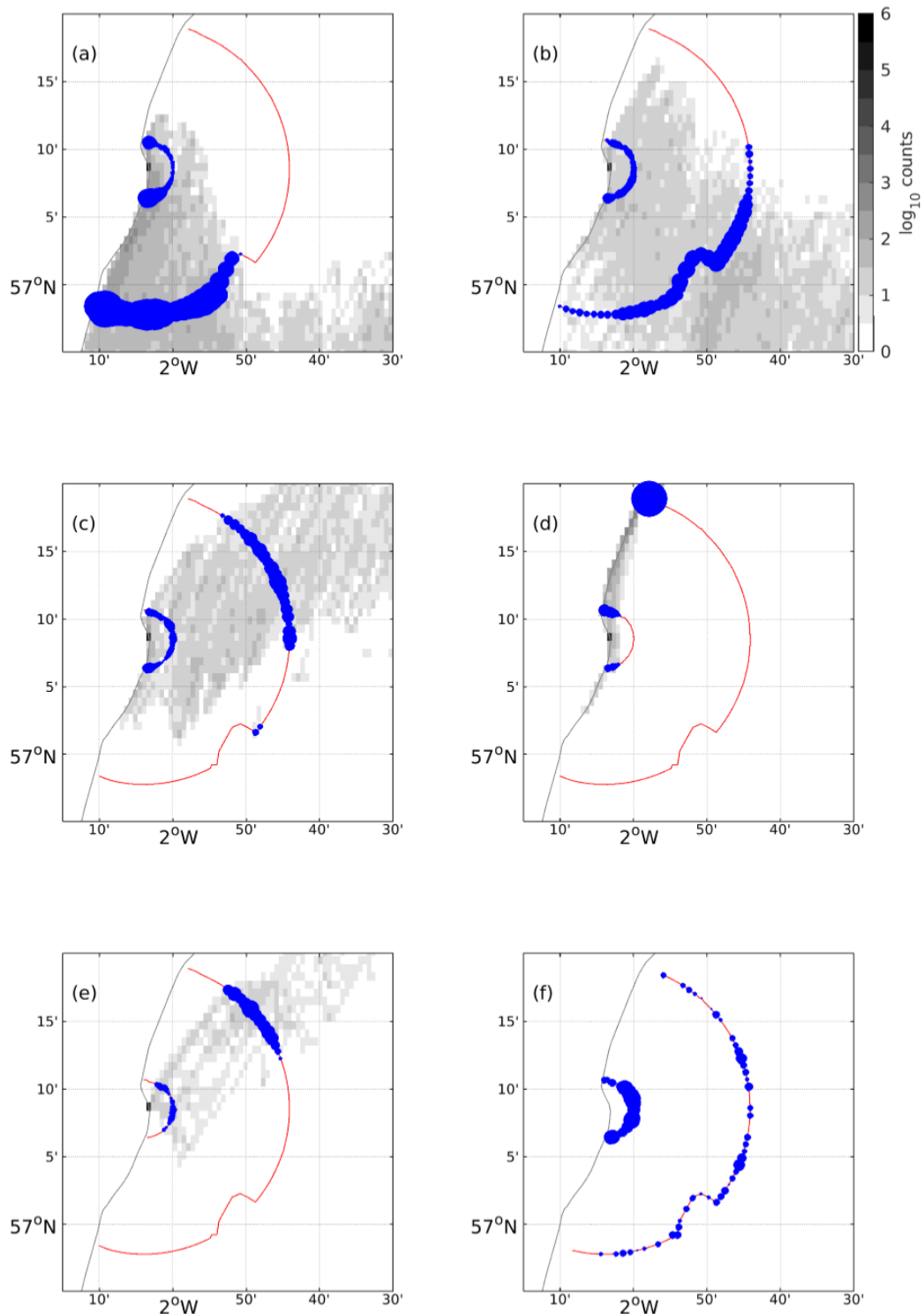


Figure 15.2 (a) – (e) show particle density plots for 2019 simulations around Aberdeen bay for (a) passive (b) negative rheotaxis (c) variable rheotaxis (d) northerly bearing and (e) north-easterly bearing behaviours, with smolt swim speed set to 3.5 bl s⁻¹ for (b)-(e). Smolt body length was initially set to 0.14 m. The 2019 inner and outer arrays of acoustic receivers are indicated with red lines. The detections of the particles are shown by the blue dots, the size of which indicate the number of particle detections at each receiver location. (f) shows the detections of tagged salmon smolts at the two arrays, with the size indicating the number of detections at any one receiver.

16 Appendix F – Near-field temporal analysis with faster swim speeds

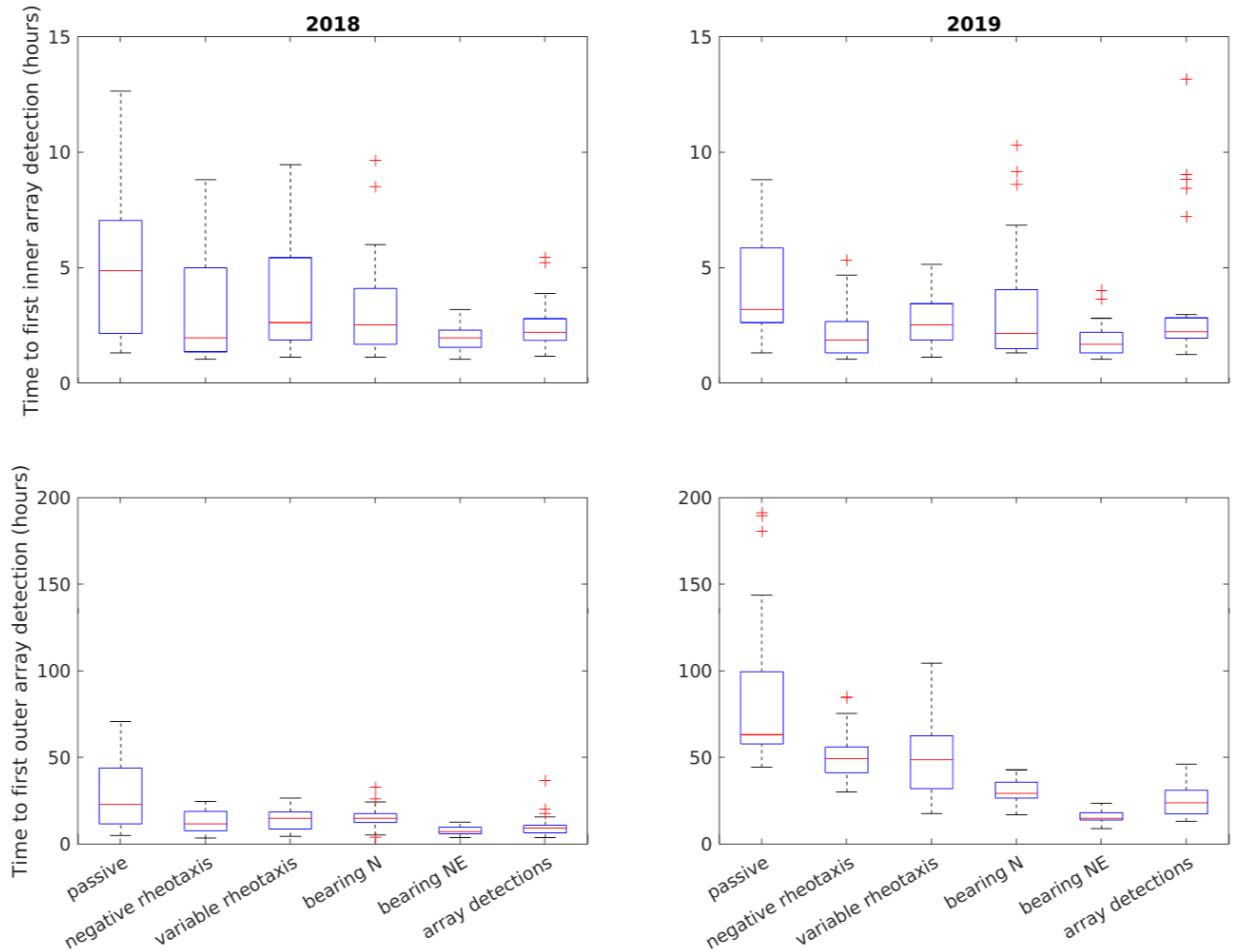


Figure 16.1 Boxplots showing the time for particles to be first detected at the inner (top) and outer (bottom) arrays for the 2018 (left) and 2019 (right) simulations, under the different behaviours with smolt swim speeds set to 2.5 bl s⁻¹. Red lines show median values for the particles tracked, or detections made, boxes show the 25th and 75th percentiles, the whiskers show the lower and upper adjacent values and the red crosses show any outliers.

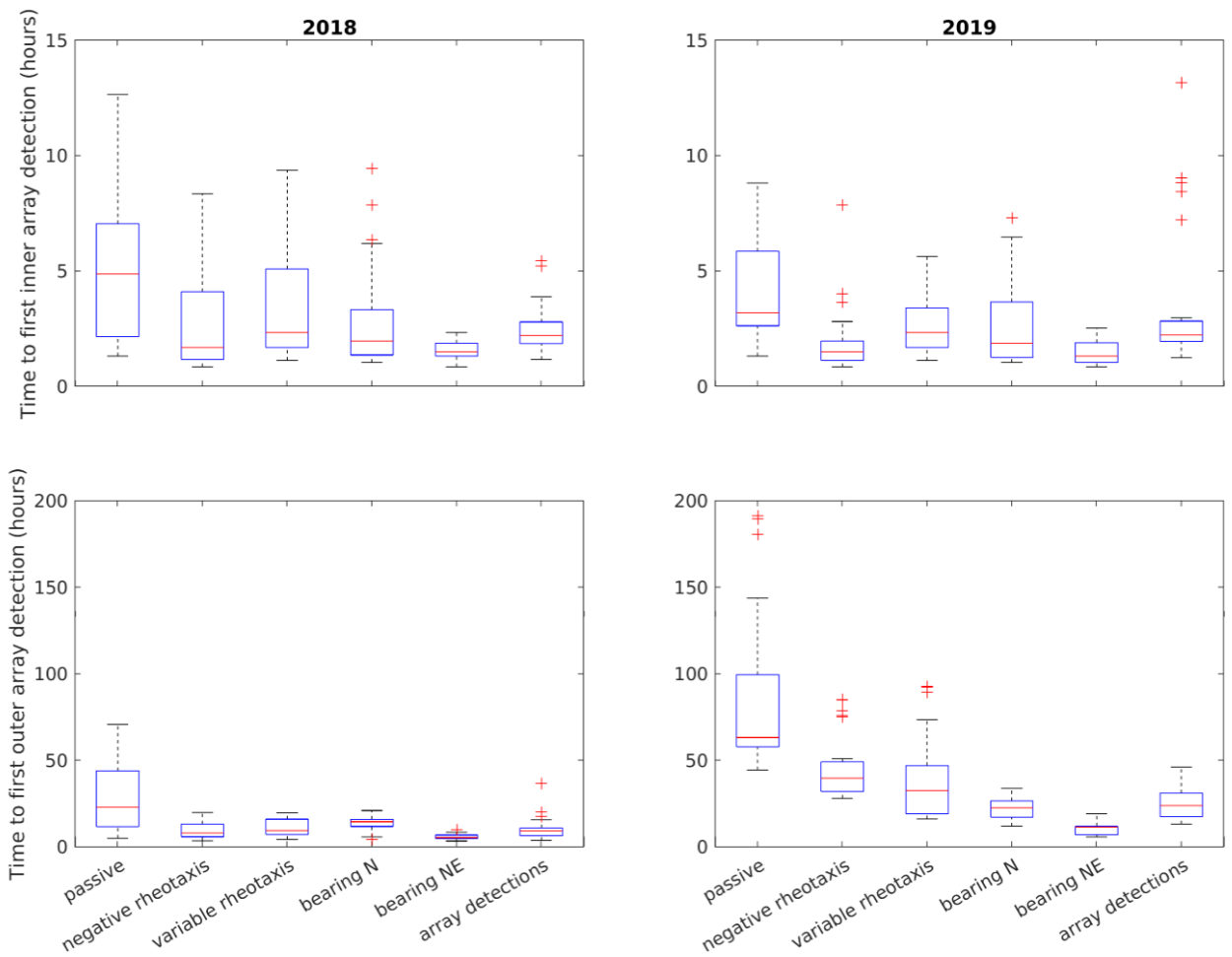


Figure 16.2 Boxplots showing the time for particles to be first detected at the inner (top) and outer (bottom) arrays for the 2018 (left) and 2019 (right) simulations, under the different behaviours with smolt swim speeds set to 3.5 bl s⁻¹. Red lines show median values for the particles tracked, or detections made, boxes show the 25th and 75th percentiles, the whiskers show the lower and upper adjacent values and the red crosses show any outliers.